Ravani, B. "Kinematics and Mechanisms"
The Engineering Handbook.
Ed. Richard C. Dorf
Boca Raton: CRC Press LLC, 2000

THE LONG TRAVEL DAMPER (LTD) CLUTCH—The introduction of the Long Travel Damper (LTD) clutch by Rockwell has addressed driver concerns of engine and drivetrain torsional vibration. The 15.5", diaphragm-spring, two-plate, pull-type clutch absorbs and dampens vibrations and torque loads passed through from the engine flywheel, providing a smoother ride for drivers and increased drivetrain component life. The LTD is available in three different capacities for use in low, medium and high horsepower ranges and features a fifth rivet to help alleviate clutch drag. (Photo courtesy of Rockwell Automotive.)

IV
Kinematics and Mechanisms

Bahram Ravani
University of California, Davis

THIS SECTION COMBINES KINEMATICS AND MECHANISMS and certain aspects of mechanical design to provide an introductory coverage of certain aspects of the theory of machines and mechanisms. This is the branch of engineering that deals with design and analysis of moving devices (or mechanisms) and machinery and their components. Kinematic analysis is usually the first step in the design and evaluation of mechanisms and machinery, and involves studying the relative motion of various components of a device or evaluating the geometry of the force system acting on a mechanism or its components. Further analysis and evaluation may involve calculation of the magnitude and sense of the forces and the stresses produced in each part of a mechanism or machine as a result of such forces. The overall subject of the theory of machines and mechanisms is broad and would be difficult to cover in this section. Instead, the authors in this section provide an introduction to some topics in this area to give readers an appreciation of the broad nature of this subject as well as to provide a readily available reference on the topics covered.

The first chapter is an introductory coverage of linkages and cams. These are mechanisms found in a variety of applications, from door hinges to robot manipulators and the valve mechanisms used in present-day motor vehicles. The scope of the presentation is displacement analysis dealing with understanding the relative motion between the input and output in such mechanisms. The second chapter goes beyond kinematic analysis and deals with the effects of the interactions between two surfaces in relative motion. This subject is referred to as tribology, and it is an important topic in

mechanical design, the theory of machines, and other fields. Tribology is an old field but still has many applications in areas where mechanical movement is achieved by relative motion between two surfaces. Present applications of tribology range from understanding the traction properties of tires used in automobiles to understanding the interfacial phenomena in magnetic storage systems and devices. The third chapter in this section deals with mechanical devices used for stopping relative motion between the contacting surfaces of machine elements or for coupling two moving mechanical components. These include mechanical fasteners, brakes, and clutches. Many mechanical devices and machines require the use of bolts and nuts (which are fasteners) for their construction. Brakes are usually used to stop the relative motion between two moving surfaces, and clutches reduce any mismatch in the speed of two mechanical elements. These components are used in a variety of applications; probably their best-known application is their use in the motor vehicle.

The fourth chapter deals with another mechanical element in the automotive industry, namely, the journal bearing used in the crankshaft of the automotive engine (which is usually an internal combustion engine). The last chapter in this sectiondeals with mechanical seals used to protect against leakage of fluids from mechanical devices and machines. When two mechanical components are brought into contact or relative motion as part of a machine, the gap between the contacting surfaces must be sealed if fluid is used for lubrication or other purposes in the machine. This chapter provides an introduction to the mechanical seals used to protect against leakage of fluids.

In summary, the authors in this section have provided easy-to-read introductions to selected topics in the field of theory of machines and mechanisms that can be used as a basis for further studies or as a readily available reference on the subject.

McCarthy, J. M., Long, G. L. "Linkages and Cams"
The Engineering Handbook.
Ed. Richard C. Dorf
Boca Raton: CRC Press LLC, 2000

20

Linkages and Cams

J. Michael McCarthy
University of California, Irvine

Gregory L. Long
University of California, Irvine

Mechanical movement of various machine components can be coordinated using linkages and cams. These devices are assembled from hinges, ball joints, sliders, and contacting surfaces and transform an input movement such as a rotation into an output movement that may be quite complex.

20.1 Linkages

Rigid links joined together by hinges parallel to each other are constrained to move in parallel planes and the system is called a **planar linkage.** A generic value for the **degree of freedom,** or mobility, of the system is given by the formula $F = 3(n - 1) - 2j$, where *n* is the number of links and *j* is the number of hinges.

Two links and one hinge form the simplest *open chain linkage*. Open chains appear as the structure of robot manipulators. In particular, a three-degree-of-freedom planar robot is formed by four bodies joined in a series by three hinges, as in Fig. 20.1(b).

If the series of links close to form a loop, the linkage is a simple *closed chain.* The simplest case is a quadrilateral ($n = 4$, $j = 4$) with one degree of freedom (See Figs. 20.1(a) and 20.3); notice that a triangle has mobility zero. A single loop with five links has two degrees of freedom and one with six links has three degrees of freedom. This latter linkage also appears when two planar robots hold the same object.

A useful class of linkages is obtained by attaching a two-link chain to a four-link quadrilateral in various ways to obtain a one-degree-of-freedom linkage with two loops. The two basic forms of this linkage are known as the Stephenson and Watt six-bar linkages, shown in Fig. 20.2.

Figure 20.1 (a) Planar four-bar linkage; and (b) planar robot.

(a)   (b)

Figure 20.2 (a) A Watt six-bar linkage; and (b) a Stephenson six-bar linkage.

(a)   (b)
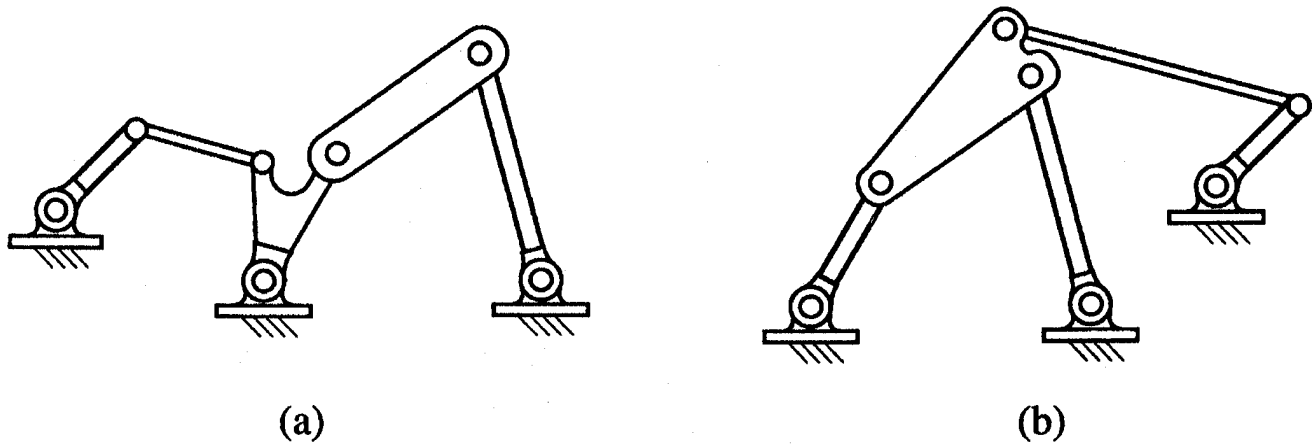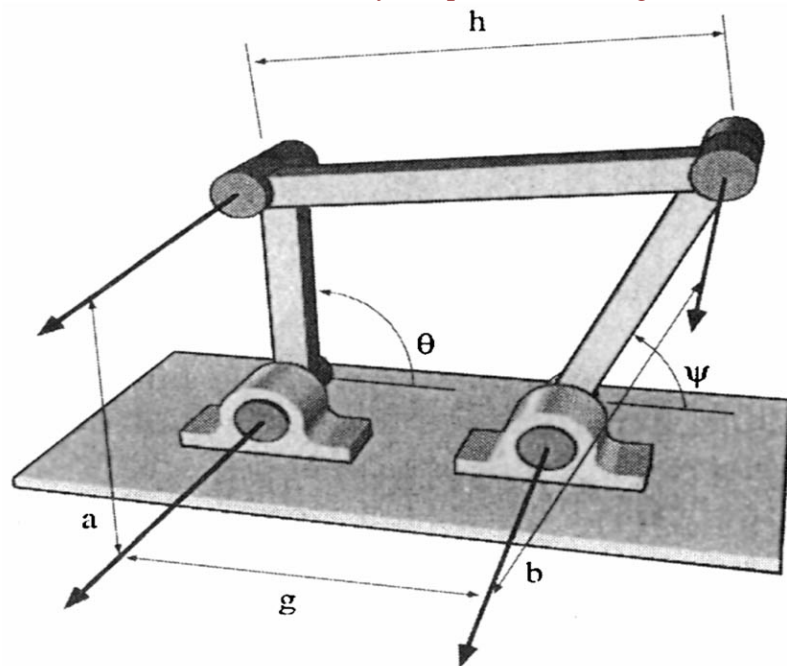
Figure 20.3 Dimensions used to analyze a planar 4R linkage.

In each of these linkages a sliding joint, which constrains a link to a straight line rather than a circle, can replace a hinge to obtain a different movement. For example, a slider-crank linkage is a four-bar closed chain formed by three hinges and a sliding joint.

20.2 Spatial Linkages

The axes of the hinges connecting a set of links need not be parallel. In this case the system is no longer constrained to move in parallel planes and forms a **spatial linkage**. The robot manipulator with six hinged joints (denoted R for **revolute joint**) is an example of a spatial 6R open chain.

Spatial linkages are often constructed using joints that constrain a link to a sphere about a point, such as a ball-in-socket joint, or a gimbal mounting formed by three hinges with concurrent axes—each termed a **spherical joint** (denoted S). The simplest spatial closed chain is the RSSR linkage, which is often used in place of a planar four-bar linkage to allow for misalignment of the cranks (Fig. 20.4).

Figure 20.4 A spatial RSSR linkage.
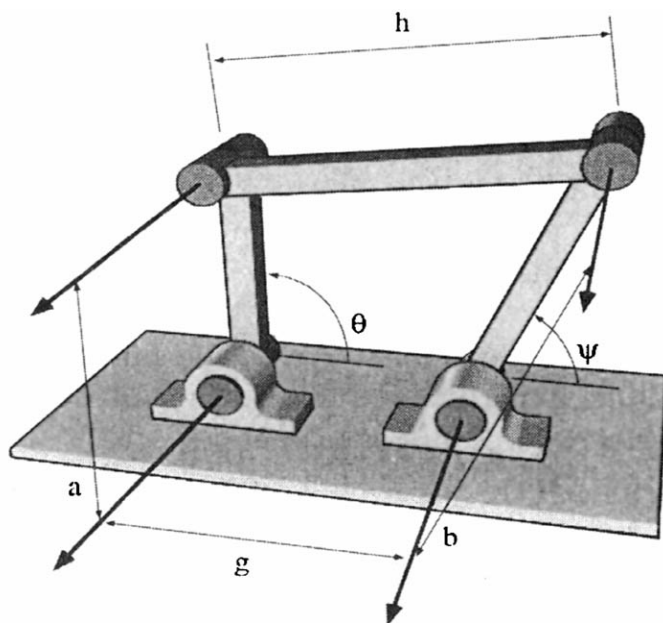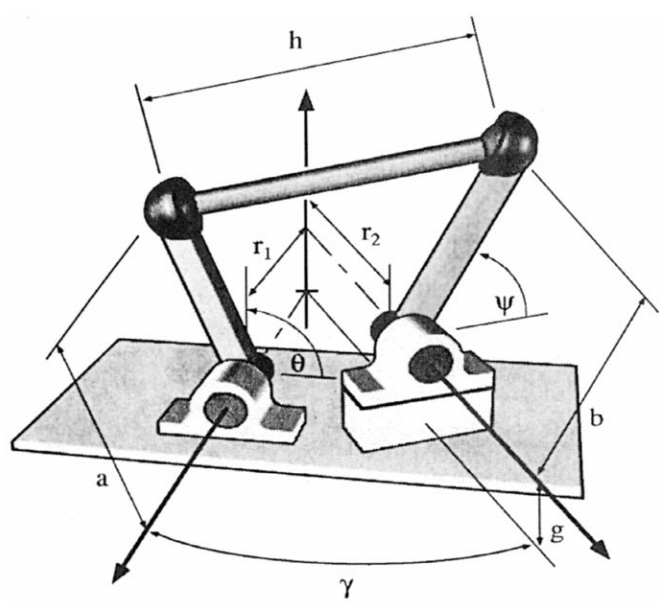
Figure 20.5 A spherical 4R linkage.

Another useful class of spatial mechanisms is produced by four hinges with concurrent axes that form a spherical quadrilateral known as a **spherical linkage.** These linkages provide a controlled reorientation movement of a body in space (Fig. 20.5).

20.3 Displacement Analysis

The closed loop of the planar 4R linkage (Fig. 20.3) introduces a constraint between the crank angles θ and ψ given by the equation

$$A\cos\psi + B\sin\psi = C \qquad (20.1)$$

where

$$A = 2gb - 2ab\cos\theta$$
$$B = -2ab\sin\theta$$
$$C = h^2 - g^2 - b^2 - a^2 + 2ga\cos\theta$$

This equation can be solved to give an explicit formula for the angle ψ of the output crank in terms of the input crank rotation θ:

$$\psi(\theta) = \tan^{-1}\left(\frac{B}{A}\right) \pm \cos^{-1}\left(\frac{C}{\sqrt{A^2 + B^2}}\right) \qquad (20.2)$$

The constraint equations for the spatial RSSR and spherical 4R linkages have the same form as that of the planar 4R linkage, but with coefficients as follows. For spatial RSSR linkage (Fig. 20.4):

$$A = -2ab\cos\gamma\cos\theta - 2br_1\sin\gamma$$
$$B = 2bg - 2ab\sin\theta$$
$$C = h^2 - g^2 - b^2 - a^2 - r_1^2 - r_2^2 + 2r_1r_2\cos\gamma$$
$$\quad + 2ar_2\sin\gamma\cos\theta + 2ga\sin\theta$$

For spherical 4R linkage (Fig. 20.5):

$$A = \sin\alpha\sin\beta\cos\gamma\cos\theta - \cos\alpha\sin\beta\sin\gamma$$
$$B = \sin\alpha\sin\beta\sin\theta$$
$$C = \cos\eta - \sin\alpha\cos\beta\sin\gamma\cos\theta$$
$$\quad - \cos\alpha\cos\beta\cos\gamma$$

The formula for the output angle ψ in terms of θ for both cases is identical to that already given for the planar 4R linkage.
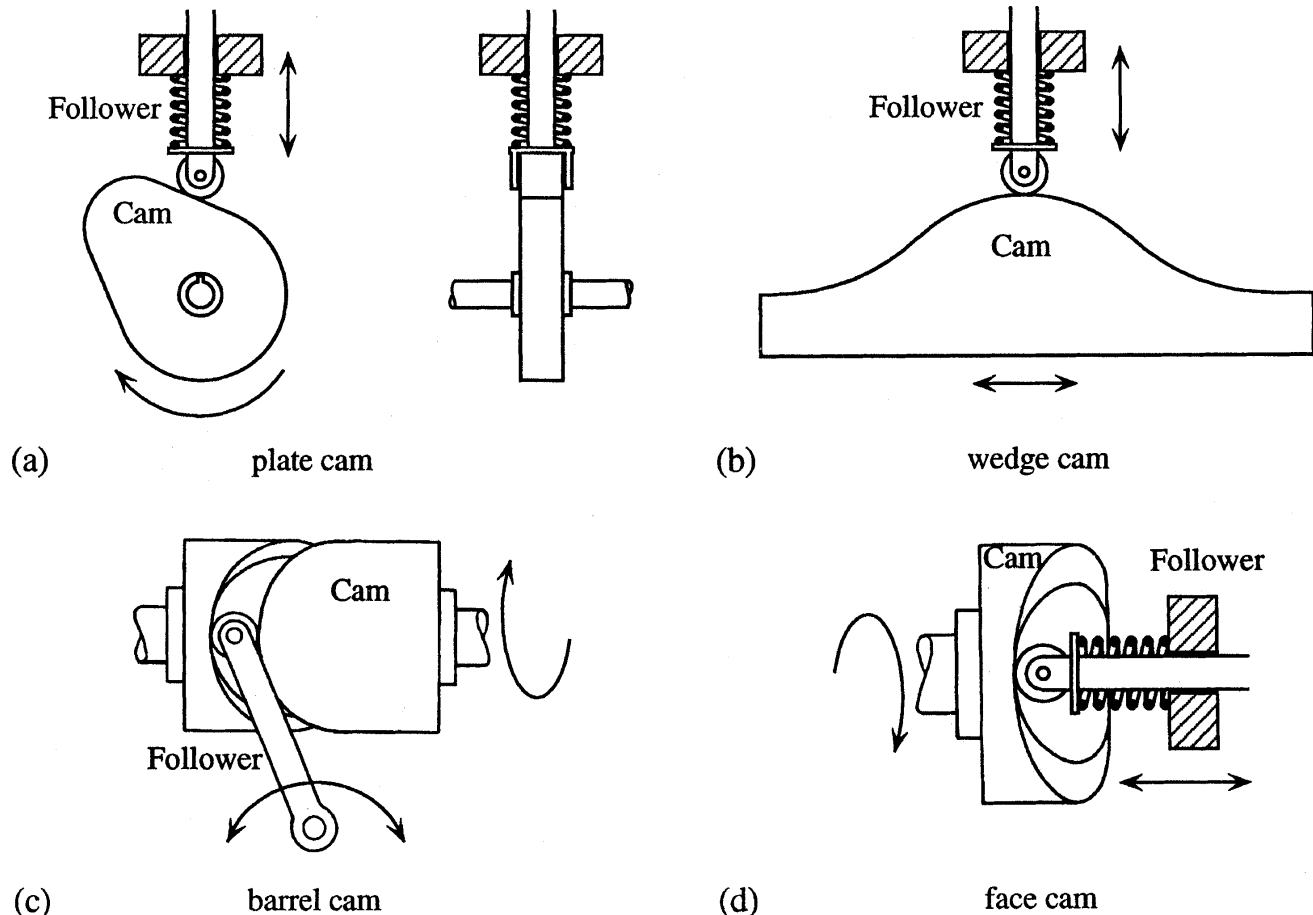
20.4 Cam Design

A *cam pair* (or *cam-follower*) consists of two primary elements called the *cam* and *follower*. The cam's motion, which is usually rotary, is transformed into either follower translation, oscillation, or combination, through direct mechanical contact. Cam pairs are found in numerous manufacturing and commercial applications requiring motion, path, and/or function generation. Cam pair mechanisms are usually simple, inexpensive, compact, and robust for the most demanding design applications. Moreover, a **cam profile** can be designed to generate virtually any desired follower motion, by either graphical or analytical methods.

20.5 Classification of Cams and Followers
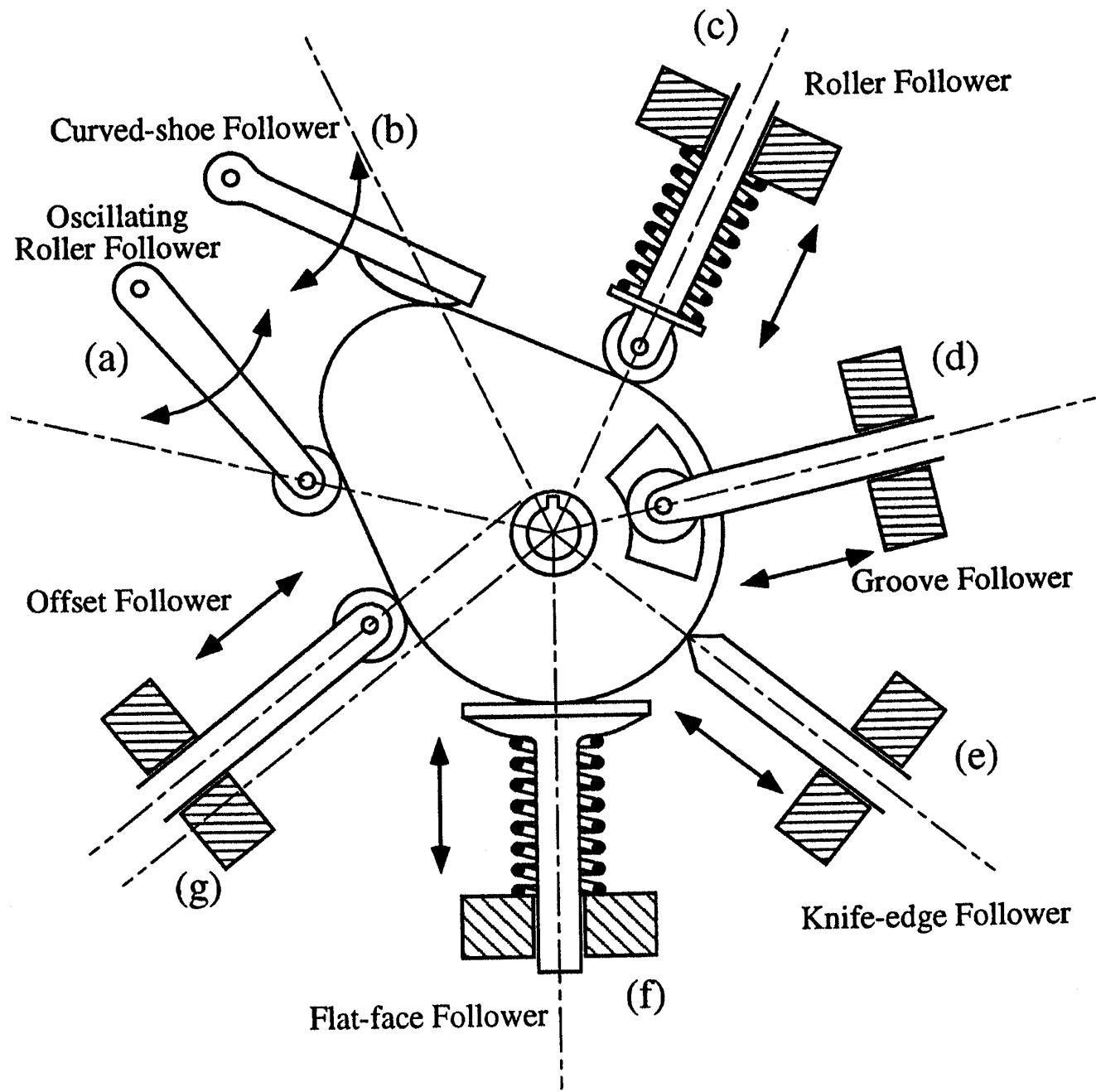
The versatility of cam pairs is evidenced by the variety of shapes, forms, and motions for both cam and follower. Cams are usually classified according to their basic shape as illustrated in Fig. 20.6: (a) plate cam, (b) wedge cam, (c) cylindric or barrel cam, and (d) end or face cam.

Figure 20.6 Basic types of cams.

(a) plate cam

(b) wedge cam

(c) barrel cam

(d) face cam

Followers are also classified according to their basic shape with optional modifiers describing their motion characteristics. For example, a follower can oscillate [Figs. 20.7(a–b)] or translate [20.7(c–g)]. As required by many applications, follower motion may be offset from the cam shaft's center as illustrated in Fig. 20.7(g). For all cam pairs, however, the follower must maintain constant contact with cam surface. Constant contact can be achieved by gravity, springs, or other mechanical constraints such as grooves.
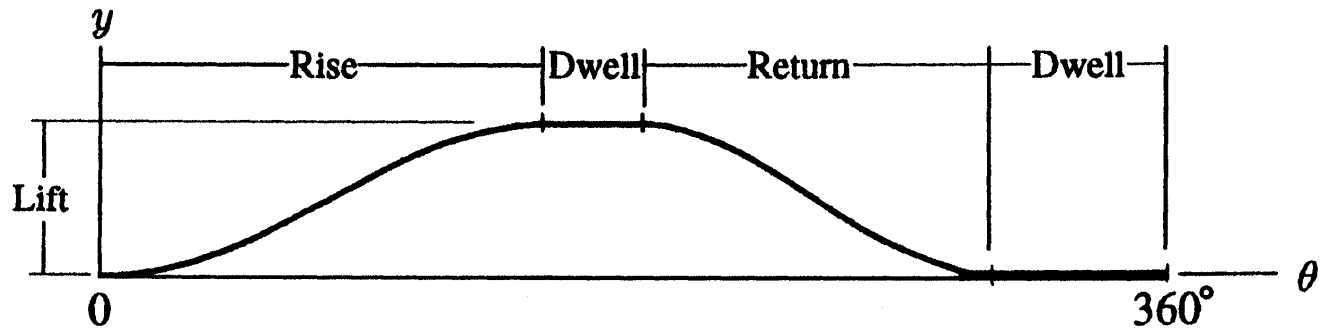
20.6 Displacement Diagrams

The cam's primary function is to create a well-defined follower displacement. If the cam's displacement is designated by θ and follower displacement by y, a given cam is designed such that a displacement function

$$y = f(\theta) \qquad (20.3)$$

is satisfied. A graph of *y* versus θ is called the *follower displacement diagram* (Fig. 20.8). On a displacement diagram, the abscissa represents one revolution of cam motion (θ) and the ordinate represents the corresponding follower displacement (y). Portions of the displacement diagram, when follower motion is away from the cam's center, are called *rise*. The maximum rise is called *lift*. Periods of follower rest are referred to as *dwells,* and *returns* occur when follower motion is toward the cam's center.

Figure 20.8 Displacement diagram.

The cam profile is generated from the follower displacement diagram via graphical or analytical methods that use parabolic, simple harmonic, cycloidal, and/or polynomial profiles. For many applications, the follower's velocity, acceleration, and higher time derivatives are necessary for proper cam design.

Cam profile generation is best illustrated using graphical methods where the cam profile can be constructed from the follower displacement diagram using the principle of kinematic inversion. As shown in Fig. 20.9, the prime circle is divided into a number of equal angular segments and assigned station numbers. The follower displacement diagram is then divided along the abscissa into corresponding segments. Using dividers, the distances are then transferred from the displacement diagram directly onto the cam layout to locate the corresponding trace point position. A smooth curve through these points is the pitch curve. For the case of a roller follower, the roller is drawn in its proper position at each station and the cam profile is then constructed as a smooth curve tangent to all roller positions. Analytical methods can be employed to facilitate computer-aided design of cam profiles.

Figure 20.9 Cam layout.
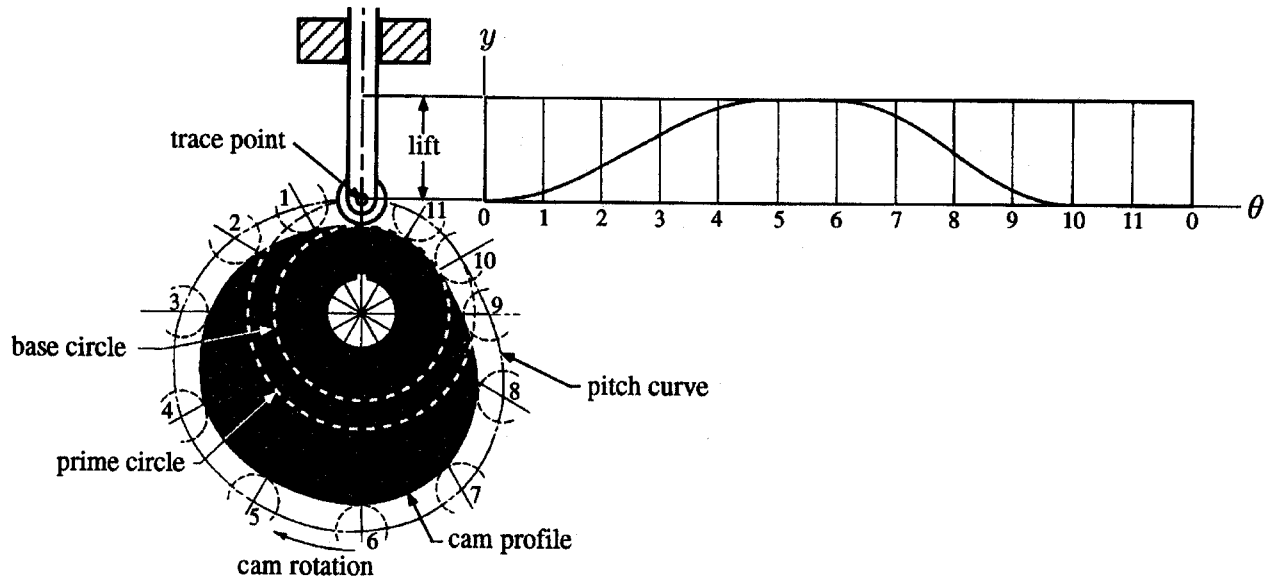
Figure 20.9   Cam layout.

Defining Terms

Linkage Terminology
Standard terminology for linkages includes the following:
Degree of freedom: The number of parameters, available as input, that prescribe the configuration of a given linkage, also known as its *mobility*.
Planar linkage: A collection of links constrained to move in parallel planes.
Revolute joint: A hinged connection between two links that constrains their relative movement to the plane perpendicular to the hinge axis.
Spatial linkage: A linkage with at least one link that moves out of a plane.
Spherical joint: A connection between two links that constrains their relative movement to a sphere about a point at the center of the joint.
Spherical linkage: A collection of links constrained to move on concentric spheres.

Cam Terminology
The standard cam terminology is illustrated in Fig. 20.10 and defined as follows:
Base circle: The smallest circle, centered on the cam axis, that touches the cam profile (radius R_b).
Cam profile: The cam's working surface.
Pitch circle: The circle through the pitch point, centered on the cam axis (radius R_p).
Pitch curve: The path of the trace point.
Pitch point: The point on the pitch curve where pressure angle is maximum.
Pressure angle: The angle between the normal to the pitch curve and the instantaneous direction
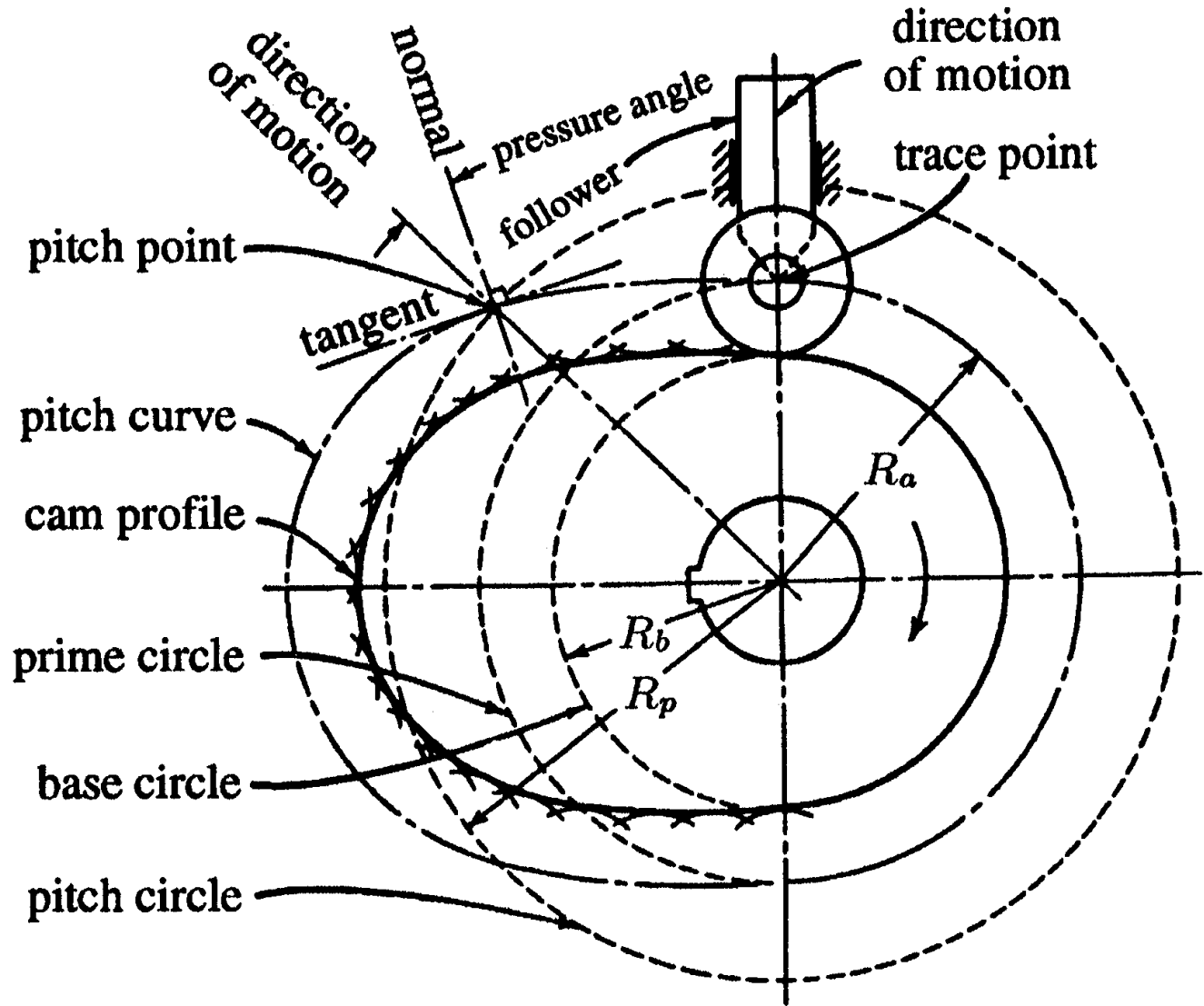
of trace point motion.

Prime circle: The smallest circle, centered on the cam axis, that touches the pitch curve (radius R_a).

Trace point: The contact point of a knife-edge follower, the center of a roller follower, or a reference point on a flat-faced follower.

Figure 20.10 Cam terminology.

References

Chironis, N. P. 1965. *Mechanisms, Linkages, and Mechanical Controls.* McGraw-Hill, New York.
Erdman, A. G. and Sandor, G. N. 1984. *Mechanism Design: Analysis and Synthesis*, vol. 1. Prentice Hall, Englewood Cliffs, NJ.

Paul, B. 1979. *Kinematics and Dynamics of Planar Machinery*. Prentice Hall, Englewood Cliffs, NJ.

Shigley, J. E. and Uicker, J. J. 1980. *Theory of Machines and Mechanisms.* McGraw-Hill, New York.

Suh, C. H. and Radcliffe, C. W. 1978. *Kinematics and Mechanism Design.* John Wiley & Sons, New York.

Further Information

An interesting array of linkages that generate specific movements can be found in *Mechanisms and Mechanical Devices Sourcebook* by Nicholas P. Chironis.

Design methodologies for planar and spatial linkages to guide a body in a desired way are found in *Mechanism Design: Analysis and Synthesis* by George Sandor and Arthur Erdman and in *Kinematics and Mechanism Design* by Chung Ha Suh and Charles W. Radcliffe.

Theory of Machines and Mechanisms by Joseph E. Shigley and John J. Uicker is particularly helpful in design of cam profiles for various applications.

Proceedings of the ASME Design Engineering Technical Conferences are published annually by the American Society of Mechanical Engineers. These proceedings document the latest developments in mechanism and machine theory.

The quarterly *ASME Journal of Mechanical Design* reports on advances in the design and analysis of linkage and cam systems. For a subscription contact American Society of Mechanical Engineers, 345 E. 47th St., New York, NY 10017.

Bhushan, B. "Tribology: Friction, Wear, and Lubrication"
The Engineering Handbook.
Ed. Richard C. Dorf
Boca Raton: CRC Press LLC, 2000

21

Tribology: Friction, Wear, and Lubrication

Bharat Bhushan
Ohio State University

In this chapter we first present the history of macrotribology and micro/nanotribology and their significance. We then describe mechanisms of friction, wear, and lubrication, followed by micro/nanotribology.
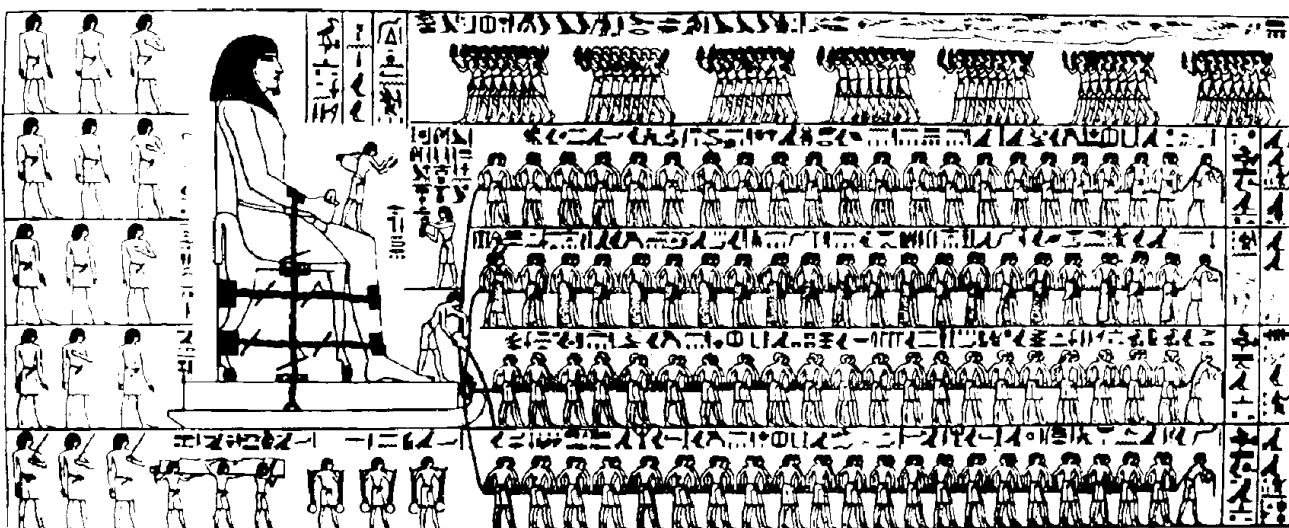
21.1 History of Tribology and Its Significance to Industry

Tribology is the science and technology of two interacting surfaces in relative motion and of related subjects and practices. The popular equivalent is friction, wear, and lubrication. The word *tribology,* coined in 1966, is derived from the Greek word *tribos* meaning "rubbing," so the literal translation would be the science of rubbing [Jost, 1966]. It is only the name tribology that is relatively new, because interest in the constituent parts of tribology is older than recorded history [Dowson, 1979]. It is known that drills made during the Paleolithic period for drilling holes or producing fire were fitted with bearings made from antlers or bones, and potters' wheels or stones for grinding cereals clearly had a requirement for some form of bearings [Davidson, 1957]. A ball thrust bearing dated about 40 A.D. was found in Lake Nimi near Rome.

Records show the use of wheels from 3500 B.C., which illustrates our ancestors' concern with reducing friction in translationary motion. The transportation of large stone building blocks and monuments required the know-how of frictional devices and lubricants, such as water-lubricated

sleds. Figure 21.1 illustrates the use of a sledge to transport a heavy statue by Egyptians circa 1880 B.C. [Layard, 1853]. In this transportation, 172 slaves are being used to drag a large statue weighing about 600 kN along a wooden track. One man, standing on the sledge supporting the statue, is seen pouring a liquid into the path of motion; perhaps he was one of the earliest lubrication engineers. [Dowson (1979) has estimated that each man exerted a pull of about 800 N. On this basis the total effort, which must at least equal the friction force, becomes 172×800 N. Thus, the coefficient of friction is about 0.23.] A tomb in Egypt that was dated several thousand years B.C. provides the evidence of use of lubricants. A chariot in this tomb still contained some of the original animal-fat lubricant in its wheel bearings.

Figure 21.1 Egyptians using lubricant to aid movement of Colossus, El-Bersheh, c. 1880 B.C.

During and after the glory of the Roman empire, military engineers rose to prominence by devising both war machinery and methods of fortification, using tribological principles. It was the Renaissance engineer and artist Leonardo da Vinci (1452−1519), celebrated in his days for his genius in military construction as well as for his painting and sculpture, who first postulated a scientific approach to friction. Leonardo introduced for the first time the concept of coefficient of friction as the ratio of the friction force to normal load. In 1699 Amontons found that the friction force is directly proportional to the normal load and is independent of the apparent area of contact. These observations were verified by Coulomb in 1781, who made a clear distinction between static friction and kinetic friction.

Many other developments occurred during the 1500s, particularly in the use of improved bearing materials. In 1684 Robert Hooke suggested the combination of steel shafts and bell-metal bushes as preferable to wood shod with iron for wheel bearings. Further developments were associated with the growth of industrialization in the latter part of the eighteenth century. Early developments in the petroleum industry started in Scotland, Canada, and the U.S. in the 1850s [Parish, 1935; Dowson, 1979].

Though essential laws of viscous flow had earlier been postulated by Newton, scientific

understanding of lubricated bearing operations did not occur until the end of the nineteenth century. Indeed, the beginning of our understanding of the principle of hydrodynamic lubrication was made possible by the experimental studies of Tower [1884] and the theoretical interpretations of Reynolds [1886] and related work by Petroff [1883]. Since then developments in hydrodynamic bearing theory and practice have been extremely rapid in meeting the demand for reliable bearings in new machinery.

Wear is a much younger subject than friction and bearing development, and it was initiated on a largely empirical basis.

Since the beginning of the 20th century, from enormous industrial growth leading to demand for better tribology, our knowledge in all areas of tribology has expanded tremendously [Holm, 1946; Bowden and Tabor, 1950, 1964; Bhushan, 1990, 1992; Bhushan and Gupta, 1991].

Tribology is crucial to modern machinery, which uses sliding and rolling surfaces. Examples of productive wear are writing with a pencil, machining, and polishing. Examples of productive friction are brakes, clutches, driving wheels on trains and automobiles, bolts, and nuts. Examples of unproductive friction and wear are internal combustion and aircraft engines, gears, cams, bearings, and seals. According to some estimates, losses resulting from ignorance of tribology amount in the U.S. to about 6% of its gross national product or about 200 billion dollars per year, and approximately one-third of the world's energy resources in present use appear as friction in one form or another. Thus, the importance of friction reduction and wear control cannot be overemphasized for economic reasons and long-term reliability. According to Jost [1966, 1976], the United Kingdom could save approximately 500 million pounds per annum and the U.S. could save in excess of 16 billion dollars per annum by better tribological practices. The savings are both substantial and significant and could be obtained without the deployment of large capital investment.
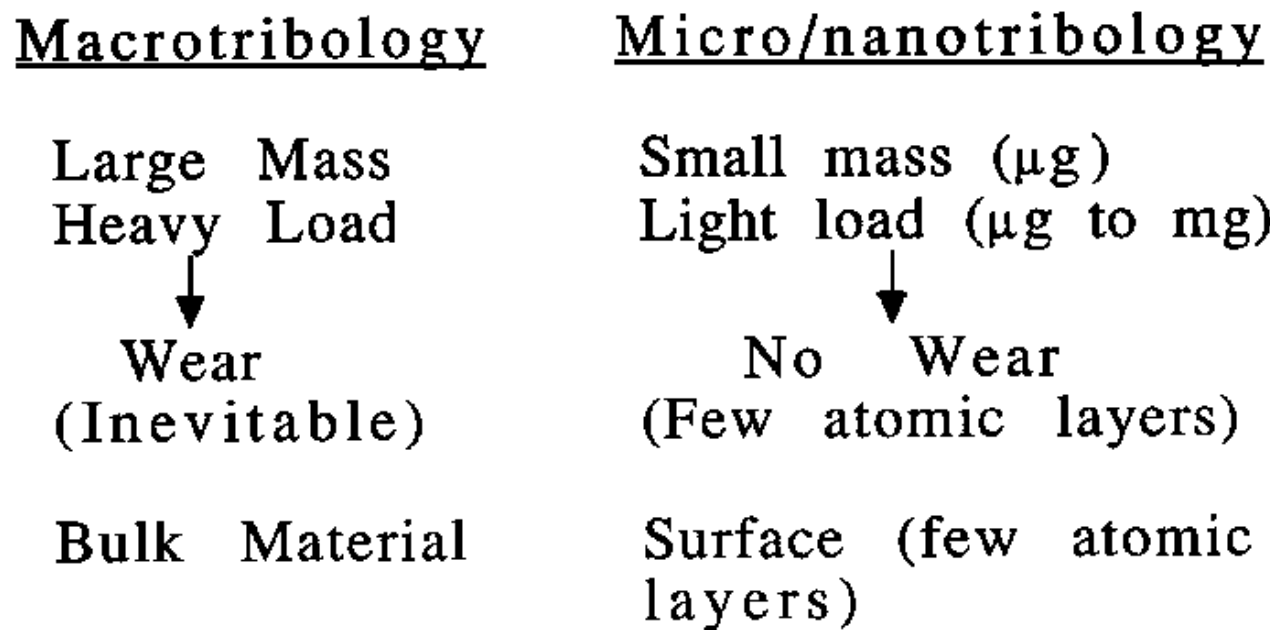
The purpose of research in tribology is understandably the minimization and elimination of losses resulting from friction and wear at all levels of technology where the rubbing of surfaces are involved. Research in tribology leads to greater plant efficiency, better performance, fewer breakdowns, and significant savings.

21.2 Origins and Significance of Micro/nanotribology

The advent of new techniques to measure surface topography, adhesion, friction, wear, lubricant film thickness, and mechanical properties all on micro- to nanometer scale; to image lubricant molecules; and to conduct atomic-scale simulations with the availability of supercomputers has led to development of a new field referred to as *microtribology, nanotribology, molecular tribology,* or *atomic-scale tribology.* This field deals with experimental and theoretical investigations of processes ranging from atomic and molecular scales to micro scales, occurring during adhesion, friction, wear, and thin-film lubrication at sliding surfaces. The differences between the conventional or macrotribology and micro/nanotribology are contrasted in Fig. 21.2. In macrotribology, tests are conducted on components with relatively large mass under heavily loaded conditions. In these tests, wear is inevitable and the bulk properties of mating components dominate the tribological performance. In **micro/nanotribology,** measurements are made on components, at least one of the mating components with relatively small mass under lightly loaded

conditions. In this situation negligible wear occurs and the surface properties dominate the tribological performance.

Figure 21.2 Comparison between macrotribology and micro/nanotribology.

Macrotribology

Large Mass
Heavy Load
↓
Wear
(Inevitable)

Bulk Material

Micro/nanotribology

Small mass (μg)
Light load (μg to mg)
↓
No Wear
(Few atomic layers)

Surface (few atomic layers)

The micro/nanotribological studies are needed to develop fundamental understanding of interfacial phenomena on a small scale and to study interfacial phenomena in micro- and nanostructures used in magnetic storage systems, microelectromechanical systems (MEMS) and other industrial applications [Bhushan, 1990, 1992]. The components used in micro- and nanostructures are very light (on the order of few micrograms) and operate under very light loads (on the order of few micrograms to few milligrams). As a result, friction and wear (on a nanoscale) of lightly loaded micro/nanocomponents are highly dependent on the surface interactions (few atomic layers). These structures are generally lubricated with molecularly thin films. Micro- and nanotribological techniques are ideal to study the friction and wear processes of micro- and nanostructures. Although micro/nanotribological studies are critical to study micro- and nanostructures, these studies are also valuable in fundamental understanding of interfacial phenomena in macrostructures to provide a bridge between science and engineering. Friction and wear on micro- and nanoscales have been found to be generally small compared to that at macroscales. Therefore, micro/nanotribological studies may identify the regime for ultra-low friction and near zero wear.

To give a historical perspective of the field [Bhushan, 1995], the *scanning tunneling microscope* (STM) developed by Dr. Gerd Binnig and his colleagues in 1981 at the IBM Zurich Research Laboratory, Forschungslabor, is the first instrument capable of directly obtaining three-dimensional (3-D) images of solid surfaces with atomic resolution [Binnig *et al.,* 1982]. G. Binnig and H. Rohrer received a Nobel Prize in Physics in 1986 for their discovery. STMs can

only be used to study surfaces that are electrically conductive to some degree. Based on their design of STM Binnig *et al.* developed, in 1985, an *atomic force microscope* (AFM) to measure ultrasmall forces (less than 1 μN) present between the AFM tip surface and the sample surface [1986]. AFMs can be used for measurement of *all engineering surfaces,* which may be either electrically conducting or insulating. AFM has become a popular surface profiler for topographic measurements on micro- to nanoscale. Mate *et al.* [1987] were the first to modify an AFM in order to measure both normal and friction forces and this instrument is generally called *friction force microscope* (FFM) or *lateral force microscope* (LFM). Since then, Bhushan and other researchers have used FFM for atomic-scale and microscale friction and boundary lubrication studies [Bhushan and Ruan, 1994; Bhushan *et al.,* 1994; Ruan and Bhushan, 1994; Bhushan, 1995; Bhushan *et al.,* 1995]. By using a standard or a sharp diamond tip mounted on a stiff cantilever beam, Bhushan and other researchers have used AFM for scratching, wear, and measurements of elastic/plastic mechanical properties (such as indentation hardness and modulus of elasticity) [Bhushan *et al.,* 1994; Bhushan and Koinkar, 1994a,b; Bhushan, 1995; Bhushan *et al.,* 1995].
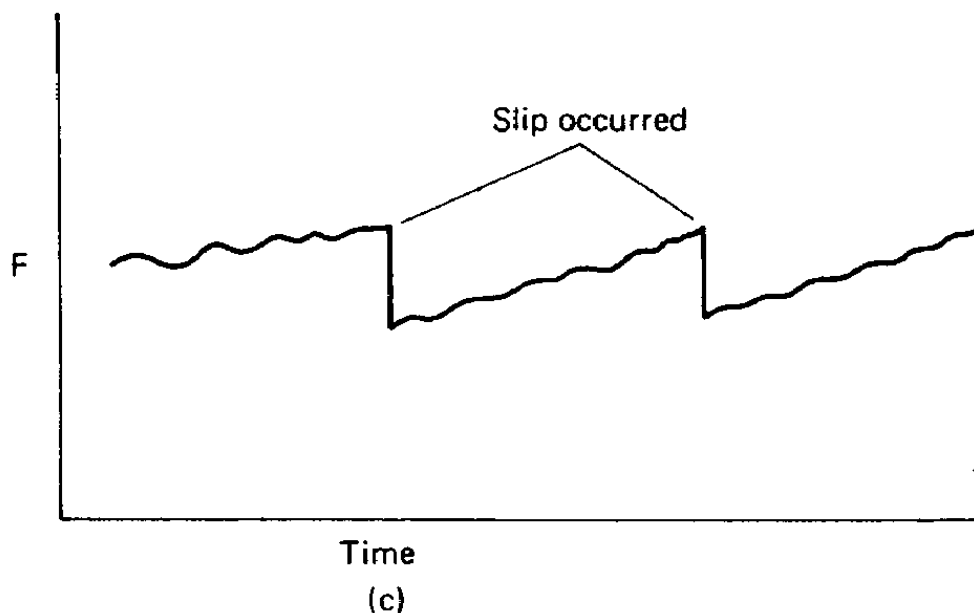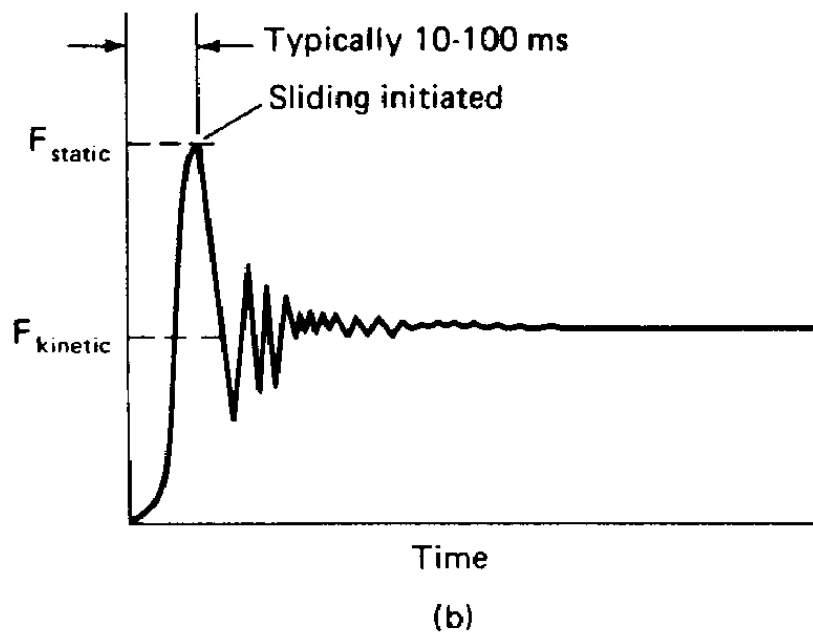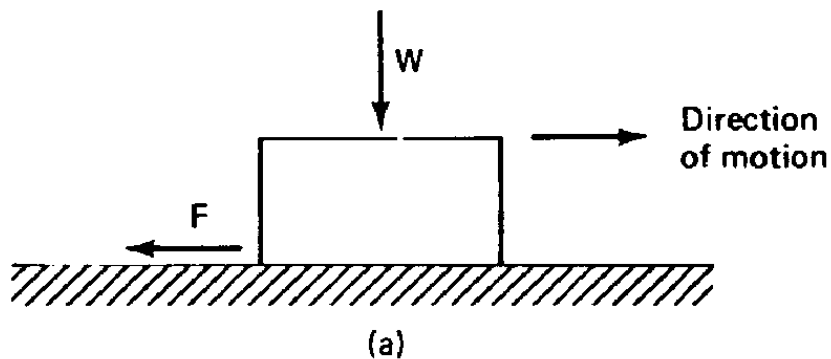
Surface force apparatuses (SFAs), first developed in 1969 [Tabor and Winterton, 1969], are other instruments used to study both static and dynamic properties of the molecularly thin liquid films sandwiched between two molecularly smooth surfaces [Israelachvili and Adams, 1978; Klein, 1980; Tonck *et al.,* 1988; Georges *et al.,* 1993,1994]. These instruments have been used to measure the dynamic shear response of liquid films [Bhushan, 1995]. Recently, new friction attachments were developed that allow for two surfaces to be sheared past each other at varying sliding speeds or oscillating frequencies while simultaneously measuring both the friction forces and normal forces between them [Peachey *et al.,* 1991; Bhushan, 1995]. The distance between two surfaces can also be independently controlled to within ± 0.1 nm and the force sensitivity is about 10 nN. The SFAs are used to study rheology of molecularly thin liquid films; however, the liquid under study has to be confined between molecularly smooth optically transparent surfaces with radii of curvature on the order of 1 mm (leading to poorer lateral resolution as compared to AFMs). SFAs developed by Tonck *et al.* [1988] and Georges *et al.* [1993, 1994] use an opaque and smooth ball with large radius (≈ 3 mm) against an opaque and smooth flat surface. Only AFMs/FFMs can be used to study *engineering surfaces* in the *dry and wet conditions* with *atomic resolution.*

21.3 Friction

Definition of Friction

Friction is the resistance to motion that is experienced whenever one solid body slides over another. The resistive force, which is parallel to the direction of motion, is called the friction force, Fig. 21.3(a). If the solid bodies are loaded together and a tangential force (F) is applied, then the value of the tangential force that is required to initiate sliding is the static friction force. It may take a few milliseconds before sliding is initiated at the interface (F_{static}). The tangential force required to maintain sliding is the kinetic (or dynamic) friction force (F_{kinetic}). The kinetic friction force is either lower than or equal to the static friction force, Fig. 21.3(b).

Figure 21.3 (a) Schematic illustration of a body sliding on a horizontal surface. *W* is the normal load and *F* is the friction force. (b) Friction force versus time or displacement. F_{static} is the force required to initiate sliding and $F_{kinetic}$ is the force required to sustain sliding. (c) Kinetic friction force versus time or displacement showing irregular stick-slip.

It has been found experimentally that there are two basic laws of intrinsic (or conventional) friction that are generally obeyed over a wide range of applications. The first law states that the friction is independent of the apparent area of contact between the contacting bodies, and the second law states that the friction force F is proportional to the normal load W between the bodies. These laws are often referred to as *Amontons laws,* after the French engineer Amontons, who presented them in 1699 [Dowson, 1979].

The second law of friction enables us to define a *coefficient of friction.* The law states that the friction force F is proportional to the normal load W. That is,

$$F = \mu W \qquad (21.1)$$

where μ is a constant known as the *coefficient of friction.* It should be emphasized that μ is a constant only for a given pair of sliding materials under a given set of operating conditions (temperature, humidity, normal pressure, and sliding velocity). Many materials show sliding speed and normal load dependence on the coefficients of static and kinetic friction in dry and lubricated contact.

It is a matter of common experience that the sliding of one body over another under a steady pulling force proceeds sometimes at constant or nearly constant velocity, and on other occasions at velocities that fluctuate widely. If the friction force (or sliding velocity) does not remain constant as a function of distance or time and produces a form of oscillation, it is generally called a *stick-slip phenomena,* Fig. 21.3(c). During the stick phase, the friction force builds up to a certain value and then slip occurs at the interface. Usually, a sawtooth pattern in the friction force−time curve [Fig. 21.3(c)] is observed during the stick-slip process. Stick-slip generally arises whenever the coefficient of static friction is markedly greater than the coefficient of kinetic friction or whenever the rate of change of coefficient of kinetic friction as a function of velocity at the sliding velocity employed is negative. The stick-slip events can occur either repetitively or in a random manner.

The stick-slip process generally results in squealing and chattering of sliding systems. In most sliding systems the fluctuations of sliding velocity resulting from the stick-slip process and associated squeal and chatter are considered undesirable, and measures are normally taken to eliminate, or at any rate to reduce, the amplitude of the fluctuations.

Theories of Friction

All engineering surfaces are rough on a microscale. When two nominally flat surfaces are placed in contact under load, the contact takes place at the tips of the asperities and the load is supported by the deformation of contacting asperities, and the discrete contact spots (junctions) are formed, Fig. 21.4. The sum of the areas of all the contact spots constitutes the real (true) area of the contact (A_r) and for most materials at normal loads, this will be only a small fraction of the apparent (nominal) area of contact (A_a). The proximity of the asperities results in adhesive contacts caused by either physical or chemical interaction. When these two surfaces move relative to each other, a lateral force is required to overcome adhesion. This force is referred to as *adhesional friction*

force. From classical theory of adhesion, this friction force (F_A) is defined as follows [Bowden and Tabor, 1950]. For a dry contact,

$$F_A = A_r \tau_a \qquad (21.2a)$$

and for a lubricated contact,
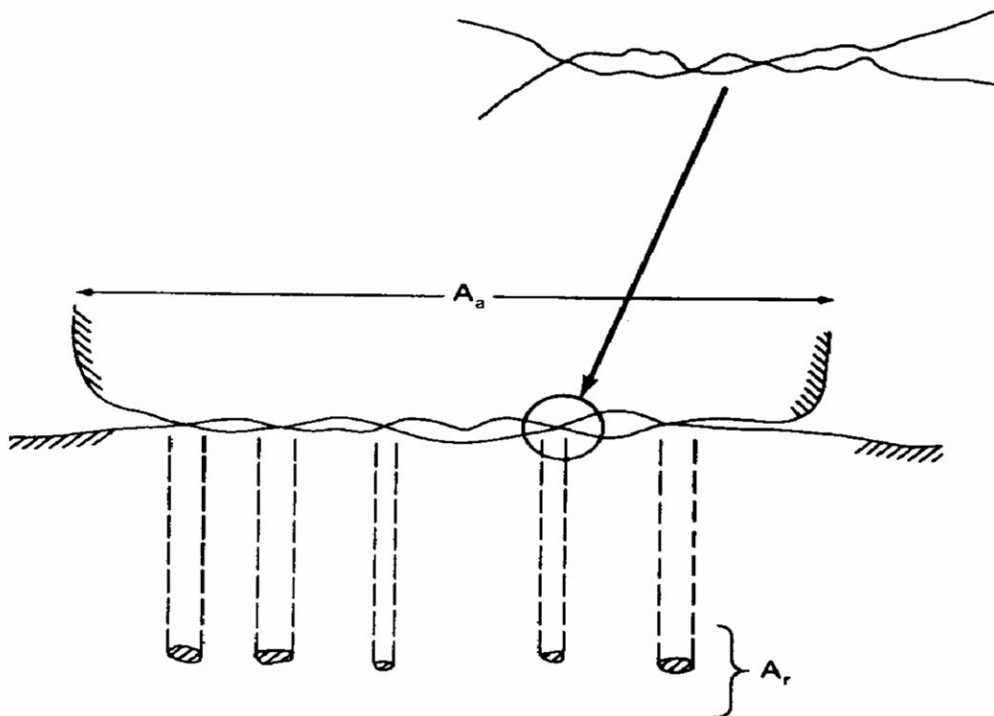
$$F_A = A_r[\alpha\tau_a + (1 - \alpha)\tau_l] \qquad (21.2b)$$

and

$$\tau_l = \eta_l V/h \qquad (21.2c)$$

where τ_a and τ_l are the shear strengths of the dry contact and of the lubricant film, respectively; α is the fraction of unlubricated area; η_l is the dynamic viscosity of the lubricant; V is the relative sliding velocity; and h is the lubricant film thickness.

Figure 21.4 Schematic representation of an interface, showing the apparent (A_a) and real (A_r) areas of contact. Typical size of an asperity contact is from submicron to a few microns. Inset shows the details of a contact on a submicron scale.

The contacts can be either elastic or plastic, depending primarily on the surface topography and the mechanical properties of the mating surfaces. The expressions for real area of contact for elastic (e) and plastic (p) contacts are as follows [Greenwood and Williamson, 1966; Bhushan, 1984, 1990]. For $\psi < 0.6$, elastic contacts,

$$A_{re}/W \sim 3.2/E_c \left(\sigma_p/R_p\right)^{1/2} \qquad (21.3a)$$

For $\psi > 1$, plastic contacts,

$$A_{rp}/W = 1/H \qquad (21.3b)$$

Finally,

$$\psi = (E_c/H) \ (\sigma_p/R_p)^{1/2} \qquad (21.3c)$$

where E_c is the composite modulus of elasticity, H is the hardness of the softer material, and σ_p and $1/R_p$ are the composite standard deviation and composite mean curvature of the summits of the mating surfaces. The real area of contact is reduced by improving the mechanical properties and in some cases by increasing the roughness (in the case of bulk of the deformation being in the elastic contact regime).

The adhesion strength depends upon the mechanical properties and the physical and chemical interaction of the contacting bodies. The adhesion strength is reduced by reducing surface interactions at the interface. For example, presence of contaminants or deliberately applied fluid film (e.g., air, water, or lubricant) would reduce the adhesion strength. Generally, most interfaces in vacuum with intimate solid-solid contact would exhibit very high values for coefficient of friction. Few pp of contaminants (air, water) may be sufficient to reduce μ dramatically. Thick films of liquids or gases would further reduce μ, as it is much easier to shear into a fluid film than to shear a solid-solid contact.

So far we have discussed theory of adhesional friction. If one of the sliding surfaces is harder than the other, the asperities of the harder surface may penetrate and plough into the softer surface. Ploughing into the softer surface may also occur as a result of impacted wear debris. In addition, interaction of two rather rough surfaces may result into mechanical interlocking on micro or macro scale. During sliding, interlocking would result into ploughing of one of the surfaces. In tangential motion the ploughing resistance is in addition to the adhesional friction. There is yet other mechanism of friction—deformation (or hysteresis) friction —which may be prevalent in materials with elastic hysteresis losses such as in polymers. In boundary lubricated conditions or unlubricated interfaces exposed to humid environments, presence of some liquid may result in formation of menisci or adhesive bridges and the meniscus/viscous effects may become important; in some cases these may even dominate the overall friction force [Bhushan, 1990].

Measurements of Friction

In a friction measurement apparatus two test specimens are loaded against each other at a desired normal load, one of the specimens is allowed to slide relative to the other at a desired sliding speed, and the tangential force required to initiate or maintain sliding is measured. There are numerous apparatuses used to measure friction force [Benzing *et al.,* 1976; Bhushan and Gupta, 1991]. The simplest method is an inclined-plane technique. In this method the flat test specimen of weight *W* is placed on top of another flat specimen whose inclination can be adjusted, as shown in Fig. 21.5. The inclination of the lower specimen is increased from zero to an angle at which the block begins to slide. At this point, downward horizontal force being applied at the interface exceeds the static friction force, F_{static}. At the inclination angle θ, at which the block just begins to slide,
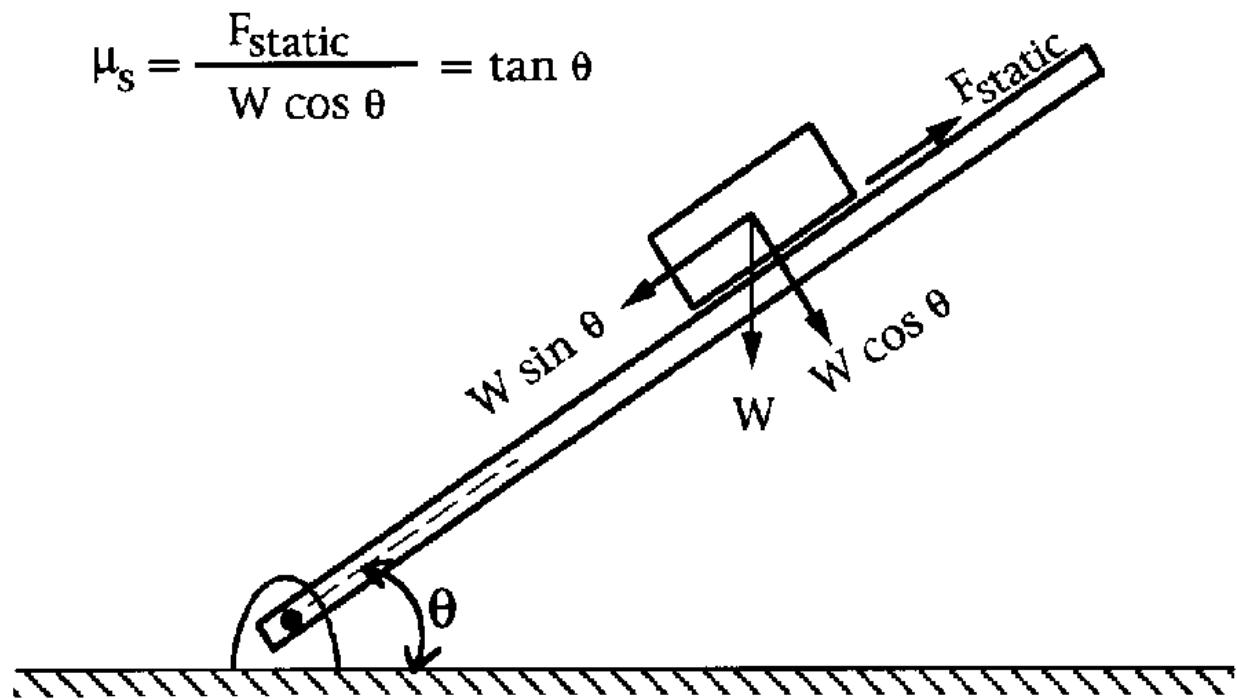
$$F_{\text{static}} = W \sin \theta$$

and the coefficient of static friction μ_s is

$$\mu_s = \frac{F_{\text{static}}}{W \cos \theta} = \tan \theta \qquad (21.4)$$

The angle θ is referred to as *friction angle.* This simple method only measures the coefficient of static friction and does not allow the measurements of the effect of sliding. However, this method demonstrates the effects of friction and provides the simplest method to measure coefficient of static friction.

Figure 21.5 Inclined-plane technique to measure static friction force.

Typical values of coefficient of friction of various material pairs are presented in Table 21.1 [Avallone and Baumeister, 1987]. It should be noted that values of coefficient of friction depend on the operating conditions—loads, speeds, and the environment —and the values reported in Table 21.1 should therefore be used with caution.

Table 21.1 Coefficient of Friction μ for Various Material Combinations

Materials	μ, static		μ, sliding (kinetic)	
	Dry	Greasy	Dry	Greasy
Hard steel on hard steel	0.78	0.11(*a*)	0.42	0.029(*h*)
		0.23(*b*)		0.081(*c*)
		0.15(*c*)		0.080(*i*)
		0.11(*d*)		0.058(*j*)

Material combination	Static dry	Static greasy	Kinetic dry	Kinetic greasy
		0.0075(p)		0.084(d)
		0.0052(h)		0.105(k)
				0.096(l)
				0.108(m)
				0.12(a)
Mild steel on mild steel	0.74		0.57	0.09(a)
				0.19(u)
Hard steel on graphite	0.21	0.09(a)		
Hard steel on babbitt (ASTM 1)	0.70	0.23(b)	0.33	0.16(b)
		0.15(c)		0.06(c)
		0.08(d)		0.11(d)
		0.085(e)		
Hard steel on babbitt (ASTM 8)	0.42	0.17(b)	0.35	0.14(b)
		0.11(c)		0.065(c)
		0.09(d)		0.07(d)
		0.08(e)		0.08(h)
Hard steel on babbitt (ASTM 10)		0.25(b)		0.13(b)
		0.12(c)		0.06(c)
		0.10(d)		0.055(d)
		0.11(e)		
Mild steel on cadmium silver				0.097(f)
Mild steel on phosphor bronze			0.34	0.173(f)
Mild steel on copper lead				0.145(f)
Mild steel on cast iron		0.183(c)	0.23	0.133(f)
Mild steel on lead	0.95	0.5(f)	0.95	0.3(f)
Nickel on mild steel			0.64	0.178(x)
Aluminum on mild steel	0.61		0.47	
Magnesium on mild steel			0.42	
Magnesium on magnesium	0.6	0.08(y)		
Teflon on Teflon	0.04			0.04(f)
Teflon on steel	0.04			0.04(f)
Tungsten carbide on tungsten carbide	0.2	0.12(a)		
Tungsten carbide on steel	0.5	0.08(a)		
Tungsten carbide on copper	0.35			
Tungsten carbide on iron	0.8			
Bonded carbide on copper	0.35			
Bonded carbide on iron	0.8			
Cadmium on mild steel			0.46	
Copper on mild steel	0.53		0.36	0.18(a)
Nickel on nickel	1.10		0.53	0.12(w)

	Static, dry	Static, lubricated	Kinetic, dry	Kinetic, lubricated
Brass on mild steel	0.51		0.44	
Brass on cast iron			0.30	
Zinc on cast iron	0.85		0.21	
Magnesium on cast iron			0.25	
Copper on cast iron	1.05		0.29	
Tin on cast iron			0.32	
Lead on cast iron			0.43	
Aluminum on aluminum	1.05		1.4	
Glass on glass	0.94	0.01(p) 0.005(q)	0.40	0.09(a) 0.116(v)
Carbon on glass			0.18	
Garnet on mild steel			0.39	
Glass on nickel	0.78		0.56	
Copper on glass	0.68		0.53	
Cast iron on cast iron	1.10		0.15	0.070(d) 0.064(n)
Bronze on cast iron			0.22	0.077(n)
Oak on oak (parallel to grain)	0.62		0.48	0.164(r) 0.067(s)
Oak on oak (perpendicular)	0.54		0.32	0.072(s)
Leather on oak (parallel)	0.61		0.52	
Cast iron on oak			0.49	0.075(n)
Leather on cast iron			0.56	0.36(t) 0.13(n)
Laminated plastic on steel			0.35	0.05(t)
Fluted rubber bearing on steel				0.05(t)

Source: Adapted from Avallone, E. A. and Baumeister, T., III, 1987. *Marks' Standard Handbook for Mechanical Engineers,* 9th ed. McGraw-Hill, New York.

Note: Reference letters indicate the lubricant used:

a = oleic acid
b = Atlantic spindle oil (light mineral)
c = castor oil
d = lard oil
e = Atlantic spindle oil plus 2% oleic acid
f = medium mineral oil
g = medium mineral oil plus ½% oleic acid
h = stearic acid
i = grease (zinc oxide base)
j = graphite
k = turbine oil plus 1% graphite
l = turbine oil plus 1% stearic acid
m = turbine oil (medium mineral)
n = olive oil
p = palmitic acid

q = ricinoleic acid
r = dry soap
s = lard
t = water
u = rape oil
v = 3-in-1 oil
w = octyl alcohol
x = triolein
y = 1% lauric acid in paraffin oil

21.4 Wear

Wear is the removal of material from one or both of two solid surfaces in a solid-state contact. It occurs when solid surfaces are in a sliding, rolling, or impact motion relative to one another. Wear occurs through surface interactions at asperities, and components may need replacement after a relatively small amount of material has been removed or if the surface is unduly roughened. In well-designed tribological systems, the removal of material is usually a very slow process but it is very steady and continuous. The generation and circulation of wear debris—particularly in machine applications where the clearances are small relative to the wear particle size—may be more of a problem than the actual amount of wear.

Wear includes six principal, quite distinct phenomena that have only one thing in common: the removal of solid material from rubbing surfaces. These are (1) adhesive; (2) abrasive; (3) fatigue; (4) impact by erosion or percussion; (5) corrosive; and (6) electrical arc–induced wear [Archard, 1980; Bhushan *et al.,* 1985a,b; Bhushan, 1990]. Other commonly encountered wear types are fretting and fretting corrosion. These are not distinct mechanisms, but rather combinations of the adhesive, corrosive, and abrasive forms of wear. According to some estimates, two-thirds of all wear encountered in industrial situations occurs because of adhesive- and abrasive-wear mechanisms.

Of the aforementioned wear mechanisms, one or more may be operating in one particular machinery. In many cases wear is initiated by one mechanism and results in other wear mechanisms, thereby complicating failure analysis.
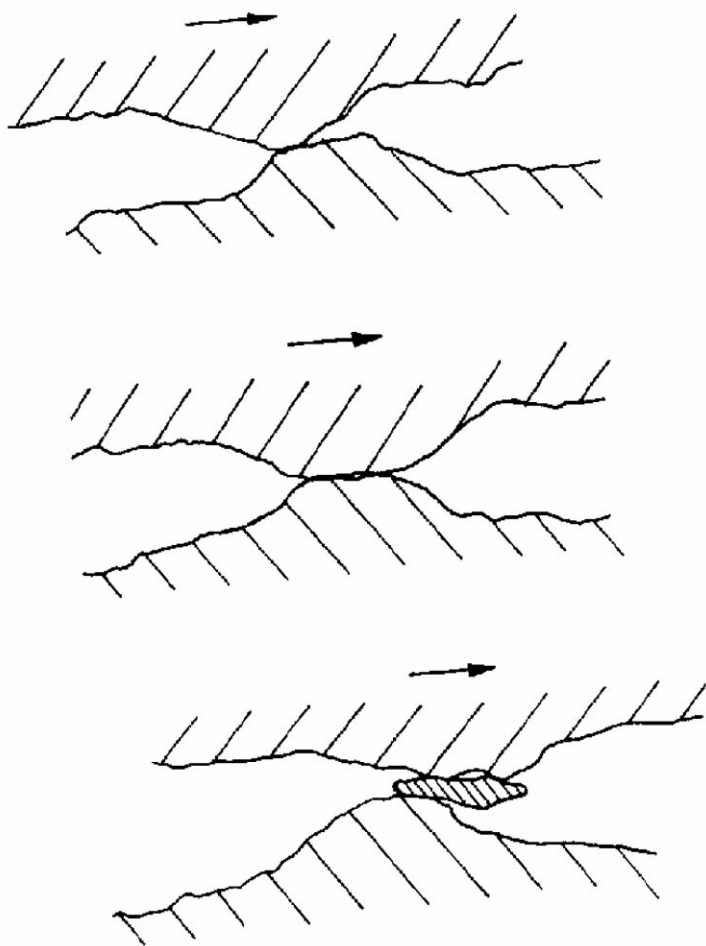
Adhesive Wear

Adhesive wear occurs when two nominally flat solid bodies are in rubbing contact, whether lubricated or not. Adhesion (or bonding) occurs at the asperity contacts on the interface, and fragments are pulled off one surface to adhere to the other surface. Subsequently, these fragments may come off the surface on which they are formed and either be transferred back to the original surface or form loose wear particles. Severe types of adhesive wear are often called *galling, scuffing, scoring,* or *smearing,* although these terms are sometimes used loosely to describe other types of wear.

Although the adhesive-wear theory can explain transferred wear particles, it does not explain how loose wear particles are formed. We now describe the actual process of formation of wear

particles. Asperity contacts are sheared by sliding and a small fragment of *either surface* becomes attached to the other surface. As sliding continues, the fragment constitutes a new asperity that becomes attached once more to the original surface. This transfer element is repeatedly passed from one surface to the other and grows quickly to a large size, absorbing many of the transfer elements so as to form a flakelike particle from materials of both rubbing elements. Rapid growth of this transfer particle finally accounts for its removal as a wear particle, as shown in Fig. 21.6. The occurrence of wear of the harder of the two rubbing surfaces is difficult to understand in terms of the adhesion theory. It is believed that the material transferred by adhesion to the harder surface may finally get detached by a fatigue process.

Figure 21.6 Schematic showing generation of wear particle as a result of adhesive wear mechanism.

As a result of experiments carried out with various unlubricated materials—the vast majority being metallic—it is possible to write the laws of adhesive wear, commonly referred to as Archard's law, as follows [Archard, 1953]. For plastic contacts,

$$V = kWx/H \qquad (21.5)$$

where V is the volume worn away, W is the normal load, x is the sliding distance, H is the hardness of the surface being worn away, and k is a nondimensional wear coefficient dependent on the materials in contact and their exact degree of cleanliness. The term k is usually interpreted as the probability that a wear particle is formed at a given asperity encounter.

Equation (21.5) suggests that the probability of a wear-particle formation increases with an increase in the real area of contact, A_r ($A_r = W/H$ for plastic contacts), and the sliding distance. For elastic contacts occurring in materials with a low modulus of elasticity and a very low surface roughness Eq. (21.5) can be rewritten for elastic contacts (Bhushan's law of adhesive wear) as [Bhushan, 1990]

$$V = k'Wx/E_c(\sigma_p/R_p)^{1/2} \qquad (21.6)$$

where k' is a nondimensional wear coefficient. According to this equation, elastic modulus and surface roughness govern the volume of wear. We note that in an elastic contact—though the normal stresses remain compressive throughout the entire contact—strong adhesion of some contacts can lead to generation of wear particles. Repeated elastic contacts can also fail by surface/subsurface fatigue. In addition, as the total number of contacts increases, the probability of a few plastic contacts increases, and the plastic contacts are specially detrimental from the wear standpoint.

Based on studies by Rabinowicz [1980], typical values of wear coefficients for metal on metal and nonmetal on metal combinations that are unlubricated (clean) and in various lubricated conditions are presented in Table 21.2. Wear coefficients and coefficients of friction for selected material combinations are presented in Table 21.3 [Archard, 1980].

Table 21.2 Typical Values of Wear Coefficients for Metal on Metal and Nonmetal on Metal Combinations

| Condition | Metal on Metal | | Nonmetal on Metal |
	Like	Unlike*	
Clean (unlubricated)	$1500 \cdot 10^{-6}$	15 to $500 \cdot 10^{-6}$	$1.5 \cdot 10^{-6}$
Poorly lubricated	300	3 to 100	1.5
Average lubrication	30	0.3 to 10	0.3
Excellent lubrication	1	0.03 to 0.3	0.03

*The values depend on the metallurgical compatibility (degree of solid solubility when the two metals are melted together). Increasing degree of incompatibility reduces wear, leading to higher value of the wear coefficients.

Table 21.3 Coefficient of Friction and Wear Coefficients for Various Materials in the Unlubricated Sliding

Materials				
Wearing Surface	Counter Surface	Vickers Microhardness (kg/mm²)	Coefficient of Friction	Wear Coefficient (k)
Mild steel	Mild steel	186	0.62	$7.0 \cdot 10^{-3}$
60/40 leaded brass	Tool steel	95	0.24	$6.0 \cdot 10^{-4}$
Ferritic stainless steel	Tool steel	250	0.53	$1.7 \cdot 10^{-5}$
Stellite	Tool steel	690	0.60	$5.5 \cdot 10^{-5}$
PTFE	Tool steel	5	0.18	$2.4 \cdot 10^{-5}$
Polyethylene	Tool steel	17	0.53	$1.3 \cdot 10^{-7}$
Tungsten carbide	Tungsten carbide	1300	0.35	$1.0 \cdot 10^{-6}$

Source: Archard, J. F. 1980. Wear theory and mechanisms. In *Wear Control Handbook,* ed. M. B. Peterson and W. O. Winer, pp. 35–80. ASME, New York.

Note: Load = 3.9 N; speed = 1.8 m/s. The stated value of the hardness is that of the softer (wearing) material in each example.

Abrasive Wear
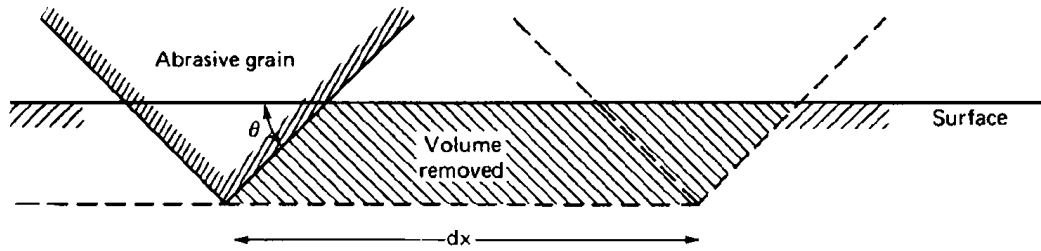
Abrasive wear occurs when a rough, hard surface slides on a softer surface and ploughs a series of grooves in it. The surface can be ploughed (plastically deformed) without removal of material. However, after the surface has been ploughed several times, material removal can occur by a low-cycle fatigue mechanism. Abrasive wear is also sometimes called *ploughing, scratching, scoring, gouging,* or *cutting,* depending on the degree of severity. There are two general situations for this type of wear. In the first case the hard surface is the harder of two rubbing surfaces (two-body abrasion), for example, in mechanical operations such as grinding, cutting, and machining. In the second case the hard surface is a third body, generally a small particle of grit or abrasive, caught between the two other surfaces and sufficiently harder that it is able to abrade either one or both of the mating surfaces (three-body abrasion), for example, in lapping and polishing. In many cases the wear mechanism at the start is adhesive, which generates wear debris that gets trapped at the interface, resulting in a three-body abrasive wear.

To derive a simple quantitative expression for abrasive wear, we assume a conical asperity on the hard surface (Fig. 21.7). Then the volume of wear removed is given as follows [Rabinowicz, 1965]:

$$V = kWx\,\overline{\tan\theta}/H \qquad (21.7)$$

where $\overline{\tan\theta}$ is a weighted average of the $\tan\theta$ values of all the individual cones and k is a factor that includes the geometry of the asperities and the probability that a given asperity cuts (removes) rather than ploughs. Thus, the roughness effect on the volume of wear is very distinct.

Figure 21.7 Abrasive wear model in which a cone removes material from a surface. (*Source:* Rabinowicz, E. 1965. *Friction and Wear of Materials.* John Wiley & Sons, New York. With permission.)

Fatigue Wear

Subsurface and surface fatigue are observed during repeated rolling and sliding, respectively. For pure rolling condition the maximum shear stress responsible for nucleation of cracks occurs some distance below the surface, and its location moves towards the surface with an application of the friction force at the interface. The repeated loading and unloading cycles to which the materials are exposed may induce the formation of subsurface or surface cracks, which eventually, after a critical number of cycles, will result in the breakup of the surface with the formation of large fragments, leaving large pits in the surface. Prior to this critical point, negligible wear takes place, which is in marked contrast to the wear caused by adhesive or abrasive mechanism, where wear causes a gradual deterioration from the start of running. Therefore, the amount of material removed by fatigue wear is not a useful parameter. Much more relevant is the useful life in terms of the number of revolutions or time before fatigue failure occurs. Time to fatigue failure is dependent on the amplitude of the reversed shear stresses, the interface lubrication conditions, and the fatigue properties of the rolling materials.

Impact Wear

Two broad types of wear phenomena belong in the category of impact wear: erosive and percussive wear. Erosion can occur by jets and streams of solid particles, liquid droplets, and implosion of bubbles formed in the fluid. Percussion occurs from repetitive solid body impacts. Erosive wear by impingement of solid particles is a form of abrasion that is generally treated rather differently because the contact stress arises from the kinetic energy of a particle flowing in an air or liquid stream as it encounters a surface. The particle velocity and impact angle combined with the size of the abrasive give a measure of the kinetic energy of the erosive stream. The volume of wear is proportional to the kinetic energy of the impinging particles, that is, to the square of the velocity.

Wear rate dependence on the impact angle differs between ductile and brittle materials. [Bitter, 1963].

When small drops of liquid strike the surface of a solid at high speeds (as low as 300 m/s), very high pressures are experienced, exceeding the yield strength of most materials. Thus, plastic deformation or fracture can result from a single impact, and repeated impact leads to pitting and erosive wear. Caviation erosion arises when a solid and fluid are in relative motion and bubbles formed in the fluid become unstable and implode against the surface of the solid. Damage by this process is found in such components as ships' propellers and centrifugal pumps.

Percussion is a repetitive solid body impact, such as experienced by print hammers in high-speed electromechanical applications and high asperities of the surfaces in a gas bearing (e.g., head-medium interface in magnetic storage systems). In most practical machine applications the impact is associated with sliding; that is, the relative approach of the contacting surfaces has both normal and tangential components known as *compound impact* [Engel, 1976].

Corrosive Wear

Corrosive wear occurs when sliding takes place in a corrosive environment. In the absence of sliding, the products of the corrosion (e.g., oxides) would form a film typically less than a micrometer thick on the surfaces, which would tend to slow down or even arrest the corrosion, but the sliding action wears the film away, so that the corrosive attack can continue. Thus, corrosive wear requires both corrosion and rubbing. Machineries operating in an industrial environment or near the coast generally corrode more rapidly than those operating in a clean environment. Corrosion can occur because of chemical or electrochemical interaction of the interface with the environment. Chemical corrosion occurs in a highly corrosive environment and in high temperature and high humidity environments. Electrochemical corrosion is a chemical reaction accompanied by the passage of an electric current, and for this to occur a potential difference must exist between two regions.

Electrical Arc-Induced Wear

When a high potential is present over a thin air film in a sliding process, a dielectric breakdown results that leads to arcing. During arcing, a relatively high-power density (on the order of 1 kW/mm^2) occurs over a very short period of time (on the order of 100 μs). The heat affected zone is usually very shallow (on the order of 50 μm). Heating is caused by the Joule effect due to the high power density and by ion bombardment from the plasma above the surface. This heating results in considerable melting, corrosion, hardness changes, other phase changes, and even the direct ablation of material. Arcing causes large craters, and any sliding or oscillation after an arc either shears or fractures the lips, leading to abrasion, corrosion, surface fatigue, and fretting. Arcing can thus initiate several modes of wear, resulting in catastrophic failures in electrical machinery [Bhushan and Davis, 1983].

Fretting and Fretting Corrosion

Fretting occurs where low-amplitude vibratory motion takes place between two metal surfaces loaded together [Anonymous, 1955]. This is a common occurrence because most machinery is subjected to vibration, both in transit and in operation. Examples of vulnerable components are shrink fits, bolted parts, and splines. Basically, fretting is a form of adhesive or abrasive wear where the normal load causes adhesion between asperities and vibrations cause ruptures, resulting in wear debris. Most commonly, fretting is combined with corrosion, in which case the wear mode is known as *fretting corrosion.*

21.5 Lubrication

Sliding between clean solid surfaces is generally characterized by a high coefficient of friction and severe wear due to the specific properties of the surfaces, such as low hardness, high surface energy, reactivity, and mutual solubility. Clean surfaces readily adsorb traces of foreign substances, such as organic compounds, from the environment. The newly formed surfaces generally have a much lower coefficient of friction and wear than the clean surfaces. The presence of a layer of foreign material at an interface cannot be guaranteed during a sliding process; therefore, lubricants are deliberately applied to produce low friction and wear. The term **lubrication** is applied to two different situations: solid lubrication and fluid (liquid or gaseous) film lubrication.

Solid Lubrication
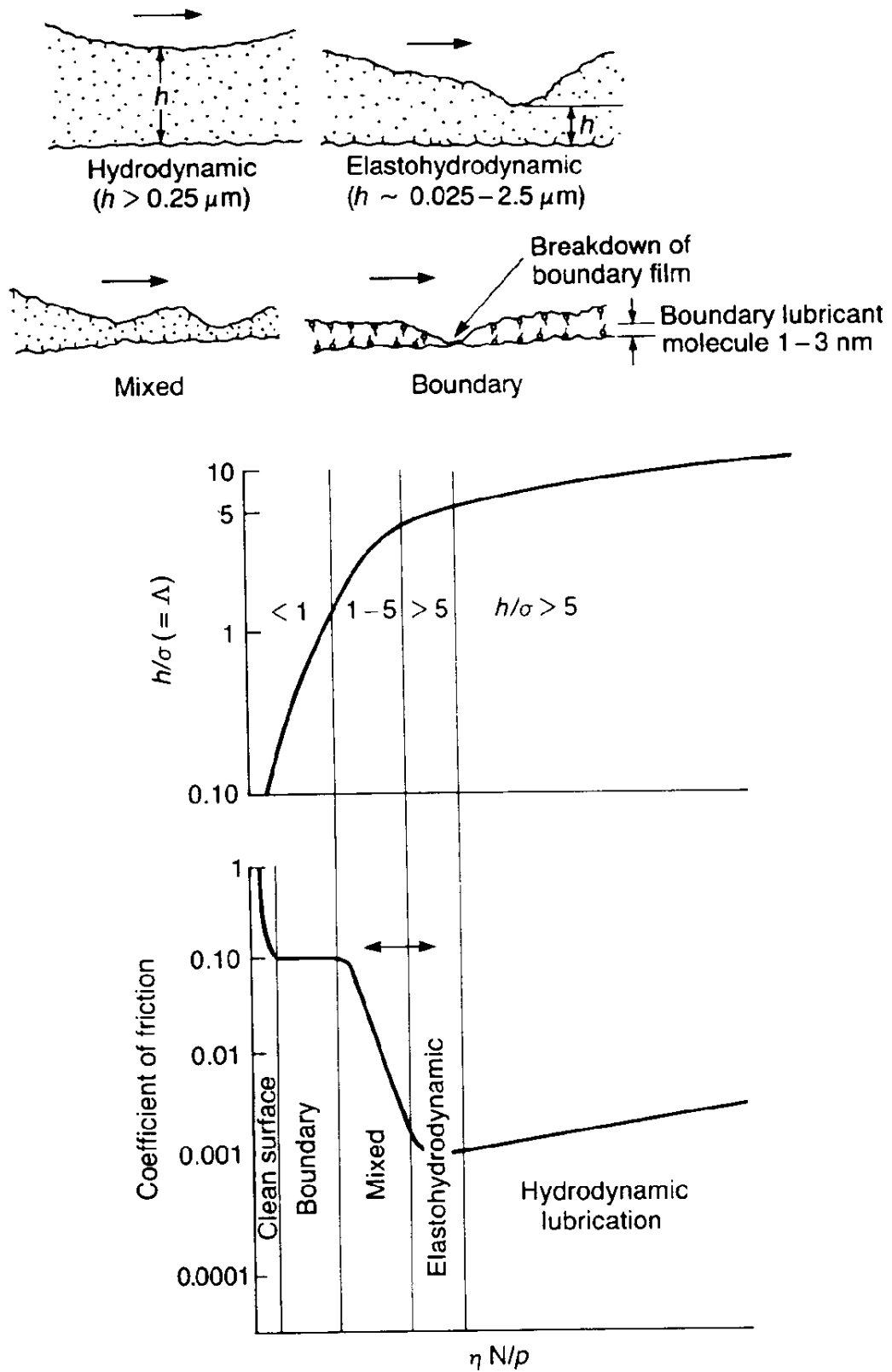
A solid lubricant is any material used in bulk or as a powder or a thin, solid film on a surface to provide protection from damage during relative movement to reduce friction and wear. Solid lubricants are used for applications in which any sliding contact occurs, for example, a bearing operative at high loads and low speeds and a hydrodynamically lubricated bearing requiring start/stop operations. The term *solid lubricants* embraces a wide range of materials that provide low friction and wear [Bhushan and Gupta, 1991]. Hard materials are also used for low wear under extreme operating conditions.

Fluid Film Lubrication

A regime of lubrication in which a thick fluid film is maintained between two sliding surfaces by an external pumping agency is called *hydrostatic lubrication.*

A summary of the lubrication regimes observed in fluid (liquid or gas) lubrication without an external pumping agency (self-acting) can be found in the familiar Stribeck curve in Fig. 21.8. This plot for a hypothetical fluid-lubricated bearing system presents the coefficient of friction as a function of the product of viscosity (η) and rotational speed (N) divided by the normal pressure (p). The curve has a minimum, which immediately suggests that more than one lubrication mechanism is involved. The regimes of lubrication are sometimes identified by a lubricant film parameter Λ equal to h/σ, which is mean film thickness divided by composite standard deviation of surface roughnesses. Descriptions of different regimes of lubrication follow [Booser, 1984; Bhushan, 1990].

Figure 21.8 Lubricant film parameter (Λ) and coefficient of friction as a function of $\eta N/p$ (Stribeck curve) showing different lubrication regimes observed in fluid lubrication without an external pumping agency. Schematics of interfaces operating in different lubrication regimes are also shown.

Hydrostatic Lubrication

Hydrostatic bearings support load on a thick film of fluid supplied from an external pressure source—a pump—which feeds pressurized fluid to the film. For this reason, these bearings are often called "externally pressurized." Hydrostatic bearings are designed for use with both incompressible and compressible fluids. Since hydrostatic bearings do not require relative motion of the bearing surfaces to build up the load-supporting pressures as necessary in hydrodynamic bearings, hydrostatic bearings are used in applications with little or no relative motion between the surfaces. Hydrostatic bearings may also be required in applications where, for one reason or another, touching or rubbing of the bearing surfaces cannot be permitted at startup and shutdown. In addition, hydrostatic bearings provide high stiffness. Hydrostatic bearings, however, have the disadvantage of requiring high-pressure pumps and equipment for fluid cleaning, which adds to space and cost.

Hydrodynamic Lubrication

Hydrodynamic (HD) lubrication is sometimes called *fluid-film* or *thick-film lubrication.* As a bearing with convergent shape in the direction of motion starts to spin (slide in the longitudinal direction) from rest, a thin layer of fluid is pulled through because of viscous entrainment and is then compressed between the bearing surfaces, creating a sufficient (hydrodynamic) pressure to support the load without any external pumping agency. This is the principle of hydrodynamic lubrication, a mechanism that is essential to the efficient functioning of the self-acting journal and thrust bearings widely used in modern industry. A high load capacity can be achieved in the bearings that operate at high speeds and low loads in the presence of fluids of high viscosity.

Fluid film can also be generated only by a reciprocating or oscillating motion in the normal direction (*squeeze*), which may be fixed or variable in magnitude (transient or steady state). This load-carrying phenomenon arises from the fact that a viscous fluid cannot be instantaneously squeezed out from the interface with two surfaces that are approaching each other. It takes time for these surfaces to meet, and during that interval—because of the fluid's resistance to extrusion—a pressure is built up and the load is actually supported by the fluid film. When the load is relieved or becomes reversed, the fluid is sucked in and the fluid film often can recover its thickness in time for the next application. The squeeze phenomenon controls the buildup of a water film under the tires of automobiles and airplanes on wet roadways or landing strips (commonly known as *hydroplaning*) that have virtually no relative sliding motion.

HD lubrication is often referred to as the ideal lubricated contact condition because the lubricating films are normally many times thicker (typically $5-500 \ \mu\mathrm{m}$) than the height of the irregularities on the bearing surface, and solid contacts do not occur. The coefficient of friction in the HD regime can be as small as 0.001 (Fig. 21.8). The friction increases slightly with the sliding speed because of viscous drag. The behavior of the contact is governed by the bulk physical properties of the lubricant, notable viscosity, and the frictional characteristics arise purely from the shearing of the viscous lubricant.

Elastohydrodynamic Lubrication

Elastohydrodynamic (EHD) lubrication is a subset of HD lubrication in which the elastic deformation of the bounding solids plays a significant role in the HD lubrication process. The film thickness in EHD lubrication is thinner (typically $0.5-2.5~\mu m$) than that in HD lubrication (Fig. 21.8), and the load is still primarily supported by the EHD film. In isolated areas, asperities may actually touch. Therefore, in liquid lubricated systems, boundary lubricants that provide boundary films on the surfaces for protection against any solid-solid contact are used. Bearings with heavily loaded contacts fail primarily by a fatigue mode that may be significantly affected by the lubricant. EHD lubrication is most readily induced in heavily loaded contacts (such as machine elements of low geometrical conformity), where loads act over relatively small contact areas (on the order of one-thousandth of journal bearing), such as the point contacts of ball bearings and the line contacts of roller bearings and gear teeth. EHD phenomena also occur in some low elastic modulus contacts of high geometrical conformity, such as seals and conventional journal and thrust bearings with soft liners.

Mixed Lubrication

The transition between the hydrodynamic/elastohydrodynamic and boundary lubrication regimes constitutes a gray area known as *mixed lubrication,* in which two lubrication mechanisms may be functioning. There may be more frequent solid contacts, but at least a portion of the bearing surface remains supported by a partial hydrodynamic film (Fig. 21.8). The solid contacts, if between unprotected virgin metal surfaces, could lead to a cycle of adhesion, metal transfer, wear particle formation, and snowballing into seizure. However, in liquid lubricated bearings, the physi- or chemisorbed or chemically reacted films (boundary lubrication) prevent adhesion during most asperity encounters. The mixed regime is also sometimes referred to as *quasihydrodynamic, partial fluid,* or *thin-film* (typically $0.5-2.5~\mu m$) *lubrication.*

Boundary Lubrication

As the load increases, speed decreases or the fluid viscosity decreases in the Stribeck curve shown in Fig. 21.8; the coefficient of friction can increase sharply and approach high levels (about 0.2 or much higher). In this region it is customary to speak of boundary lubrication. This condition can also occur in a starved contact. Boundary lubrication is that condition in which the solid surfaces are so close together that surface interaction between monomolecular or multimolecular films of lubricants (liquids or gases) and the solids dominate the contact. (This phenomenon does not apply to solid lubricants.) The concept is represented in Fig. 21.8, which shows a microscopic cross section of films on two surfaces and areas of asperity contact. In the absence of boundary lubricants and gases (no oxide films), friction may become very high (>1).

21.6 Micro/nanotribology

AFM/FFMs are commonly used to study engineering surfaces on micro- to nanoscales. These instruments measure the normal and friction forces between a sharp tip (with a tip radius of $30-100$ nm) and an engineering surface. Measurements can be made at loads as low as less than 1 nN and at scan rates up to about 120 Hz. A sharp AFM/ FFM tip sliding on a surface simulates a single asperity contact. FFMs are used to measure coefficient of friction on micro- to nanoscales

and AFMs are used for studies of surface topography, scratching/wear and boundary lubrication, mechanical property measurements, and nanofabrication/nanomachining [Bhushan and Ruan, 1994; Bhushan *et al.,* 1994; Bhushan and Koinkar, 1994a,b; Ruan and Bhushan, 1994; Bhushan, 1995; Bhushan *et al.,* 1995]. For surface roughness, friction force, nanoscratching and nanowear measurements, a microfabricated square pyramidal Si_3N_4 tip with a tip radius of about 30 nm is generally used at loads ranging from 10 to 150 nN. For microscratching, microwear, nanoindentation hardness measurements, and nanofabrication, a three-sided pyramidal single-crystal natural diamond tip with a tip radius of about 100 nm is used at relatively high loads ranging from 10 μN to 150 μN. Friction and wear on micro- and nanoscales are found to be generally smaller compared to that at macroscales. For an example of comparison of coefficients of friction at macro- and microscales see Table 21.4.

Table 21.4 Surface Roughness and Micro- and Macroscale Coefficients of Friction of Various Samples

Material	RMS Roughness,nm	Microscale Coefficient of Friction versus Si_3N_4 Tip[1]	Macroscale Coefficient of Friction versus Alumina Ball[2]	
			0.1 N	1 N
Si (111)	0.11	0.03	0.18	0.60
C^+-implanted Si	0.33	0.02	0.18	0.18

[1]Si_3N_4 tip (with about 50 nm radius) in the load range of 10–150 nN (1.5–3.8 GPa), a scanning speed of 4 μm/s and scan area of 1 μm $\times$ 1 μm .

[2]Alumina ball with 3-mm radius at normal loads of 0.1 and 1 N (0.23 and 0.50 GPa) and average sliding speed of 0.8 mm/s.

Defining Terms

Friction: The resistance to motion whenever one solid slides over another.

Lubrication: Materials applied to the interface to produce low friction and wear in either of two situations—solid lubrication or fluid (liquid or gaseous) film lubrication.

Micro/nanotribology: The discipline concerned with experimental and theoretical investigations of processes (ranging from atomic and molecular scales to microscales) occurring during adhesion, friction, wear, and lubrication at sliding surfaces.

Tribology: The science and technology of two interacting surfaces in relative motion and of related subjects and practices.

Wear: The removal of material from one or both solid surfaces in a sliding, rolling, or impact motion relative to one another.

References

Anonymous. 1955. Fretting and fretting corrosion. *Lubrication.* 41:85−96.

Archard, J. F. 1953. Contact and rubbing of flat surfaces. *J. Appl. Phys.* 24:981−988.

Archard, J. F. 1980. Wear theory and mechanisms. *Wear Control Handbook,* ed. M. B. Peterson and W. O. Winer, pp. 35−80. ASME, New York.

Avallone, E. A. and Baumeister, T., III. 1987. *Marks' Standard Handbook for Mechanical Engineers,* 9th ed. McGraw-Hill, New York.

Benzing, R., Goldblatt, I., Hopkins, V., Jamison, W., Mecklenburg, K., and Peterson, M. 1976. *Friction and Wear Devices,* 2nd ed. ASLE, Park Ridge, IL.

Bhushan, B. 1984. Analysis of the real area of contact between a polymeric magnetic medium and a rigid surface. *ASME J. Lub. Tech.* 106:26−34.

Bhushan, B. 1990. *Tribology and Mechanics of Magnetic Storage Devices.* Springer-Verlag, New York.

Bhushan, B. 1992. *Mechanics and Reliability of Flexible Magnetic Media.* Springer-Verlag, New York.

Bhushan, B. 1995. *Handbook of Micro/Nanotribology.* CRC Press, Boca Raton, FL.

Bhushan, B. and Davis, R. E. 1983. Surface analysis study of electrical-arc-induced wear. *Thin Solid Films.* 108:135−156.

Bhushan, B., Davis, R. E., and Gordon, M. 1985a. Metallurgical re-examination of wear modes. I: Erosive, electrical arcing and fretting. *Thin Solid Films.* 123:93−112.

Bhushan, B., Davis, R. E., and Kolar, H. R. 1985b. Metallurgical re-examination of wear modes. II: Adhesive and abrasive. *Thin Solid Films.* 123:113−126.

Bhushan, B. and Gupta, B. K. 1991. *Handbook of Tribology: Materials, Coatings, and Surface Treatments.* McGraw-Hill, New York.

Bhushan, B., Israelachvili, J. N., and Landman, U. 1995. Nanotribology: Friction, Wear and Lubrication at the Atomic Scale. *Nature.* 374:607−616.

Bhushan, B. and Koinkar, V. N. 1994a. Tribological studies of silicon for magnetic recording applications. *J. Appl. Phys.* 75:5741−5746.

Bhushan, B. and Koinkar, V. N. 1994b. Nanoindentation hardness measurements using atomic force microscopy. *Appl. Phys. Lett.* 64:1653−1655.

Bhushan, B., Koinkar, V. N., and Ruan, J. 1994. Microtribology of magnetic media. *Proc. Inst. Mech. Eng., Part J: J. Eng. Tribol.* 208:17−29.

Bhushan, B. and Ruan, J. 1994. Atomic-scale friction measurements using friction force microscopy: Part II— Application to magnetic media. *ASME J. Tribology.* 116:389−396.

Binnig, G., Quate, C. F., and Gerber, C. 1986. Atomic force microscope. *Phys. Rev. Lett.* 56:930−933.

Binnig, G., Rohrer, H., Gerber, C., and Weibel, E. 1982. Surface studies by scanning tunnelling microscopy. *Phys. Rev. Lett.* 49:57−61.

Bitter, J. G. A. 1963. A study of erosion phenomena. *Wear.* 6:5−21; 169−190.

Booser, E. R. 1984. *CRC Handbook of Lubrication,* vol. 2. CRC Press, Boca Raton, FL.

Bowden, F. P. and Tabor, D. 1950. *The Friction and Lubrication of Solids,* vols. I and II. Clarendon Press, Oxford.

Davidson, C. S. C. 1957. Bearing since the stone age. *Engineering.* 183:2−5.

Dowson, D. 1979. *History of Tribology.* Longman, London.

Engel, P. A. 1976. *Impact Wear of Materials.* Elsevier, Amsterdam.

Fuller, D. D. 1984. *Theory and Practice of Lubrication for Engineers,* 2nd ed. John Wiley & Sons, New York.

Georges, J. M., Millot, S., Loubet, J. L., and Tonck, A. 1993. Drainage of thin liquid films between relatively smooth surfaces. *J. Chem. Phys.* 98:7345−7360.

Georges, J. M., Tonck, A., and Mazuyer, D. 1994. Interfacial friction of wetted monolayers. *Wear.* 175:59−62.

Greenwood, J. A. and Williamson, J. B. P. 1966. Contact of nominally flat surfaces. *Proc. R. Soc. Lond.* A295:300−319.

Holm, R. 1946. *Electrical Contact.* Springer-Verlag, New York.

Israelachvili, J. N. and Adams, G. E. 1978. Measurement of friction between two mica surfaces in aqueous electrolyte solutions in the range 0−100 nm. *Chem. Soc. J., Faraday Trans. I.* 74:975−1001.

Jost, P. 1966. *Lubrication (Tribology)¾A Report on the Present Position and Industry's Needs.* Department of Education and Science, H.M. Stationary Office, London.

Jost, P. 1976. Economic impact of tribology. *Proc. Mechanical Failures Prevention Group.* NBS Special Pub. 423, Gaithersburg, MD.

Klein, J. 1980. Forces between mica surfaces bearing layers of adsorbed polystyrene in Cyclohexane. *Nature.* 288:248−250.

Layard, A. G. 1853. *Discoveries in the Ruins of Nineveh and Babylon,* I and II. John Murray, Albemarle Street, London.

Mate, C. M., McClelland, G. M., Erlandsson, R., and Chiang, S. 1987. Atomic-scale friction of a tungsten tip on a graphite surface. *Phys. Rev. Lett.* 59:1942− 1945.

Parish, W. F. 1935. Three thousand years of progress in the development of machinery and lubricants for the hand crafts. *Mill and Factory.* Vols. 16 and 17.

Peachey, J., Van Alsten, J., and Granick, S. 1991. Design of an apparatus to measure the shear response of ultrathin liquid films. *Rev. Sci. Instrum.* 62:463−473.

Petroff, N. P. 1883. Friction in machines and the effects of the lubricant. *Eng. J.* (in Russian; St. Petersburg) 71−140, 228−279, 377−436, 535−564.

Rabinowicz, E. 1965. *Friction and Wear of Materials.* John Wiley & Sons, New York.

Rabinowicz, E. 1980. Wear coefficients—metals. *Wear Control Handbook,* ed. M. B. Peterson and W. O. Winer, pp. 475−506. ASME, New York.

Reynolds, O. O. 1886. On the theory of lubrication and its application to Mr. Beauchamp Tower's experiments. *Phil. Trans. R. Soc.* (Lond.) 177:157 −234.

Ruan, J. and Bhushan, B. 1994. Atomic-scale and microscale friction of graphite and diamond using friction force microscopy. *J. Appl. Phys.* 76:5022−5035.

Tabor, D. and Winterton, R. H. S. 1969. The direct measurement of normal and retarded van der Waals forces. *Proc. R. Soc. Lond.* A312:435−450.

Tonck, A., Georges, J. M., and Loubet, J. L. 1988. Measurements of intermolecular forces and the rheology of dodecane between alumina surfaces. *J. Colloid Interf. Sci.* 126:1540−1563.

Tower, B. 1884. Report on friction experiments. *Proc. Inst. Mech. Eng.* 632.

Further Information

Major conferences:

> ASME/STLE Tribology Conference held every October in the U.S.
> Leeds-Lyon Symposium on Tribology held every year at Leeds, U.K., or Lyon, France (alternating locations).
> International Symposium on Advances in Information Storage and Processing Systems held annually at ASME International Congress and Exposition in November/December in the U.S.
> International Conference on Wear of Materials held every two years; next one to be held in 1995.
> Eurotrib held every four years; next one to be held in 1997.

Societies:

> Information Storage and Processing Systems Division, The American Society of Mechanical Engineers, New York.
> Tribology Division, The American Society of Mechanical Engineers, New York.
> Institution of Mechanical Engineers, London, U.K.
> Society of Tribologists and Lubrication Engineers, Park Ridge, IL.

Pennock, G. R. "Machine Elements"
The Engineering Handbook.
Ed. Richard C. Dorf
Boca Raton: CRC Press LLC, 2000

22

Machine Elements

Gordon R. Pennock
Purdue University

Section 22.1 presents a discussion of threaded fasteners, namely, the nut and bolt, the machine screw, the cap screw, and the stud. Equations are presented for the spring stiffness of the portion of a bolt, or a cap screw, within the clamped zone, which generally consists of the unthreaded shank portion and the threaded portion. Equations for the resultant bolt load and the resultant load on the members are also included in the discussion. The section concludes with a relation that provides an estimate of the torque that is required to produce a given preload. Section 22.2 presents a discussion of clutches and brakes and the important features of these machine elements. Various types of frictional-contact clutches and brakes are included in the discussion, namely, the radial, axial, disk, and cone types. Information on positive-contact clutches and brakes is also provided. The section includes energy considerations, equations for the temperature-rise, and the characteristics of a friction material.

22.1 Threaded Fasteners

The bolted joint with hardened steel washers is a common solution when a connection is required that can be easily disassembled (without destructive methods) and is strong enough to resist external tensile loads and shear loads. The clamping load, which is obtained by twisting the nut until the bolt is close to the elastic limit, stretches or elongates the bolt. This bolt tension will remain as the clamping force, or preload, providing the nut does not loosen. The preload induces compression in the members, which are clamped together, and exists in the connection after the nut has been properly tightened, even if there is no external load. Care must be taken to ensure that a bolted joint is properly designed and assembled [Blake, 1986]. When tightening the connection, the bolt head should be held stationary and the nut twisted. This procedure will ensure that the bolt shank will not experience the thread-friction torque. During the tightening process, the first thread on the nut tends to carry the entire load. However, yielding occurs with some strengthening due to the cold work that takes place, and the load is eventually distributed over about three nut threads. For this reason, it is recommended that nuts should not be reused; in fact, it can be dangerous if

this practice is adopted [Shigley and Mischke, 1989].

There are several styles of hexagonal nut, namely, (1) the general hexagonal nut, (2) the washer-faced regular nut, (3) the regular nut chamfered on both sides, (4) the jam nut with washer face, and (5) the jam nut chamfered on both sides. Flat nuts only have a chamfered top [Shigley and Mischke, 1986]. The material of the nut must be selected carefully to match that of the bolt. Carbon steel nuts are usually made to conform to ASTM A563 Grade A specifications or to SAE Grade 2. A variety of machine screw head styles also exist; they include (1) fillister head, (2) flat head, (3) round head, (4) oval head, (5) truss head, (6) binding head, and (7) hexagonal head (trimmed and upset). There are also many kinds of locknuts, which have been designed to prevent a nut from loosening in service. Spring and lock washers placed beneath an ordinary nut are also common devices to prevent loosening.

Another tension-loaded connection uses cap screws threaded into one of the members. Cap screws can be used in the same applications as nuts and bolts and also in situations where one of the clamped members is threaded. The common head styles of the cap screw include (1) hexagonal head, (2) fillister head, (3) flat head, and (4) hexagonal socket head. The head of a hexagon-head cap screw is slightly thinner than that of a hexagon-head bolt. An alternative to the cap screw is the stud, which is a rod threaded on both ends. Studs should be screwed into the lower member first, then the top member should be positioned and fastened down with hardened steel washers and nuts. The studs are regarded as permanent and the joint should be disassembled by removing only the nuts and washers. In this way, the threaded part of the lower member is not damaged by reusing the threads.

The grip of a connection is the total thickness of the clamped material [Shigley and Mischke, 1989]. In the bolted joint the grip is the sum of the thicknesses of both the members and the washers. In a stud connection the grip is the thickness of the top member plus that of the washer. The spring stiffness, or spring rate, of an elastic member such as a bolt is the ratio of the force applied to the member and the deflection caused by that force. The spring stiffness of the portion of a bolt, or cap screw, within the clamped zone generally consists of two parts, namely, (1) that of the threaded portion, and (2) that of the unthreaded shank portion. Therefore, the stiffness of a bolt is equivalent to the stiffness of two springs in series:

$$\frac{1}{k_b} = \frac{1}{k_T} + \frac{1}{k_d} \quad \text{or} \quad k_b = \frac{k_T k_d}{k_T + k_d} \qquad (22.1)$$

The spring stiffnesses of the threaded and unthreaded portions of the bolt in the clamped zone, respectively, are

$$k_T = \frac{A_t E}{L_T} \quad \text{and} \quad k_d = \frac{A_d E}{L_d} \qquad (22.2)$$

where A_t is the tensile-stress area, L_T is the length of the threaded portion in the grip, A_d is the major-diameter area of the fastener, L_d is the length of the unthreaded portion in the grip, and E is the modulus of elasticity. Substituting Eq. (22.2) into Eq. (22.1), the estimated effective stiffness of the bolt (or cap screw) in the clamped zone can be expressed as

$$k_b = \frac{A_t A_d E}{A_t L_d + A_d L_T} \qquad (22.3)$$

For short fasteners the unthreaded area is small and so the first of the expressions in Eq. (22.2) can be used to evaluate k_b. In the case of long fasteners the threaded area is relatively small, so the second expression in Eq. (22.2) can be used to evaluate the effective stiffness of the bolt. Expressions can also be obtained for the stiffness of the members in the clamped zone [Juvinall, 1983]. Both the stiffness of the fastener and the stiffness of the members in the clamped zone must be known in order to understand what happens when the connection is subjected to an external tensile load. There may of course be more than two members included in the grip of the fastener. Taken together the members act like compressive springs in series, and hence the total spring stiffness of the members is

$$\frac{1}{k_m} = \frac{1}{k_1} + \frac{1}{k_2} + \frac{1}{k_3} + \cdots \qquad (22.4)$$

If one of the members is a soft gasket, its stiffness relative to the other members is usually so small that for all practical purposes the other members can be neglected and only the gasket stiffness need be considered. If there is no gasket, the stiffness of the members is difficult to obtain, except by experimentation, because the compression spreads out between the bolt head and the nut and hence the area is not uniform. There are, however, some cases in which this area can be determined. Ultrasonic techniques have been used to determine the pressure distribution at the member interface in a bolt-flange assembly [Ito *et al.,* 1977]. The results show that the pressure stays high out to about 1.5 times the bolt radius and then falls off farther away from the bolt. Rotsher's pressure-cone method has been suggested for stiffness calculations with a variable cone angle. This method is quite complicated and a simpler approach is to use a fixed cone angle [Little, 1967].

Consider what happens when an external tensile load is applied to a bolted connection. Assuming that the preload has been correctly applied (by tightening the nut before the external tensile load is applied), the tensile load causes the connection to stretch through some distance. This elongation can be related to the stiffness of the bolts, or the members, by the equation

$$\delta = \frac{P_b}{k_b} = \frac{P_m}{k_m} \quad \text{or} \quad P_b = \frac{k_b}{k_m} P_m \qquad (22.5)$$

where P_b is the portion of the external tensile load P taken by the bolt and P_m is the portion of P taken by the members. Since the external tensile load P is equal to $P_b + P_m$,

$$P_b = \left(\frac{k_b}{k_b + k_m} \right) P \quad \text{and} \quad P_m = \left(\frac{k_m}{k_b + k_m} \right) P \qquad (22.6)$$

The resultant bolt load is $F_b = P_b + F_i$ and the resultant load on the members is $F_m = P_m - F_i$, where F_i is the preload. Therefore, the resultant bolt load can be written as

$$F_b = \left(\frac{k_b}{k_b + k_m} \right) P + F_i, \qquad F_m < 0 \qquad (22.7)$$

and the resultant load on the members can be written as

$$F_m = \left(\frac{k_m}{k_b + k_m} \right) P - F_i, \qquad F_m < 0 \qquad (22.8)$$

Equations (22.7) and (22.8) are only valid for the case when some clamping load remains in the members, which is indicated by the qualifier in the two equations. Making the grip longer causes the members to take an even greater percentage of the external load. If the external load is large enough to completely remove the compression, then the members will separate and the entire load will be carried by the bolts.

Since it is desirable to have a high preload in important bolted connections, methods of ensuring that the preload is actually developed when the parts are assembled must be considered. If the overall length of the bolt, L_b, can be measured (say with a micrometer) when the parts are assembled, then the bolt elongation due to the preload F_i can be computed from the relation

$$\delta = \frac{F_i L_b}{AE} \qquad (22.9)$$

where A is the cross-sectional area of the bolt. The nut can then be tightened until the bolt elongates through the distance δ, which ensures that the desired preload has been obtained. In many cases, however, it is not practical or possible to measure the bolt elongation. For example, the elongation of a screw cannot be measured if the threaded end is in a blind hole. In such cases the wrench torque that is required to develop the specified preload must be estimated. Torque wrenching, pneumatic-impact wrenching, or the **turn-of-the-nut method** can be used [Blake and Kurtz, 1965]. The torque wrench has a built-in dial that indicates the proper torque. With pneumatic-impact wrenching, the air pressure is adjusted so that the wrench stalls when the proper torque is obtained or, in some cases, the air shuts off automatically at the desired torque.

The **snug-tight condition** is defined as the tightness attained by a few impacts of an impact wrench or the full effort of a person using an ordinary wrench. When the snug-tight condition is attained, all additional turning develops useful tension in the bolt. The turn-of-the-nut method requires that fractional number of turns necessary to develop the required preload from the snug-tight condition be computed. For example, for heavy hexagon structural bolts, the turn-of-the-nut specification requires that under optimum conditions the nut should be turned a minimum of $180°$ from the snug-tight condition. A good estimate of the torque required to produce a given preload F_i can be obtained from the relation [Shigley and Mischke, 1989]

$$T = \frac{F_i d_m}{2} \left(\frac{L + \pi \mu d_m \sec \alpha}{\pi d_m - \mu L \sec \alpha} \right) + \frac{F_i \mu_c d_c}{2} \qquad (22.10)$$

where d_m is the mean diameter of the bolt, L is the lead of the thread, α is half the thread angle, μ_c is the coefficient of thread friction, μ_c is the coefficient of collar friction, and d_c is the mean collar diameter. The coefficients of friction depend upon the surface smoothness, the accuracy, and the degree of lubrication. Although these items may vary considerably, it is interesting to note that on the average both μ and μ_c are approximately 0.15.

22.2 Clutches and Brakes

A clutch is a coupling that connects two shafts rotating at different speeds and brings the output shaft smoothly and gradually to the same speed as the input shaft. Clutches and brakes are machine elements associated with rotation and have in common the function of storing or transferring rotating energy [Remling, 1983]. When the rotating members are caused to stop by means of a brake, the kinetic energy of rotation must be absorbed by the brake. In the same way, when the members of a machine that are initially at rest are brought up to speed, slipping must occur in the clutch until the driven members have the same speed as the driver. Kinetic energy is absorbed during slippage of either a clutch or a brake, and this energy appears in the form of heat. The important features in the performance of these devices are (1) the actuating force, (2) the transmitted torque, (3) the energy loss, and (4) the temperature rise. The torque that is transmitted is related to the actuating force, the coefficient of friction, and the geometry of the device. Essentially this is a problem in statics and can be studied separately for each geometric configuration. The rise in temperature, however, can be studied without regard to the type of device because the heat-dissipating surfaces are the geometry of interest. An approximate guide to the rise in temperature in a drum brake is the horsepower per square inch [Spotts, 1985].

The torque capacity of a clutch or brake depends upon the coefficient of friction of the material and a safe normal pressure. The character of the load may be such, however, that if this torque value is permitted, the clutch or brake may be destroyed by the generated heat. Therefore, the capacity of a clutch is limited by two factors: (a) the characteristics of the material, and (b) the ability of the clutch to dissipate the frictional heat. The temperature rise of a clutch or brake assembly can be approximated by the relation

$$\Delta T = \frac{H}{CW} \qquad (22.11)$$

where ΔT is in $°F$, H is the heat generated in Btu, C is the specific heat in Btu/(lbm $°F$), and W is the mass of the clutch or brake assembly in lbm. If SI units are used, then

$$\Delta T = \frac{E}{Cm} \qquad (22.12)$$

where ΔT is in $°C$, E is the total energy dissipated during the clutching operation or the braking cycle in J, C is in J/kg $°C$, and m is the mass of the clutch or brake assembly in kg. Equation (22.11) or (22.12) can be used to explain what happens when a clutch or a brake is operated. However, there are so many variables involved that it is most unlikely that the analytical results

would approximate experimental results. For this reason such analyses are only useful, for repetitive cycling, in pinpointing the design parameters that have the greatest effect on performance.

The friction material of a clutch or brake should have the following characteristics, to a degree that is dependent upon the severity of the service: (a) a high and uniform coefficient of friction, (b) imperviousness to environmental conditions, such as moisture, (c) the ability to withstand high temperatures, as well as a good heat conductivity, (d) good resiliency, and (e) high resistance to wear, scoring, and galling. The manufacture of friction materials is a highly specialized process, and the selection of a friction material for a specific application requires some expertise. Selection involves a consideration of all the characteristics of a friction material as well as the standard sizes that are available. The woven-cotton lining is produced as a fabric belt, which is impregnated with resins and polymerized. It is mostly used in heavy machinery and can be purchased in rolls up to 50 feet in length. The thicknesses that are available range from 0.125 to 1 in. and the width may be up to 12 in. A woven-asbestos lining is similar in construction to the cotton lining and may also contain metal particles. It is not quite as flexible as the cotton lining and comes in a smaller range of sizes. The woven-asbestos lining is also used as a brake material in heavy machinery.

Molded-asbestos linings contain asbestos fiber and friction modifiers; a thermoset polymer is used, with heat, to form a rigid or a semirigid molding. The principal use is in drum brakes. Molded-asbestos pads are similar to molded linings but have no flexibility; they are used for both clutches and brakes. Sintered-metal pads are made of a mixture of copper and/or iron particles with friction modifiers, molded under high pressure and then heated to a high temperature to fuse the material. These pads are used in both brakes and clutches for heavy-duty applications. Cermet pads are similar to the sintered-metal pads and have a substantial ceramic content. Typical brake linings may consist of a mixture of asbestos fibers to provide strength and ability to withstand high temperatures; various friction particles to obtain a degree of wear resistance and higher coefficient of friction; and bonding materials. Some clutch friction materials may be run wet by allowing them to dip in oil or to be sprayed by oil. This reduces the coefficient of friction, but more heat can be transferred and higher pressure can be permitted.

The two most common methods of coupling are the frictional-contact clutch and the positive-contact clutch. Other methods include the overrunning or freewheeling clutch, the magnetic clutch, and the fluid coupling. In general, the types of frictional-contact clutches and brakes can be classified as rim type or axial type [Marks, 1987]. The analysis of all types of frictional-clutches and brakes follows the same general procedure, namely, (a) determine the pressure distribution on the frictional surfaces, (b) find a relation between the maximum pressure and the pressure at any point, and (c) apply the conditions of static equilibrium to find the actuating force, the torque transmitted, and the support reactions. The analysis is useful when the dimensions are known and the characteristics of the friction material are specified. In design, however, synthesis is of more interest than analysis. Here the aim is to select a set of dimensions that will provide the best device within the limitations of the frictional material that is specified by the designer [Proctor, 1961].

Rim-Type Clutches and Brakes
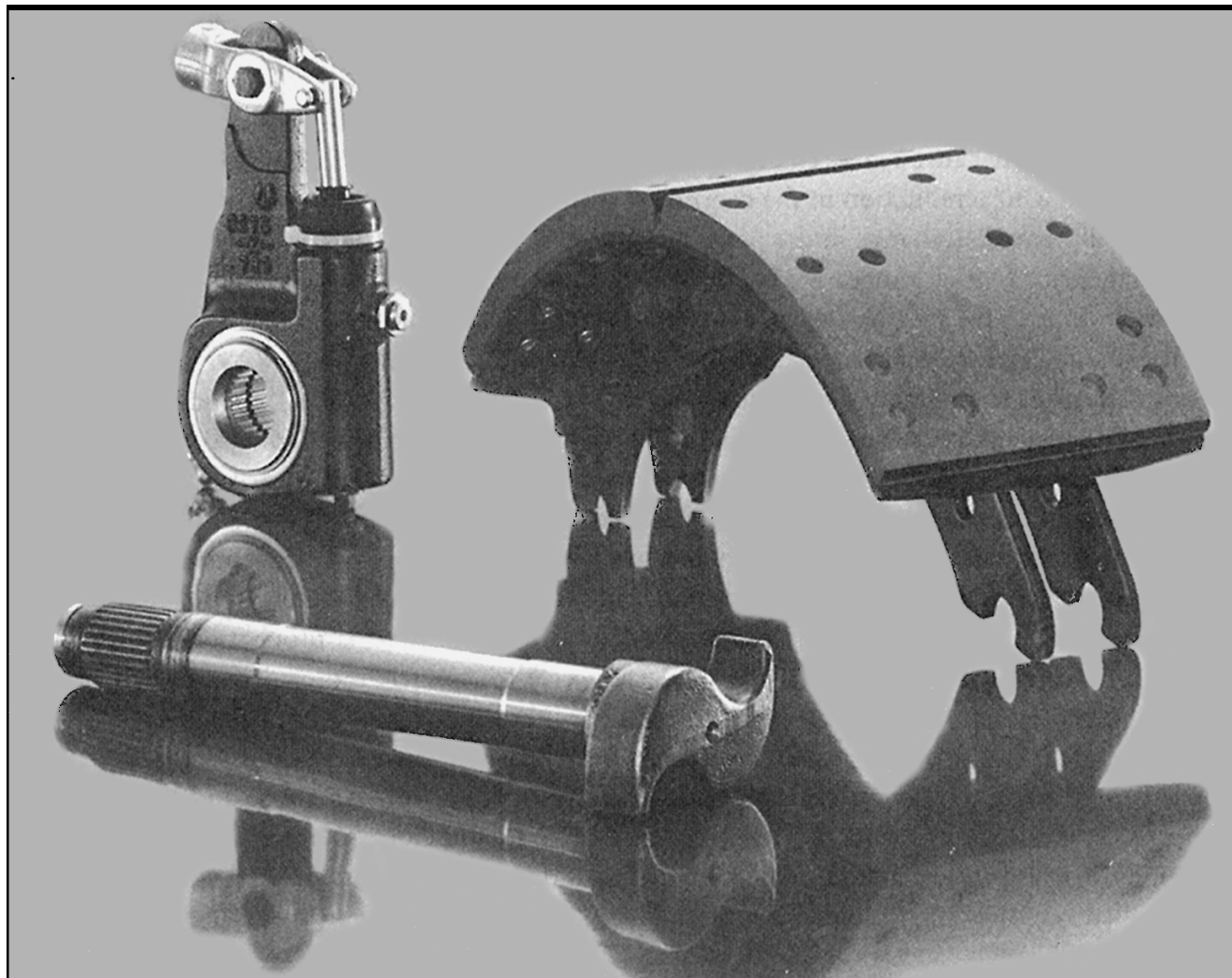
The rim-type brake can be designed for **self-energizing,** that is, using friction to reduce the actuating force. Self-energization is important in reducing the required braking effort; however, it also has a disadvantage. When rim-type brakes are used as vehicle brakes, a small change in the coefficient of friction will cause a large change in the pedal force required for braking. For example, it is not unusual for a 30% reduction in the coefficient of friction (due to a temperature change or moisture) to result in a 50% change in the pedal force required to obtain the same braking torque that was possible prior to the change.

The rim types may have internal expanding shoes or external contracting shoes. An internal shoe clutch consists essentially of three elements: (1) a mating frictional surface, (2) a means of transmitting the torque to and from the surfaces, and (3) an actuating mechanism. Depending upon the operating mechanism, such clutches can be further classified as expanding-ring, centrifugal, magnetic, hydraulic, or pneumatic. The expanding-ring clutch benefits from centrifugal effects, transmits high torque even at low speeds, and requires both positive engagement and ample release force. This type of clutch is often used in textile machinery, excavators, and machine tools in which the clutch may be located within the driving pulley. The centrifugal clutch is mostly used for automatic operation. If no spring is present, the torque transmitted is proportional to the square of the speed [Beach, 1962]. This is particularly useful for electric motor drives in which, during starting, the driven machine comes up to speed without shock. Springs can be used to prevent engagement until a certain motor speed has been reached, but some shock may occur. Magnetic clutches are particularly useful for automatic and remote-control systems and are used in drives subject to complex load cycles. Hydraulic and pneumatic clutches are useful in drives having complex loading cycles, in automatic machinery, and in manipulators. Here the fluid flow can be controlled remotely using solenoid valves. These clutches are available as disk, cone, and multiple-plate clutches.

In braking systems the internal-shoe or drum brake is used mostly for automotive applications. The actuating force of the device is applied at the end of the shoe away from the pivot. Since the shoe is usually long, the distribution of the normal forces cannot be assumed to be uniform. The mechanical arrangement permits no pressure to be applied at the heel; therefore, frictional material located at the heel contributes very little to the braking action. It is standard practice to omit the friction material for a short distance away from the heel, which also eliminates interference. In some designs the hinge pin is allowed to move to provide additional heel pressure. This gives the effect of a floating shoe. A good design concentrates as much frictional material as possible in the neighborhood of the point of maximum pressure. Typical assumptions made in an analysis of the shoe include the following: (1) the pressure at any point on the shoe is proportional to the distance from the hinge pin (zero at the heel); (2) the effect of centrifugal force is neglected (in the case of brakes, the shoes are not rotating and no centrifugal force exists; in clutch design, the effect of this force must be included in the equations of static equilibrium); (3) the shoe is rigid (in practice, some deflection will occur depending upon the load, pressure, and stiffness of the shoe; therefore, the resulting pressure distribution may be different from the assumed distribution); and (4) the entire analysis is based upon a coefficient of friction that does not vary with pressure. Actually, the coefficient may vary with a number of conditions, including temperature, wear, and the environment.

For pivoted external shoe brakes and clutches, the operating mechanisms can be classified as

solenoids, levers, linkages or toggle devices, linkages with spring loading, hydraulic devices, and pneumatic devices. It is common practice to concentrate on brake and clutch performance without the extraneous influences introduced by the need to analyze the statics of the control mechanisms. The moments of the frictional and normal forces about the hinge pin are the same as for the internal expanding shoes. It should be noted that when external contracting designs are used as clutches, the effect of the centrifugal force is to decrease the normal force. Therefore, as the speed increases, a larger value of the actuating force is required. A special case arises when the pivot is symmetrically located and also placed so that the moment of the friction forces about the pivot is zero.

AFTERMARKET BRAKE PRODUCTS

The genuine OEM quality brake replacement parts by Rockwell are the exact components that are used for new vehicles' original equipment. Shown above are non-asbestos lined brake shoes, automatic slack adjusters, and cold-rolled 28-tooth spline camshafts. Rockwell genuine replacement parts are reliable and offer long-lasting quality. Other original OEM aftermarket brake

products include major and minor overhaul kits, unlined brake shoes, manual slack adjusters, a variety of s-cam shafts, and air dryers. (Photo courtesy of Rockwell Automotive.)

Axial-Type Clutches and Brakes

In an axial clutch the mating frictional members are moved in a direction parallel to the shaft. One of the earliest axial clutches was the cone clutch, which is simple in construction and, yet, quite powerful. Except for relatively simple installations, however, it has been largely replaced by the disk clutch, which employs one or more disks as the operating members. Advantages of the disk clutch include (1) no centrifugal effects, (2) a large frictional area that can be installed in a small space, (3) more effective heat dissipation surfaces, and (4) a favorable pressure distribution. There are two methods in general use to obtain the axial force necessary to produce a certain torque and pressure (depending upon the construction of the clutch). The two methods are (1) uniform wear, and (2) uniform pressure. If the disks are rigid then the greatest amount of wear will first occur in the outer areas, since the work of friction is greater in those areas. After a certain amount of wear has taken place, the pressure distribution will change so as to permit the wear to be uniform. The greatest pressure must occur at the inside diameter of the disk in order for the wear to be uniform. The second method of construction employs springs to obtain a uniform pressure over the area.

Disk Clutches and Brakes

There is no fundamental difference between a disk clutch and a disk brake [Gagne, 1953]. The disk brake has no self-energization and, hence, is not as susceptible to changes in the coefficient of friction. The axial force can be written as

$$F_a = 0.5\pi p D_1 (D_2 - D_1) \qquad (22.13)$$

where p is the maximum pressure, and D_1 and D_2 are the inner and outer diameters of the disk, respectively. The torque transmitted can be obtained from the relation

$$T = 0.5\mu F_a D_m \qquad (22.14)$$

where μ is the coefficient of friction of the clutch material, and the mean diameter

$$D_m = 0.5(D_2 + D_1) \quad \text{or} \quad D_m = \frac{2(D_2^3 - D_1^3)}{3(D_2^2 - D_1^2)} \qquad (22.15)$$

for uniform wear or for uniform pressure distribution, respectively.

A common type of disk brake is the floating caliper brake. In this design the caliper supports a single floating piston actuated by hydraulic pressure. The action is much like that of a screw

clamp, with the piston replacing the function of the screw. The floating action also compensates for wear and ensures an almost constant pressure over the area of the friction pads. The seal and boot are designed to obtain clearance by backing off from the piston when the piston is released.

Cone Clutches and Brakes

A cone clutch consists of (1) a cup (keyed or splined to one of the shafts), (2) a cone that slides axially on the splines or keys on the mating shaft, and (3) a helical spring to hold the clutch in engagement. The clutch is disengaged by means of a fork that fits into the shifting groove on the friction cone. The axial force, in terms of the clutch dimensions, can be written as

$$F_a = \pi D_m pb \sin \alpha \qquad (22.16)$$

where p is the maximum pressure, b is the face width of the cone, D_m is the mean diameter of the cone, and α is one-half the cone angle in degrees. The mean diameter can be approximated as $0.5(D_2 + D_1)$. The torque transmitted through friction can be obtained from the relation

$$T = \frac{\mu F_a D_m}{2 \sin \alpha} \qquad (22.17)$$

The cone angle, the face width of the cone, and the mean diameter of the cone are the important geometric design parameters. If the cone angle is too small, say, less than about $8°$, the force required to disengage the clutch may be quite large. The wedging effect lessens rapidly when larger cone angles are used. Depending upon the characteristics of the friction materials, a good compromise can usually be found using cone angles between $10°$ and $15°$. For clutches faced with asbestos, leather, or a cork insert, a cone angle of $12.5°$ is recommended.

Positive-Contact Clutches

A positive-contact clutch does not slip, does not generate heat, cannot be engaged at high speeds, sometimes cannot be engaged when both shafts are at rest, and, when engaged at any speed, is accompanied by shock. The greatest differences among the various types of positive-contact clutches are concerned with the design of the jaws. To provide a longer period of time for shift action during engagement, the jaws may be ratchet shaped, spiral shaped, or gear-tooth shaped. The square-jaw clutch is another common form of a positive-contact clutch. Sometimes a great many teeth or jaws are used, and they may be cut either circumferentially, so that they engage by cylindrical mating or on the faces of the mating elements. Positive-contact clutches are not used to the same extent as the frictional-contact clutches.

Defining Terms

Snug-tight condition: The tightness attained by a few impacts of an impact wrench, or the full effort of a person using an ordinary wrench.

Turn-of-the-nut method: The fractional number of turns necessary to develop the required preload from the snug-tight condition.

Self-energizing: A state in which friction is used to reduce the necessary actuating force. The design should make good use of the frictional material because the pressure is an allowable maximum at all points of contact.

Self-locking: When the friction moment assists in applying the brake shoe, the brake will be self-locking if the friction moment exceeds the normal moment. The designer must select the dimensions of the clutch, or the brake, to ensure that self-locking will not occur unless it is specifically desired.

Fail-safe and dead-man: These two terms are often encountered in studying the operation of clutches and brakes. Fail-safe means that the operating mechanism has been designed such that, if any element should fail to perform its function, an accident will not occur in the machine or befall the operator. Dead-man, a term from the railroad industry, refers to the control mechanism that causes the engine to come to a stop if the operator should suffer a blackout or die at the controls.

References

Beach, K. 1962. Try these formulas for centrifugal clutch design. *Product Eng.* 33(14): 56−57.

Blake, A. 1986. *What Every Engineer Should Know about Threaded Fasteners: Materials and Design,* p. 202. Marcel Dekker, New York.

Blake, J. C. and Kurtz, H. J. 1965. The uncertainties of measuring fastener preload. *Machine Design.* 37(23): 128−131.

Gagne, A. F., Jr. 1953. Torque capacity and design of cone and disk clutches. *Product Eng.* 24(12): 182−187.

Ito, Y., Toyoda, J., and Nagata, S. 1977. Interface pressure distribution in a bolt-flange assembly. *Trans. ASME.* Paper No. 77-WA/DE-11, 1977.

Juvinall, R. C. 1983. *Fundamentals of Machine Component Design,* p. 761. John Wiley & Sons, New York.

Little, R. E. 1967. Bolted joints: How much give? *Machine Design.* 39(26): 173−175.

Marks, L. S. 1987. *Marks' Standard Handbook for Mechanical Engineers,* 9th ed. McGraw-Hill, New York.

Proctor, J. 1961. Selecting clutches for mechanical drives. *Product Eng.* 32(25): 43−58.

Remling, J. 1983. *Brakes,* 2nd ed., p. 328. John Wiley & Sons, New York.

Shigley, J. E. and Mischke, C. R. 1986. *Standard Handbook of Machine Design.* McGraw-Hill, New York.

Shigley, J. E. and Mischke, C. R. 1989. *Mechanical Engineering Design,* 5th ed., p. 779. McGraw-Hill, New York.

Spotts, M. F. 1985. *Design of Machine Elements,* 6th ed., p. 730. Prentice Hall, Englewood Cliffs, NJ.

Further Information

ASME Publications Catalog. 1985. *Codes and Standards: Fasteners.* American Society of Mechanical Engineers, New York.

Bickford, J. H. 1981. *An Introduction to the Design and Behavior of Bolted Joints,* p. 443. Marcel Dekker, New York.

Burr, A. H. 1981. *Mechanical Analysis and Design,* p. 640. Elsevier Science, New York.

Crouse, W. H. 1971. *Automotive Chassis and Body,* 4th. ed., pp. 262−299. McGraw-Hill, New York.

Fazekas, G. A. 1972. On circular spot brakes. *Journal of Engineering for Industry, Transactions of ASME,* vol. 94, series B, no. 3, August 1972, pp. 859−863.

Ferodo, Ltd. 1968. *Friction Materials for Engineers.* Chapel-en-le-Frith, England.

Fisher, J. W. and Struik, J. H. A. 1974. *Guide to Design Criteria for Bolted and Riveted Joints,* p. 314. John Wiley & Sons, New York.

ISO Metric Screw Threads. 1981. Specifications BS 3643: Part 2, p. 10. British Standards Institute, London.

Lingaiah, K. 1994. *Machine Design Data Handbook.* McGraw-Hill, New York.

Matthews, G. P. 1964. *Art and Science of Braking Heavy Duty Vehicles.* Special Publication SP-251, Society of Automotive Engineers, Warrendale, PA.

Motosh, N. 1976. Determination of joint stiffness in bolted connections. *Journal of Engineering for Industry, Transactions of ASME,* vol. 98, series B, no. 3, August 1976, pp. 858−861.

Neale, M. J. (ed.), 1973. *Tribology Handbook.* John Wiley & Sons, New York.

Osgood, C. C. 1979. Saving weight in bolted joints. *Machine Design,* vol. 51, no. 24, 25 October 1979, pp. 128−133.

Rodkey, E. 1977. Making fastened joints reliable—ways to keep 'em tight. *Assembly Engineering,* March 1977, pp. 24−27.

Screw Threads. 1974. ANSI Specification B1.1-1974, p. 80. American Society of Mechanical Engineers, New York.

Viglione, J. 1965. Nut design factors for long bolt life. *Machine Design,* vol. 37, no. 18, 5 August 1965, pp. 137−141.

Wong, J. Y. 1993. *Theory of Ground Vehicles,* 2nd ed., p. 435. John Wiley & Sons, New York.

Dedication

This article is dedicated to the late Professor Joseph Edward Shigley who authored and coauthored several outstanding books on engineering design. The Standard Handbook of Machine Design and the Mechanical Engineering Design text (both with C. R. Mischke, see the references above) are widely used and strongly influenced the direction of this article.

Subramanyan, P. K. "Crankshaft Journal Bearings"
The Engineering Handbook.
Ed. Richard C. Dorf
Boca Raton: CRC Press LLC, 2000

23

Crankshaft Journal Bearings

P. K. Subramanyan
Glacier Clevite Heavywall Bearings

In modern internal combustion engines, there are two kinds of bearings in the category of crankshaft journal bearings—namely, the main bearings and the connecting rod bearings. Basically, these are wraparound, semicylindrical shell bearings. Two of them make up a set and, depending on the position in the assembly, one is called the upper and the other the lower bearing. They are of equal sizes. The main bearings support the crankshaft of the engine and the forces transmitted to the crankshaft from the cylinders. The connecting rod bearings (or, simply, rod bearings) are instrumental in transferring the forces from the cylinders of the internal combustion engine to the crankshaft. These connecting rod bearings are also called big end bearings or crank pin bearings. Supporting the crankshaft and transferring the pressure-volume work from the cylinders to the pure rotational mechanical energy of the crankshaft are accomplished elegantly with minimal energy loss by shearing a suitable lubricating medium between the bearings and the journals. The segment of the crankshaft within the bounds of a set of bearings, whether main bearings or rod bearings, is called the journal. Consequently, these bearings are called journal bearings.

23.1 Role of the Journal Bearings in the Internal Combustion Engine

The crankshafts of internal combustion engines of sizes from small automotive to large slow-speed engines run at widely varying rpm (e.g., 72 to 7700). When the internal combustion engine

continues to run after the start-up, the crankshaft, including the crank pins, is suspended in the lubricating oil—a fluid of very low friction. In such a condition, it is conceivable that precision-machined, semicylindrical steel shells can function as good bearings. However, there are stressful conditions, particularly in the case of automotive, truck, and medium-speed engines, when the crankshaft remains in contact with the bearings and there is little or no lubricating oil present. This condition corresponds to the initial and subsequent start-ups. The oil pump is driven directly by the engine and it takes several revolutions of the crankshaft before a good oil film is developed, as shown in Fig. 23.1, so that the journals are completely lifted and suspended. During the revolutions prior to the formation of a sufficiently thick oil film, the journal contacts the bearing surface. In such situations, the bearings provide sufficient lubrication to avoid scuffing and **seizure.** Another stressful situation, but not as critical as the start-up, is the slowing down and shutting off of the engine when the oil film reduces to a **boundary layer.**

Figure 23.1 Schematic representation of the hydrodynamic lubricant film around a rotating journal in its bearing assembly. (*Source:* Slaymaker, R. R. 1955. *Bearing Lubrication Analysis.* John Wiley & Sons, New York. With permission.)

In the case of slow-speed engines, the oil pump, which is electrically driven, is turned on to prelubricate the bearings. This provides some lubrication. Nonetheless, bearings with liners and overlays are used to avoid seizure, which can result in costly damage.

Essentially, the function of journal bearings can be stated as follows:Development of the **hydrodynamic lubricating oil films** in the journal bearings lifts the journals from the surfaces of the bearings and suspends the entire crankshaft on the oil films by the journals. [Theoretical aspects of this will be considered later.] The lifting of the crankshaft or, equivalently, lifting of the journals is in the range of 30 to 1000 micro-inch in the entire range of IC engines. This process
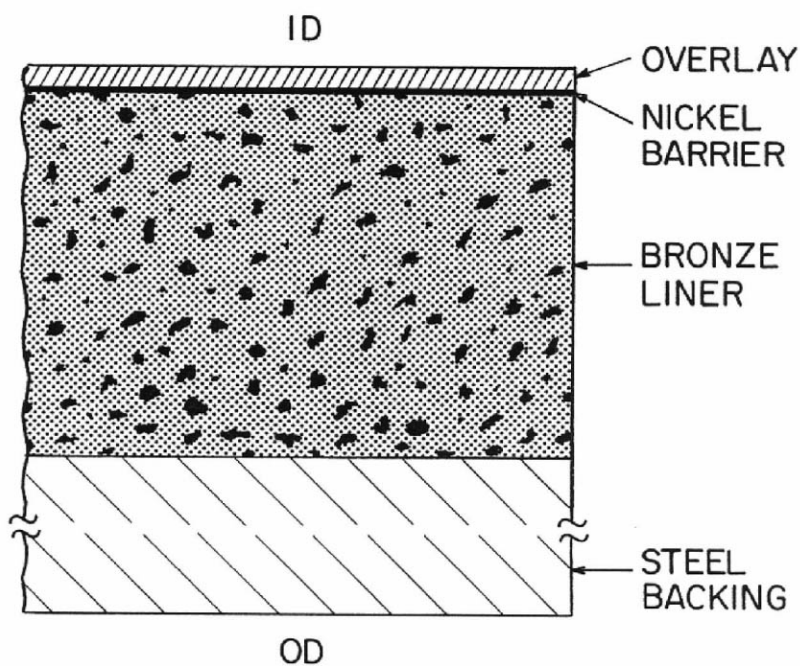
allows the crankshaft to rotate with minimal energy loss. The journal bearings make it possible so that the internal combustion engine can be started, utilized, and stopped as many times as needed.

23.2 Construction of Modern Journal Bearings

The majority of modern crankshaft journal bearings have three different layers of metallic materials with distinct characteristics and functions. Conventionally, these are called trimetal bearings. The remaining bearings belong to the class of bimetal bearings and have two different metallic material layers. Bimetallic bearings are becoming very popular in the automotive industry.

All crankshaft journal bearings have a steel backing, normally of low-carbon steels. Steel backing is the thickest layer in the bearing. The next layer bonded to the steel backing is the bearing liner. This is the layer that supports the load and determines the life of the bearing. The third layer bonded to the bearing liner is the overlay. Generally, this is a precision electrodeposited layer of (1) lead, tin, and copper, (2) lead and tin, or (3) lead and indium. A very thin electrodeposited layer of nickel (0.000 05 in.) is used as a bonding layer between the liner and the lead-tin-copper overlay. This nickel layer is considered a part of the overlay, not a separate layer. Construction of a trimetal bronze bearing is illustrated in Fig. 23.2.

Figure 23.2 Schematic representation of the construction of a trimetal bearing.

There are two classes of bearing liners in widespread use nowadays. These are the leaded bronzes and aluminum-based (frequently precipitation-strengthened) materials, such as aluminum-tin and aluminum-silicon. Bimetallic bearings have the advantage of being slightly more precise (about 0.0002 to 0.0003 in.) than the trimetal bearings. The bimetal bearings have a bored or broached internal diametral (ID) surface. The electrodeposited layer in the trimetal bearings is applied onto the bored or broached surface. The nickel bonding layer is applied first onto the liner, followed by the deposition of the lead-tin-copper overlay. The electrodeposited overlay introduces a certain degree of variation in the wall thickness of the bearings. In a limited application, babbitt overlays are centrifugally cast on bronze liners for slow-speed diesel engine journal bearings.

Another class of bearings is the single layer solid metal bearings—namely, solid bronze and solid aluminum bearings. These bearings are not generally used as crankshaft journal bearings. However, solid aluminum is used in some of the medium-speed and slow-speed diesel engines.

The most popular copper-tin-based leaded bearing liner in current use has 2 to 4% tin, 23 to 27% lead, and 69 to 75% copper (all by weight). This material is applied directly on mild steel by casting or sintering. The aluminum materials are roll-bonded to steel. The material as such is produced by powder rolling as a strip or by casting and rolling.

23.3 The Function of the Different Material Layers in Crankshaft Journal Bearings

The bulk of modern crankshaft journal bearings is mild steel (1008 to 1026 low-carbon steels). This is the strongest of the two or three layers in the bearing. It supports the bearing liner, with or without the overlay. The bearing liner derives a certain degree of strength from the steel backing. The function of the steel backing is to carry the bearing liner, which on its own is weaker, much thinner, and less ductile. With the support of the steel backing, the bearings can be seated with a high degree of conformance and good interference fit in the housing bore (steel against steel).

The bearing liners in automotive and truck bearings have a thickness in the range of 0.006 to 0.030 in. In the case of the medium-speed and slow-speed engines, the thickness of the liner ranges from 0.010 to 0.080 in. The liner material contains sufficient amounts of antifriction elements, such as lead and tin. Lead is the most valuable antifriction element in the current materials and is present as a separate phase in the matrix of copper-tin alloy in the leaded bronze materials. Similarly, tin is present as an insoluble second phase in the matrix of aluminum-based materials. Lead is also insoluble in the aluminum matrix. The liner materials play the most critical role in the bearings. Once the liner material is damaged significantly, the bearing is considered unfit for further use. In a trimetal bearing, when the overlay is lost due to wear or fatigue, the bronze liner will continue to support the load and provide adequate lubrication in times of stress. The friction coefficient of liner materials is designed to be low. Besides, the soft phases of lead (in bronze) and tin (in aluminum) function as sites for embedment of dirt particles.

The overlay, which by definition is the top layer of the bearing surface, is the softest layer in the bearing. Its functions are to provide lubrication to the journal in the initial start-up situations, adjust to any misalignment or out-of-roundness of the journal, and capture dirt particles by embedment. The overlay provides sufficient lubrication during the subsequent start-up and shut-down conditions also. The journal makes a comfortable running environment in the bearing assembly during the initial runs by "bedding in." As a result of this, the wear rate of the overlay is higher in the beginning. As long as the overlay is present, the phenomenon of seizure will not occur. Once the wear progresses through the overlay, the bearing liner will provide adequate lubrication during start-up and shut-down conditions. However, if the oil supply is severely compromised or cut off for more than several seconds to a minute or so, seizure can take place once the overlay is gone, depending on the nature of the bearing liner and the load.

23.4 The Bearing Materials

All modern crankshaft journal bearing materials are mainly composed of five elements—namely, copper, aluminum, lead, tin, and silicon. These elements account for the leaded bronze and aluminum-tin, aluminum-lead, and aluminum-silicon materials. Indium is used as a constituent of the overlays. Antimony is used in babbitts. Silver is a bearing material with good tribological properties, but it is too expensive to use as a bearing liner in journal bearings. However, it is used in special applications in some locomotive engines. An important characteristic of a good bearing material is its ability to conduct heat. Silver, copper, and aluminum are, indeed, good conductors of heat. Silver has no affinity for iron, cobalt, and nickel [Bhushan and Gupta, 1991]. Therefore, it is expected to run very well against steel shafts. Both copper and aluminum possess a certain degree of affinity for iron. Therefore, steel journals can bond to these metals in the absence of antifriction elements, such as lead and tin, or lubricating oil. Aluminum spontaneously forms an oxide layer, which is very inert, in the presence of air or water vapor. This suppresses the seizure or the bonding tendency of aluminum. Besides, the silicon particles present in the aluminum-silicon materials keep the journals polished to reduce friction.

The microstructure of the most widely used cast leaded bronze bearing liner is shown in Fig. 23.3. This has a composition of 2 to 4% tin, 23 to 27% lead, and 69 to 75% copper. Another material in widespread use, especially in automotive applications, is aluminum with 20% tin. A typical microstructure of this material is shown in Fig. 23.4. It can be used as the liner for both bimetal and trimetal bearings. The copper-tin-lead material shown in Fig. 23.3 is mainly used in trimetal bearings.

Figure 23.3 SEM photomicrograph of a typical cross section of the cast leaded bronze diesel locomotive engine bearing material manufactured by Glacier Clevite Heavywall Bearings. The nominal composition is 3% tin, 25% lead, and 72% copper. The light gray, irregular spots represent lead in a matrix of copper-tin. This material is bonded to mild steel at the bottom. (Magnification $50\times$.)]
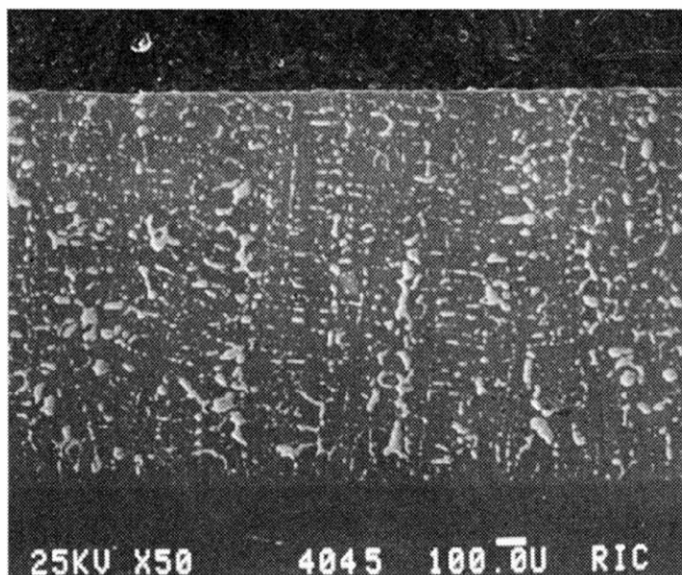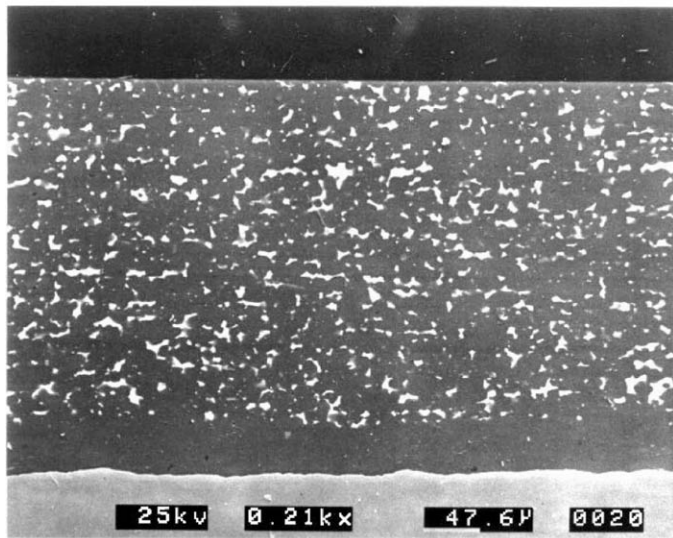
Figure 23.4 SEM photomicrograph of a typical cross section of aluminum-tin material roll bonded to mild steel, manufactured by Glacier Vandervell Ltd. The nominal composition is 20% tin, 1% copper, and 79% aluminum. The light gray, irregular spots represent tin in the aluminum-copper matrix. Below the aluminum-tin layer is a layer of pure aluminum which functions as a bonding layer to the mild steel underneath. (Magnification $210\times$.)
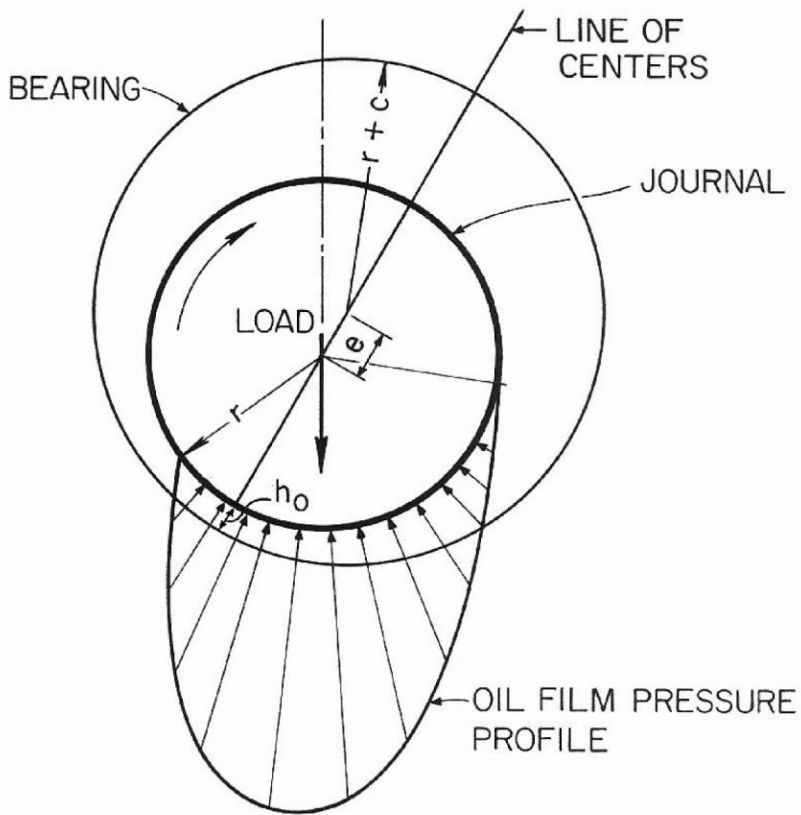
23.5 Basics of Hydrodynamic Journal Bearing Theory

Load-Carrying Ability

As mentioned previously, when running in good condition, the journal which was initially lying on the surface of the bearing is lifted and surrounded by the lubricant. It becomes suspended in the surrounding film of lubricating oil. If the engine keeps running, the journal will remain in its state of suspension indefinitely. The inertial load of the crankshaft and the forces transmitted from the cylinders to the crankshaft are supported by the lubricant films surrounding the main bearing journals. The oil film surrounding the rod bearing journal supports the gas forces developed in the cylinder and the inertial load of the piston and connecting rod assembly. Around each journal, a segment of the oil film develops a positive pressure to support the load, as shown in Fig. 23.5. In the following brief theoretical consideration, the process that develops this load-carrying positive pressure will be illustrated.

Figure 23.5 Schematic representation of the profile of the load supporting pressure in the oil film. (*Source:* Slaymaker, R. R. 1955. *Bearing Lubrication Analysis.* John Wiley & Sons, New York. By permission.)

As a background to the theoretical considerations, the following assumptions are made. The flow of the lubricating oil around the journal at all speeds is assumed to be laminar. The length of the bearing L is assumed to be infinite, or the flow of the lubricant from the edges of the bearing is negligible. The lubricant is assumed to be incompressible.

Consider a very small volume element of the lubricant moving in the direction of rotation of the journal—in this case, the x direction. The forces that act on this elemental volume and stabilize it are shown in Fig. 23.6. Here, P is the pressure in the oil film at a distance x. It is independent of the thickness of the oil film or the y dimension. S is the shear stress in the oil film at a distance y above the bearing surface, which is at $y = 0$. The length L of the bearing is in the z direction. The equilibrium condition of this volume element gives us the following relationship [Slaymaker, 1955; Fuller, 1984]:

$$\left[P + \left(\frac{dP}{dx} \right) \ dx \right] \ dy \ dz + S \ dx \ dz - \left[S + \left(\frac{dS}{dy} \right) \ dy \right] \ dx \ dz - P \ dy \ dz = 0$$

$$(23.1)$$
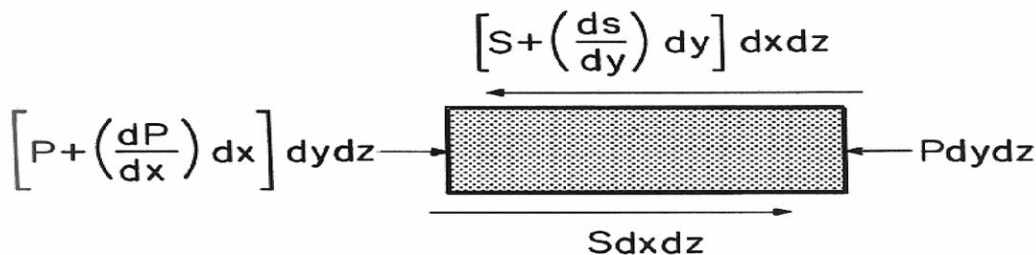
Therefore,

$$\left(\frac{dS}{dy} \right) = \left(\frac{dP}{dx} \right) \qquad (23.2)$$

Equation (23.2) represents a very important, fundamental relationship. It clearly shows how the load-carrying pressure P is developed. It is the rate of change of the shear stress in the direction of the oil film thickness that generates the hydrostatic pressure P. As we shall see from Eq. (23.3), the shear stress is directly proportional to the shearing rate of the oil film (dv/dy) —as (dv/dy) increases, (dS/dy) must increase. Since the thickness of the oil film decreases in the direction of rotation of the journal, a progressive increase in the shearing rate of the oil film automatically occurs because the same flow rate of oil must be maintained through diminishing cross sections (i.e., decreasing y dimension). This progressive increase in the shearing rate is capable of generating very high positive hydrostatic pressures to support very high loads. A profile of the pressure generated in the load-supporting segment of the oil film is shown in Fig. 23.5. By introducing the definition of the coefficient of viscosity, we can relate the shear stress to a more measurable parameter, such as the velocity, v, of the lubricant, as

$$S = \mu \left(\frac{dv}{dy} \right) \qquad (23.3)$$

Figure 23.6 Schematic representation of the forces acting on a tiny volume element in the hydrodynamic lubricant film around a rotating journal.

Substituting for (dS/dy) from Eq. (23.3) in Eq. (23.2), we obtain a second order partial differential equation in v. This is integrated to give the velocity profile as a function of y. This is then integrated to give Q, the total quantity of the lubricant flow per unit time. Applying certain boundary conditions, one can deduce the well-known Reynolds equation for the oil film pressure:

$$\left(\frac{dP}{dx}\right) = \frac{6\mu V}{h^3}(h - h_1) \qquad (23.4)$$

where h is the oil film thickness, h_1 is the oil film thickness at the line of maximum oil film pressure, and V is the peripheral velocity of the journal. The variable x in the above equation can be substituted in terms of the angle of rotation θ and then integrated to obtain the Harrison equation for the oil film pressure. With reference to the diagram in Fig. 23.7, the thickness of the oil film can be expressed as
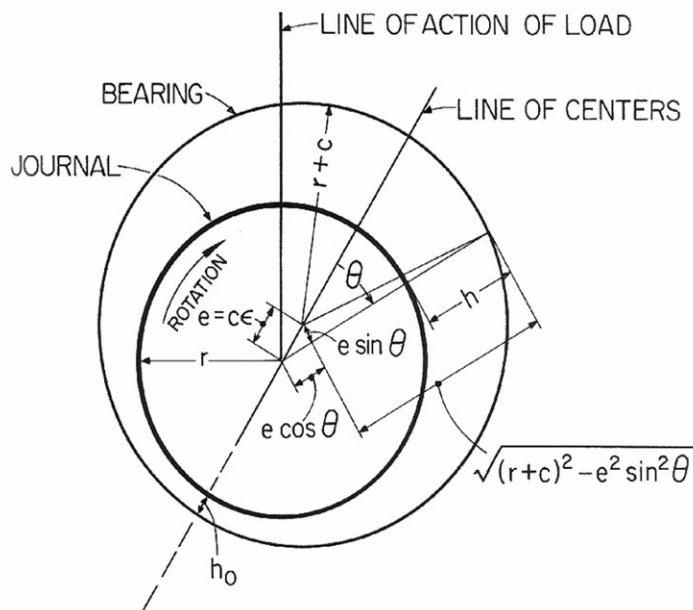
$$h = c(1 + \varepsilon \cos \theta) \qquad (23.5)$$

where c is the radial clearance and ε is the eccentricity ratio. The penultimate form of the Harrison equation can be expressed as

$$\int_0^{2\pi} dP = \int_0^{2\pi} \frac{6\mu V r \varepsilon}{c^2} \left[\frac{\cos \theta - \cos \theta_1}{(1 + \varepsilon \cos \theta)^3}\right] d\theta = P - P_0 \qquad (23.6)$$

where P_0 is the pressure of the lubricant at $\theta = 0$ in Fig. 23.7, and θ_1 is the angle at which the oil film pressure is a maximum. Brief derivations of the Reynolds equation and the Harrison equation are given in section 23.8.

Figure 23.7 Illustration of the geometric relationship of a journal rotating in its bearing assembly. (Source: Slaymaker, R. R. 1955. Bearing Lubrication Analysis. John Wiley and Sons, New York. By permission.)

For practical purposes, it is more convenient to carry out the integration of Eq. (23.6) numerically rather than using Eq. (23.14) in section 23.8. This is done with good accuracy using special computer programs. The equations presented above assume that the end leakage of the lubricating oil is equal to zero. In all practical cases, there will be end leakage and, hence, the oil film will not develop the maximum possible pressure profile. Therefore, its load-carrying capability will be diminished. The flow of the lubricant in the z direction needs to be taken into account. However, the Reynolds equation for this case has no general solution [Fuller, 1984]. Hence, a correction factor between zero and one is applied, depending on the length and diameter of the bearing (L/D ratio) and the eccentricity ratio of the bearing. Indeed, there are tabulated values available for the side leakage factors for bearings with various L/D ratios and eccentricity ratios [Fuller, 1984]. Some of these values are given in Table 23.1.

Table 23.1 Side Leakage Correction Factors for Journal Bearings

L/D Ratio	Eccentricity Ratio						
	0.80	0.90	0.92	0.94	0.96	0.98	0.99
0	1.0	1.0	1.0	1.0	1.0	1.0	1.0
2	—	0.867	0.88	0.905	0.937	0.97	0.99
1	0.605	0.72	0.745	0.79	0.843	0.91	0.958
0.5	0.33	0.50	0.56	0.635	0.732	0.84	0.908
0.3	0.17	0.30	0.355	0.435	0.551	0.705	0.81
0.1	—	0.105	0.115	0.155	0.220	0.36	0.53

Booker [1965] has done considerable work in simplifying the journal center orbit calculations without loss of accuracy by introducing new concepts, such as dimensionless journal center velocity/force ratio (i.e., mobility) and maximum film pressure/specific load ratio (i.e., maximum film pressure ratio). This whole approach is called the *mobility method.* This has been developed into computer programs which are widely used in the industry to calculate film pressures and thicknesses. Further, this program calculates energy loss due to the viscous shearing of the lubricating oil. These calculations are vital for optimizing the bearing design and selecting the appropriate bearing liner with the required fatigue life. This is determined on the basis of the **peak oil film pressure** (POFP). In Booker's mobility method, the bearing assembly, including the housing, is assumed to be rigid. In reality, the bearings and housings are flexible to a certain degree, depending on the stiffness of these components. Corrections are now being made to these deviations by the elastohydrodynamic theory, which involves finite element modeling of the bearings and the housing. Also, the increase in viscosity as a function of pressure is taken into account in this calculation. The elastohydrodynamic calculations are presently done only in very special cases and have not become part of the routine bearing analysis.

23.6 The Bearing Assembly

Housing
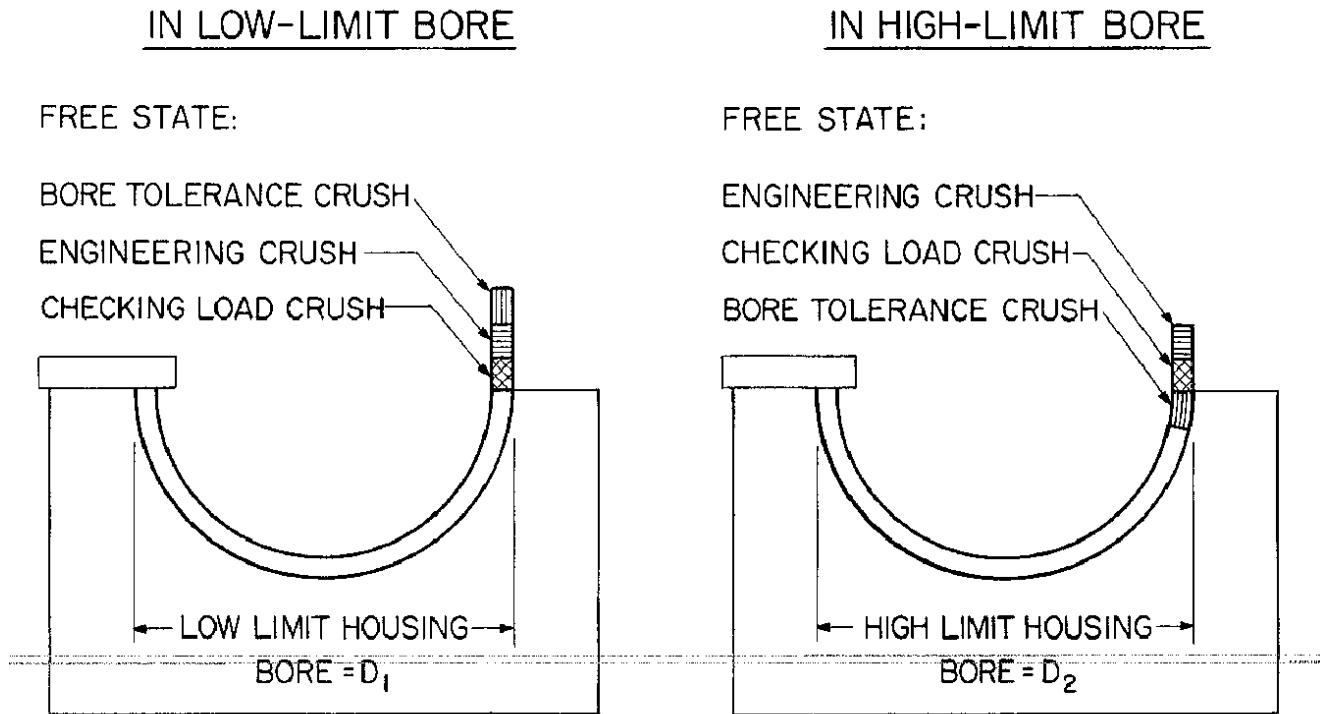
The housing into which a set of bearings is inserted and held in place is a precision-machined cylindrical bore with close tolerance. The surface finishes of the housing and the backs of the bearings must be compatible. Adequate contact between the backs of the bearings and the surface of the housing bore is a critical requirement to ensure good heat transfer through this interface. The finish of the housing bore is expected to be in the range of 60 to 90 μin. (R_a) (39.4 μin. $= 1$ micron). The finish on the back of the bearings is generally set at 80 μin. maximum. Nowadays, the finishes on the housing bore and the backs of the bearings are becoming finer. The finish at the parting line face of bearings of less than 12 in. gage size is expected to be less than 63 μin. For larger bearings, this is set at a maximum of 80 μin. The bearing backs may be rolled, turned, or ground. All the automotive and truck bearings have rolled steel finish at the back. The housing can be bored, honed, or ground, but care must be taken to avoid circumferential and axial banding.

The Bearing Crush

The term **crush** is not used in a literal sense in this context. A quantitative measure of the crush of a bearing is equal to the excess length of the exterior circumference of the bearing over half the interior circumference of the bearing housing. Effectively, this is equal to the sum of the two parting line heights. When the bearing assembly is properly torqued, the parting line height of each bearing in the set is reduced to zero. In that state, the back of the bearing makes good contact with the housing and applies a radial pressure in the range of 800 to 1200 psi (5.5 to 8.24 MPa). Thereby, a good interference fit is generated. If the bearings are taken out of the assembly, they are expected to spring back to their original state. Therefore, nothing is actually crushed.

The total crush or the parting line height of a bearing has three components—namely, the housing bore tolerance crush, the checking load crush, and the engineering crush. The housing bore tolerance crush is calculated as $0.5\pi(D_2 - D_1)$, where D_1 and D_2 are the lower and upper limits of the bore diameter, respectively. Suppose a bearing is inserted in its own inspection block (the diameter of which corresponds to the upper limit of the diameter of the bearing housing). The housing bore tolerance crush does not make a contribution to the actual crush, as shown in Fig. 23.8 (high limit bore). If load is applied on its parting lines in increasing order and the values of these loads are plotted as a function of the cumulative decrease in parting line height, one may expect it to obey Hooke's law. Initially, however, it does not obey Hooke's law, but it does so thereafter. The initial nonlinear segment corresponds to the checking load crush. The checking load corresponds to the load required to conform the bearing properly in its housing. The final crush or the parting line height of the bearing is determined in consultation with the engine manufacturer.

Figure 23.8 Schematic illustration of the components of crush of a bearing in the thinwall bearing inspection block, before application of load (i.e., in the free state). The magnitude of the crush components is exaggerated.

Other Factors Affecting Bearing Assembly

These factors are (1) freespread, (2) bore distortion, (3) cap offset or twist, (4) misalignment of the crankshaft, (5) out-of-roundness of the journal, and (6) deviation of the bearing clearance. The outside diameter of the bearing at the parting lines must be slightly greater than the diameter of the housing bore. This is called the freespread. It helps to snap the bearings into the housing. The required degree of freespread is determined by the wall thickness and the diameter. In the case of wall thickness, the freespread is inversely proportional to it. For a wide range of bearings, the freespread is in the range of 0.025 to 0.075 in. Bearings with negative freespread are not used because, when bolted, the side of the parting lines could rub against the journal and lead to possible seizure while running. It is possible to change the freespread from negative to positive by reforming the bearing. Bore distortion, cap offset or twist, and misalignment of the crankshaft can lead to the journal making rubbing contacts with the bearing surface. The conformability of the bearings can take care of these problems to a certain degree by local wearing of the overlay in a trimetal bearing or by melting the soft phase in a bimetal bearing, which results in the two-phase structure crushing and conforming. In severe cases, the liner materials in both cases are damaged.
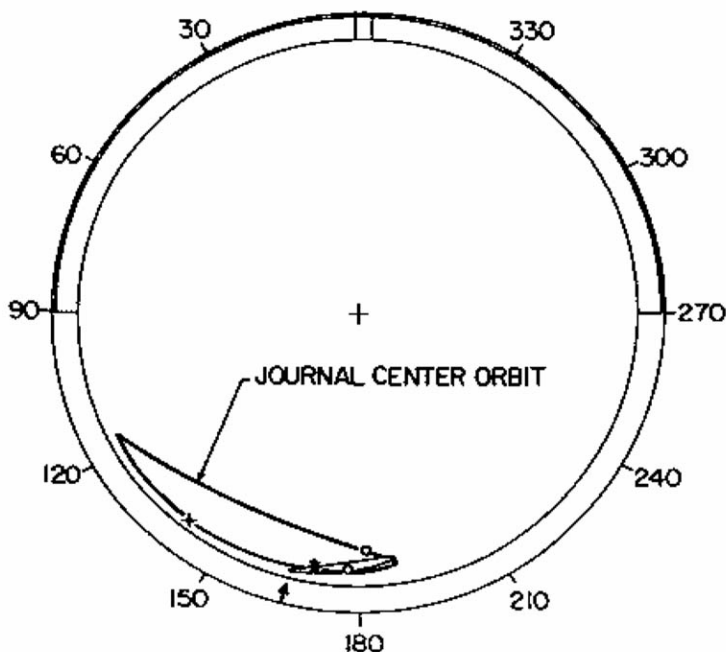
By developing high oil film pressures on the peaks of the lobes, out-of-roundness in the journal can accelerate fatigue of the bearing.

If the clearance is not adequate, the bearing will suffer from oil starvation and the temperature will rise. In extreme cases, this will lead to bearing seizure and engine damage. On the other hand, if the clearance is excessive, there will be increased noise and increased peak oil film pressure, which will bring about premature fatigue of the loaded bearing.

23.7 The Design Aspects of Journal Bearings

Even though the journal bearings are of simple semicylindrical shape and apparently of unimpressive features, there are important matters to be taken into account in their design. The bearing lengths, diameters, and wall thicknesses are generally provided by the engine builder or decided in consultation with the bearing manufacturer. A journal orbit study must be done to optimize the clearance space between the journal and the bearing surface. This study also provides the **minimum oil film thickness** (MOFT) and the POFP (Fig. 23.9). Values of these parameters for the optimized clearance are important factors. The MOFT is used in the calculation of the oil flow, temperature rise, and heat balance. According to Conway-Jones and Tarver [1993], about 52% of the heat generated in connecting rod bearings in automobile engines is carried away by the oil flow. Approximately 38% of the remaining heat flows into the adjacent main bearings via the crankshaft. The remaining 10% is lost by convection and radiation. In the case of main bearings, about 95% of the total heat is carried away by the oil flow, which is estimated to be more than five times the flow through the connecting rod bearings, which were fed by a single oil hole drilled in the crank pin. The POFP is the guiding factor in the selection of a bearing liner with adequate fatigue strength or fatigue life.

Figure 23.9 Journal center orbit diagram of two-stroke cycle medium-speed (900 rpm) diesel engine main bearings (no. 1 position). The inner circle represents the clearance circle of the bearings. It also represents the bearing surface. The entire cross section of the journal is reduced to a point coinciding with the center of the journal. The upper main bearing has an oil hole at the center with a circumferential groove at the center of the bearing represented by the dark line. Maximum unit load: 1484 psi. MOFT: 151 μin. @ 70/166. POFP: 11 212 psi @ 55/171. Oil: SAE 30W. Cylinder pressure data given by the manufacturer of the engine. Clockwise rotation. The journal orbit analysis done at Glacier Clevite Heavywall Bearings. —∗—0–180 crank angle, —+—180–360 crank angle, @ crank angle/bearing angle. Arrow indicates the location of MOFT.

The bearing must be properly located in the housing bore. This is achieved by having a notch at one end of the bearing at the parting line. There must be provisions to bring in the lubricant and remove it. Therefore, appropriate grooves and holes are required. The best groove to distribute the

lubricant is a circumferential groove with rounded edges, centrally placed in both bearings. If this is a square groove, the flow will be diminished by 10%. If these grooves are in the axial direction, the oil flow is decreased by 60% with respect to the circumferential ones. Having a circumferential groove in the loaded half of the bearings does increase the POFP. In the case of large slow-speed diesel engines, the POFPs are generally very low compared to the pressures in automotive, truck, and medium-speed diesel engines. Therefore, central circumferential grooves are best suited for slow-speed engines.

In the automotive, truck, and medium-speed engines, the loaded halves of the bearings do not have circumferential grooves. However, the other halves have the circumferential grooves. Some of the loaded bearings have partial grooves. Otherwise, some type of oil spreader machined in the location below the parting line is desirable in the case of larger bearings. If the oil is not spread smoothly, the problems of cavitation and erosion may show up. The end of the partial groove or the oil spreader must be blended.

The edges of all the bearings must be rounded or chamfered to minimize the loss of the lubricant. Edges are also chamfered to eliminate burrs. A sharp edge acts as an oil scraper and thereby enhances oil flow in the axial direction along the edges, which is harmful. Finally, bearings have a small relief just below the parting lines along the length on the inside surface. This is meant to protect the bearings in case of slight misalignment or offset at the parting lines.

23.8 Derivations of the Reynolds and Harrison Equations for Oil Film Pressure

The background for deriving these equations is given in section 23.5 of the text. The equilibrium condition of a tiny volume element of the lubricating oil (Fig. 23.6) is represented by the following equation [Slaymaker, 1955; Fuller, 1984]:

$$\left[P + \left(\frac{dP}{dx} \right) \ dx \right] \ dy \ dz + S \ dx \ dz - \left[S + \left(\frac{dS}{dy} \right) \ dy \right] \ dx \ dz - P \ dy \ dz = 0$$

$$(23.7)$$

Therefore,

$$\left(\frac{dS}{dy} \right) = \left(\frac{dP}{dx} \right) \qquad (23.8)$$

Now, by introducing the definition of the coefficient of viscosity μ, we can relate the shear stress to a more measurable parameter, like the velocity v of the lubricant, as

$$S = \mu \left(\frac{dv}{dy} \right) \qquad (23.9)$$

Substituting for (dS/dy) from Eq. (23.9) in Eq. (23.8), a second order partial differential equation in v is obtained. This is integrated to give an expression for the velocity profile as

$$v = \frac{V}{h}y - \frac{1}{2\mu}\left(\frac{dP}{dx}\right)(hy - y^2) \qquad (23.10)$$

In Eq. (23.10), V is the peripheral velocity of the journal and h is the oil film thickness. The boundary conditions used to derive Eq. (23.10) are (1) $v = V$ when $y = h$, and (2) $v = 0$ when $y = 0$ (at the surface of the bearing). Now applying the relationship of continuity, the oil flowing past any cross section in the z direction of the oil film around the journal must be equal. The quantity Q of oil flow per second is given by

$$Q = L\int_0^h v\, dy \qquad (23.11)$$

where L is the length of the bearing which is in the z direction. Now substituting for v from Eq. (23.10) in Eq. (23.11) and integrating,

$$Q = L\left[\frac{Vh}{2} - \frac{h^3}{12\mu}\left(\frac{dP}{dx}\right)\right] \qquad (23.12)$$

The pressure P varies as a function of x in the oil film, which is in the direction of rotation of the journal. At some point, it is expected to reach a maximum. At that point, (dP/dx) becomes zero. Let h_1 represent the oil film thickness at that point. Therefore,

$$Q = \frac{LV}{2}h_1 \qquad (23.13)$$

Now we can use Eq. (23.13) to eliminate Q from Eq. (23.12). Hence,

$$\left(\frac{dP}{dx}\right) = \frac{6\mu V}{h^3}(h - h_1) \qquad (23.14)$$

Equation (23.14) is the Reynolds equation for the oil film pressure as a function of distance in the direction of rotation of the journal. The variable x in Eq. (23.14) can be substituted in terms of the angle of rotation θ and then integrated to obtain the Harrison equation for the oil filmpressure. With reference to the diagram in Fig. 23.7, the oil film thickness h can be expressed as

$$h = e\cos\theta + \sqrt{(r+c)^2 - e^2\sin^2\theta} - r \qquad (23.15)$$

Here, e is the eccentricity, c is the radial clearance, and $e = c\varepsilon$, where ε is the eccentricity ratio. The quantity $e^2\sin^2\theta$ is much smaller compared to $(r+c)^2$. Therefore,

$$h = c(1 + \varepsilon\cos\theta) \qquad (23.16)$$

Now, (dP/dx) is converted into polar coordinates by substituting $rd\theta$ for dx. Therefore, Eq. (23.14) can be expressed as

$$\left(\frac{dP}{d\theta}\right) = \frac{6\mu Vr\varepsilon}{c^2}\left[\frac{\cos\theta - \cos\theta_1}{(1 + \varepsilon\cos\theta)^3}\right] \qquad (23.17)$$

where θ_1 is the angle at which the oil film pressure is a maximum. Integration of Eq. (23.17) from $\theta = 0$ to $\theta = 2\pi$ can be expressed as

$$\int_0^{2\pi} dP = \int_0^{2\pi} \frac{6\mu V r\varepsilon}{c^2} \left[\frac{\cos\theta - \cos\theta_1}{(1 + \varepsilon\cos\theta)^3} \right] d\theta = P - P_0 \qquad (23.18)$$

where P_0 is the pressure of the lubricant at the line of centers ($\theta = 0$) in Fig. 23.7. If $(P - P_0)$ is assumed to be equal to zero at $\theta = 0$ and $\theta = 2\pi$, the value of $\cos\theta_1$, upon integration of Eq. (23.18), is given by

$$\cos\theta_1 = -\frac{3\varepsilon}{2 + \varepsilon^2} \qquad (23.19)$$

and the Harrison equation for the oil film pressure for a full journal bearing by

$$P - P_0 = \frac{6\mu V r\varepsilon}{c^2} \frac{\sin\theta(2 + \varepsilon\cos\theta)}{(2 + \varepsilon^2)(1 + \varepsilon\cos\theta)^2} \qquad (23.20)$$

Acknowledgment

Defining Terms

Boundary layer lubrication: This is a marginally lubricating condition. In this case, the surfaces of two components (e.g., one sliding past the other) are physically separated by an oil film that has a thickness equal to or less than the sum of the heights of the asperities on the surfaces. Therefore, contact at the asperities can occur while running in this mode of lubrication. This is also described as "mixed lubrication." In some cases, the contacting asperities will be polished out. In other cases, they can generate enough frictional heat to destroy the two components. Certain additives can be added to the lubricating oil to reduce asperity friction drastically.

Crush: This is the property of the bearing which is responsible for producing a good interference fit in the housing bore and preventing it from spinning. A quantitative measure of the crush is equal to the excess length of the exterior circumference of the bearing over half the interior circumference of the housing. This is equal to twice the parting line height, if measured in an equalized half height measurement block.

Hydrodynamic lubrication: In this mode of lubrication, the two surfaces sliding past each other (e.g., a journal rotating in its bearing assembly) are physically separated by a liquid lubricant of suitable viscosity. The asperities do not come into contact in this case and the friction is very low.

Minimum oil film thickness (MOFT): The hydrodynamic oil film around a rotating journal develops a continuously varying thickness. The thickness of the oil film goes through a

minimum. Along this line, the journal most closely approaches the bearing. The maximum wear in the bearing is expected to occur around this line. Therefore, MOFT is an important parameter in designing bearings.

Peak oil film pressure (POFP): The profile of pressure in the load-carrying segment of the oil film increases in the direction of rotation of the journal and goes through a maximum (Fig. 23.5). This maximum pressure is a critical parameter because it determines the fatigue life of the bearing. This is also called maximum oil film pressure (MOFP).

Positive freespread: This is the excess in the outside diameter of the bearing at the parting line over the inside diameter of the housing bore. As a result of this, the bearing is clipped in position in its housing upon insertion. Bearings with negative freespread will be loose and lead to faulty assembly conditions.

Seizure: This is a critical phenomenon brought about by the breakdown of lubrication. At the core of this phenomenon is the occurrence of metal-to-metal bonding, or welding, which can develop into disastrous levels, ultimately breaking the crankshaft. With the initiation of seizure, there will be increased generation of heat, which will accelerate this phenomenon. Galling and adhesive wear are terms which mean the same basic phenomenon. The term *scuffing* is used to describe the initial stages of seizure.

References

Bhushan, B. and Gupta, B. K. 1991. *Handbook of Tribology.* McGraw-Hill, New York.

Booker, J. F. 1965. Dynamically loaded journal bearings: Mobility method of solution. *J. Basic Eng. Trans. ASME,* series D, 87:537.

Conway-Jones, J. M. and Tarver, N. 1993. Refinement of engine bearing design techniques. *SAE Technical Paper Series, 932901, Worldwide Passenger Car Conference and Exposition,* Dearborn, MI, October 25−27.

Fuller, D. D. 1984. *Theory and Practice of Lubrication for Engineers,* 2nd ed. John Wiley & Sons, New York.

Slaymaker, R. R. 1955. *Bearing Lubrication Analysis.* John Wiley & Sons, New York.

Further Information

Yahraus, W. A. 1987. Rating sleeve bearing material fatigue life in terms of peak oil film pressure. *SAE Technical Paper Series, 871685, International Off-Highway & Powerplant Congress and Exposition,* Milwaukee, WI, September 14−17.

Booker, J. F., 1971. Dynamically loaded journal bearings: Numerical application of the mobility method. *J. of Lubr. Technol. Trans. ASME,* 93:168.

Booker, J. F., 1989. Squeeze film and bearing dynamics. *Handbook of Lubrication,* ed. E. R. Booser. CRC Press, Boca Raton, FL.

Hutchings, I. M. 1992. *Tribology.* CRC Press, Boca Raton, FL.

Transactions of the ASME, Journal of Tribology.

STLE Tribology Transactions.

Spring and Fall Technical Conferences of the ASME/ICED.

Lebeck, A. O. "Fluid Sealing in Machines, Mechanical Devices..."
The Engineering Handbook.
Ed. Richard C. Dorf
Boca Raton: CRC Press LLC, 2000

24

Fluid Sealing in Machines, Mechanical Devices, and Apparatus

Alan O. Lebeck
Mechanical Seal Technology, Inc.

The passage of fluid (leakage) between the mating parts of a machine and between other mechanical elements is prevented or minimized by a fluid seal. Commonly, a gap exists between parts formed by inherent roughness or misfit of the parts—where leakage must be prevented by a seal. One may also have of necessity gaps between parts that have relative motion, but a fluid seal is still needed. The fluid to be sealed can be any liquid or gas. Given that most machines operate with fluids and must contain fluids or exclude fluids, most mechanical devices or machines require a multiplicity of seals.

Fluid seals can be categorized as *static* or *dynamic* as follows.

Static:

- Gap to be sealed is generally very small.
- Accommodates imperfect surfaces, both roughness and out-of-flatness.
- Subject to very small relative motions due to pressure and thermal cyclic loading.
- Allows for assembly/disassembly.

Dynamic:

- Gap to be sealed is much larger and exists of necessity to permit relative motion.
- Relatively large relative motions between surfaces to be sealed.
- Motion may be continuous (rotation) in one direction or large reciprocating or amount of

motion may be limited.
- Seal must not constrain motion (usually).

Although there is some crossover between static and dynamic seal types, by categorizing based on the static and dynamic classification, the distinction between the various seal types is best understood.

24.1 Fundamentals of Sealing

Sealing can be accomplished by causing the gap between two surfaces to become small but defined by the geometric relationship between the parts themselves. In this case one has a fixed-clearance seal. One may also force two materials into contact with each other, and the materials may be either sliding relative to each other or static. In this case one has a surface-guided seal where the **sealing clearance** now becomes defined by the materials themselves and the dynamics of sliding in the case of a sliding seal.

There are two broad classes of surface-guided material pairs. The first and most common involves use of an **elastomeric,** plastic, or other soft material against a hard material. In this case the soft material deforms to conform to the details of the shape of the harder surface and will usually seal off completely in the static case and nearly completely in the dynamic case. A rubber gasket on metal is an example. The second class, far less common, is where one mates a hard but wearable material to a hard material. Here the sealing gap derives from a self-lapping process plus the alignment of the faces of the material. Since both materials are relatively hard, if one material develops a roughness or grooves, the seal will leak. A mechanical face seal is an example.

24.2 Static Seals

Static seals can be categorized as follows:

Gaskets
   Single or composite compliant material
   Metal encased
   Wrapped and spiral wound
   Solid metal
Self-energized elastomeric rings
   Circular cross section (O-ring)
   Rectangular cross section
Chemical compound or liquid sealants as gaskets
   Rubbers
   Plastics

Gaskets

Within the category of static seals, gaskets comprise the greatest fraction. The sealing principle common to gaskets is that a material is clamped between the two surfaces being sealed. Clamping force is large enough to deform the gasket material and hold it in tight contact even when the pressure attempts to open the gap between the surfaces.

A simple single-material gasket clamped between two surfaces by bolts to prevent leakage is shown in Fig. 24.1. Using a compliant material the gasket can seal even though the sealing surfaces are not flat. As shown in Fig. 24.2, the gasket need not cover the entire face being sealed. A gasket can be trapped in a groove and loaded by a projection on the opposite surface as shown in Fig. 24.3. Composite material gaskets or metal gaskets may be contained in grooves as in Fig. 24.4. Gaskets are made in a wide variety of ways. A spiral-wound metal/fiber composite, metal or plastic clad, solid metal with sealing projections, and a solid fiber or rubber material are shown in Fig. 24.5.

Figure 24.1 Gasket.
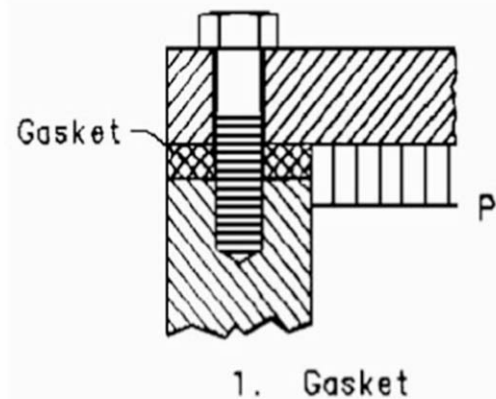
Figure 24.2 Gasket.
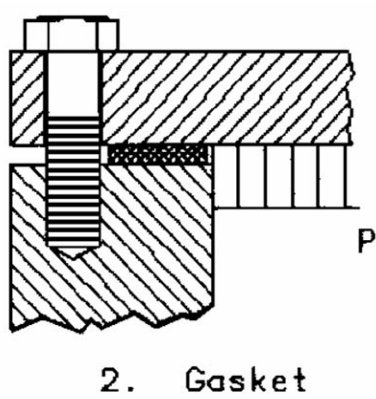
Figure 24.3 Loaded gasket.
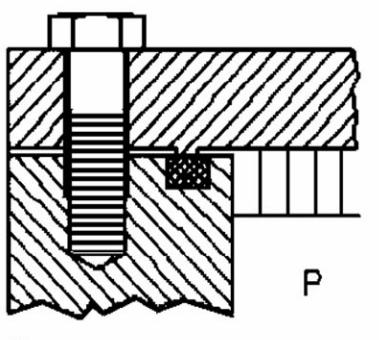
Figure 24.4 Hard ring gasket.
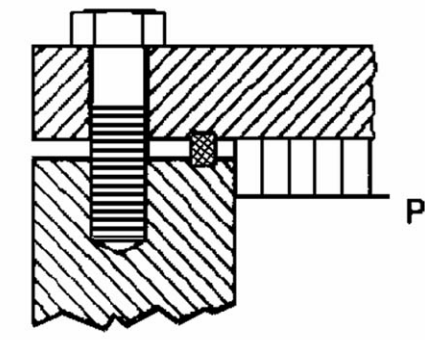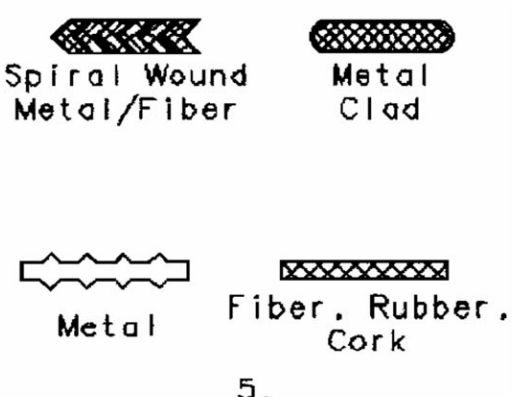
Figure 24.5 Varieties of gaskets.
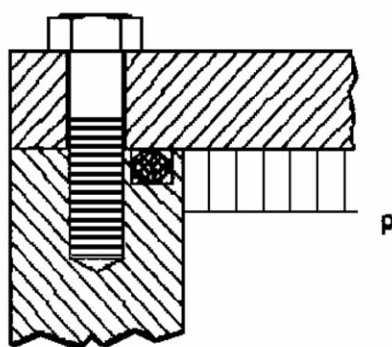
Gaskets can be made of relatively low-stiffness materials such as rubber or cork for applications at low pressures and where the surfaces are not very flat. For higher pressures and loads, one must utilize various composite materials and metal-encased materials as in Fig. 24.5.

For the highest pressures and loads a gasket may be retained in a groove and made either of very strong composite materials or even metal, as shown in Fig. 24.4.

Self-Energized Seals
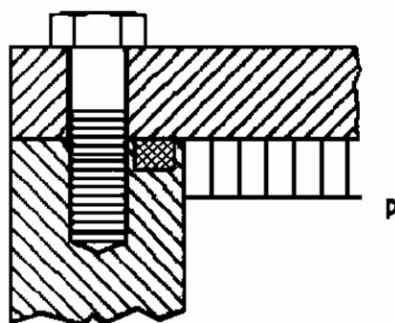
Elastomeric or **self-energized** rings can seal pressures to 20 MPa or even higher. As shown in Figs. 24.6 and 24.7, the two metal parts are clamped tightly together and they are not supported by the elastomer. As the pressure increases, the rubber is pushed into the corner through which leakage would otherwise flow. An elastomer acts much like a fluid so that the effect of pressure on one side is to cause equal pressure on all sides. Thus, the elastomer pushes tightly against the metal walls and forms a seal. The limitation of this type of seal is that the rubber will flow or extrude out of the clearance when the pressure is high enough. This is often not a problem for static seals, since the gap can be made essentially zero as shown in Fig. 24.6, which represents a typical way to utilize an elastomeric seal for static sealing.

Figure 24.6 Elastomeric O-ring.

Figure 24.7 Elastomeric rectangular ring.

Although the O-ring (circular cross section) is by far the most common elastomeric seal, one can also utilize rectangular cross sections (and even other cross sections) as shown in Fig. 24.7.

Chemical Compound or Liquid Sealants as Gaskets

Formed-in-place gaskets such as in Fig. 24.8 are made by depositing a liquid-state compound on one of the surfaces before assembly. After curing, the gasket retains a thickness and flexibility, allowing it to seal very much like a separate gasket. Such gaskets are most commonly created using room temperature vulcanizing rubbers (RTV), but other materials including epoxy can be used.

Figure 24.8 Formed-in-place elastomeric gasket.

While formed-in-place gaskets retain relatively high flexibility, there are other types of plastic materials (including epoxy and anaerobic hardening fluids) that can be used to seal two surfaces. These fluids are coated on the surfaces before assembly. Once the joint is tightened and the material hardens, it acts like a form-fitted plastic gasket, but it has the advantage that it is also bonded to the sealing surfaces. Within the limits of the ability of the materials to deform, these types of gaskets make very tight joints. But one must be aware that relative expansion of dissimilar materials so bonded can weaken the bond. Thus, such sealants are best utilized when applied to tight-fitting assemblies. These same materials are used to lock and seal threaded assemblies, including pipe fittings.

There have been many developments of chemical compounds for sealing during the past 25 years, and one is well advised to research these possibilities for sealing/assembly solutions.

24.3 Dynamic Seals

Dynamic seals can be categorized as follows:

> Rotating or oscillating shaft
> > Fixed clearance seals
> > > Labyrinth
> > > Clearance or bushing
> > > Visco seal
> > > Floating-ring seal
> > > Ferrofluid seal
> > Surface-guided seals
> > > Cylindrical surface
> > > > Circumferential seal
> > > > Packing
> > > > Lip seal
> > > > Elastomeric ring
> > > **Annular** surface (radial face)
> > > > Mechanical face seal
> > > > Lip seal
> > > > Elastomeric ring
> Reciprocating
> > Fixed clearance seals
> > > Bushing seal
> > > Floating-ring seal
> > > Clearance or bushing
> > Surface-guided seals
> > > Elastomeric rings
> > > > Solid cross section
> > > > U-cups, V-rings, chevron rings
> > > Split piston rings
> > Limited-travel seals
> > > Bellows
> > > Diaphragm
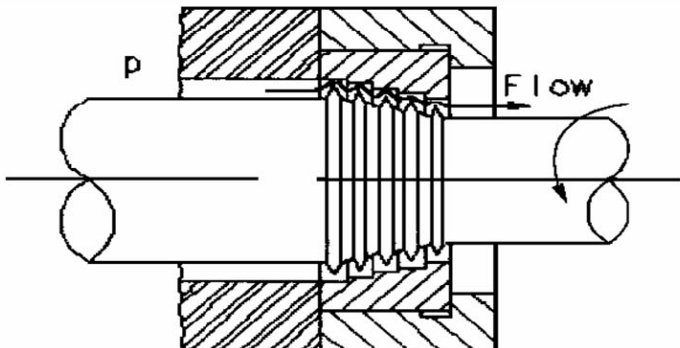
One finds considerable differences between dynamic seals for rotating shaft and dynamic seals for reciprocating motion, although there is some crossover. One of the largest differences in seal types is between fixed-clearance seals and surface-guided seals. Fixed-clearance seals maintain a sealing gap by virtue of the rigidity of the parts and purposeful creation of a fixed sealing clearance. Surface-guided seals attempt to close the sealing gap by having one of the sealing surfaces actually (or nearly) touch and rub on the other, so that the position of one surface becomes guided by the other. Fixed-clearance seals leak more than surface-guided seals as a rule, but each has its place. Finally, dynamic seals usually seal to either cylindrical surfaces or annular (radial) surfaces. Sealing to cylindrical surfaces permits easy axial freedom, whereas sealing to radial surfaces permits easy radial freedom. Many seals combine these two motions to give the needed freedom of movement in all directions.

Rotating or Oscillating Fixed-Clearance Seals
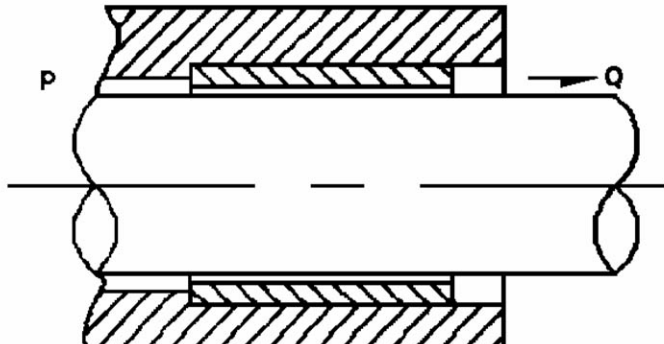
The labyrinth seal is shown in Fig. 24.9. This seal has a calculable leakage depending on the exact shape, number of stages, and clearance and is commonly used in some compressors and turbomachinery as interstage seals and sometimes as seals to atmosphere. Its components can be made of readily wearable material so that a minimum initial clearance can be utilized.

Figure 24.9 Labyrinth seal. (*Source:* Lebeck, A. O. 1991. *Principles and Design of Mechanical Face Seals.* John Wiley & Sons, New York. With permission.)

Figure 24.10 Bushing seal. (*Source:* Lebeck, A. O. 1991. *Principles and Design of Mechanical Face Seals.* John Wiley & Sons, New York. With permission.)

9. Labyrinth Seal

10. Bushing Seal

The clearance or bushing seal in Fig. 24.10 may leak more for the same clearance, but this represents the simplest type of clearance seal. Clearance bushings are often used as backup seals to limit flow in the event of failure of yet other seals in the system. As a first approximation, flow can be estimated using flow equations for fluid flow between parallel plates. Clearance-bushing leakage increases significantly if the bushing is eccentric.

In high-speed pumps and compressors, bushing seals interact with the shaft and bearing system dynamically. Bushing seals can utilize complex shapes and patterns of the shaft and seal surfaces to minimize leakage and to modify the dynamic stiffness and damping characteristics of the seal.

The visco seal or windback seal in Fig. 24.11 is used to seal highly viscous substances where it can be fairly effective. It acts like a screw conveyor, extruder, or spiral pump to make the fluid flow backward against sealed pressure. It can also be used at no differential pressure to retain oil within a shaft seal system by continuously pumping leaked oil back into the system.

Figure 24.11 Visco seal. (*Source:* Lebeck, A. O. 1991. *Principles and Design of Mechanical Face Seals.* John Wiley & Sons, New York. With permission.)
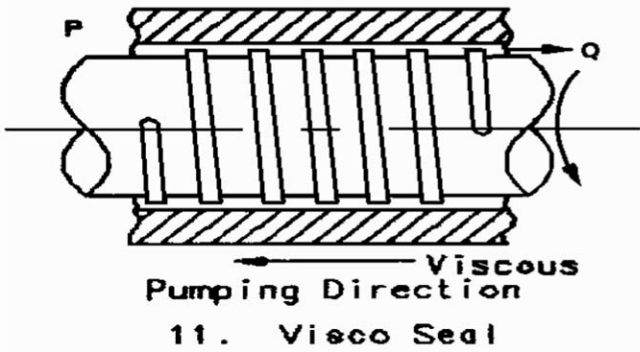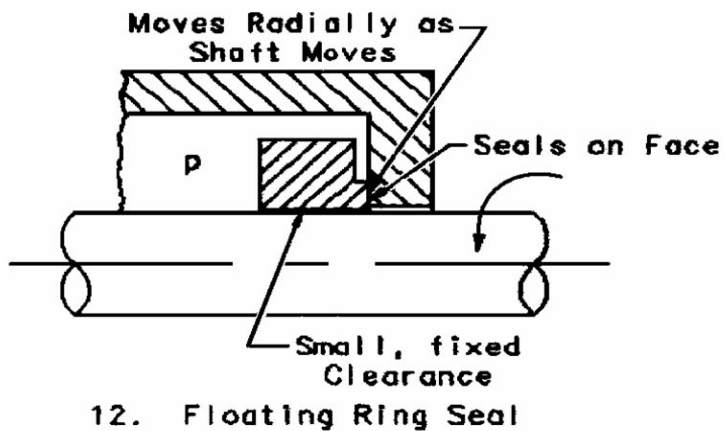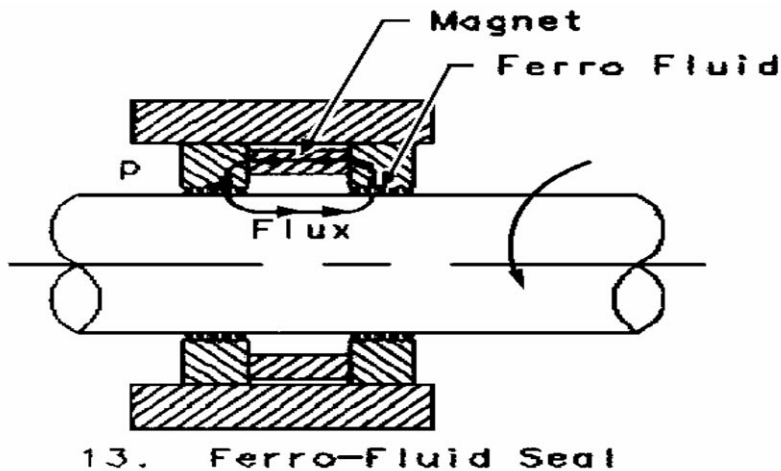
Figure 24.12 Floating-ring seal. (*Source:* Lebeck, A. O. 1991. *Principles and Design of Mechanical Face Seals.* John Wiley & Sons, New York. With permission.)

The floating-ring seal in Fig. 24.12 is used in gas compressors (can be a series of floating rings). It can be used to seal oil where the oil serves as a barrier to gas leakage or it can seal product directly. This seal can be made with a very small clearance around the shaft because the seal can float radially to handle larger shaft motions. The floating-ring seal is a combination of a journal bearing where it fits around the shaft and a face seal where it is pressed against the radial face. Most of the leakage is between the shaft and the bore of the bushing, but some leakage also occurs at the face. This seal can be used in stages to reduce leakage. It can be balanced to reduce the load on the radial face. Leakage can be less than with a fixed-bushing seal.

The **ferrofluid** seal in Fig. 24.13 has found application in computer disk drives where a true "positive seal" is necessary to exclude contaminants from the flying heads of the disk. The ferrofluid seal operates by retaining a **ferrofluid** (a suspension of iron particles in a special liquid) within the magnetic flux field, as shown. The fluid creates a continuous bridge between the rotating and nonrotating parts at all times and thus creates a positive seal. Each stage of a ferrofluid seal is capable of withstanding on the order of 20000 Pa (3 psi), so although these seals can be staged they are usually limited to low−differential pressure applications.

Figure 24.13 Ferrofluid seal. (*Source:* Lebeck, A. O. 1991. *Principles and Design of Mechanical Face Seals.* John Wiley & Sons, New York. With permission.)

Rotating Surface-Guided Seals—Cylindrical Surface

Figure 24.14 shows a segmented circumferential seal. The seal consists of angular segments with overlapping ends, and the segments are pulled radially inward by garter spring force and the sealed pressure. The seal segments are pushed against the shaft and thus are surface guided. They are also pushed against a radial face by pressure. This seal is similar to the floating-ring seal except that the seal face is pushed tight against the shaft because the segments allow for circumferential contraction. Circumferential segmented seals are commonly used in aircraft engines to seal oil and gas.

Figure 24.14 Circumferential seal.
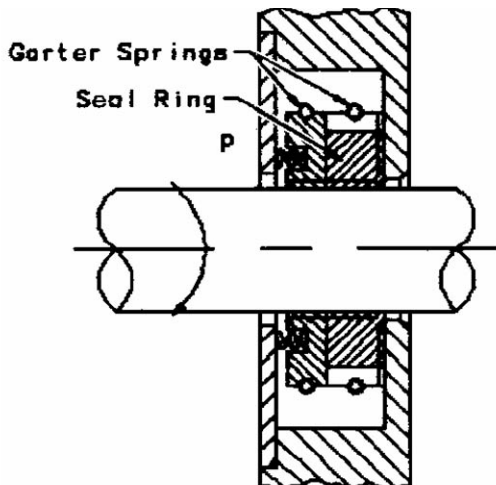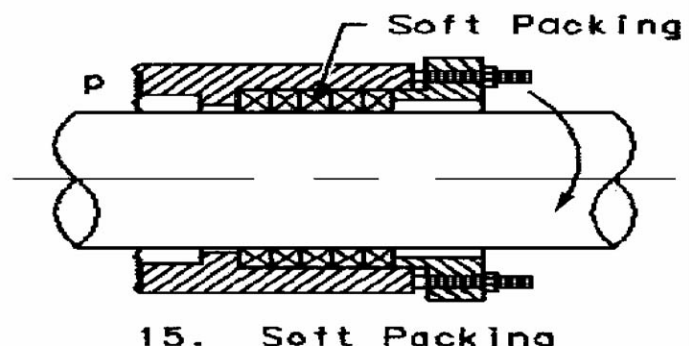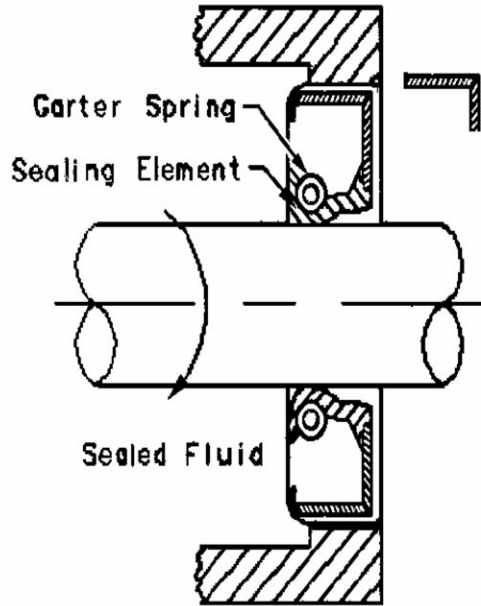
Figure 24.15 Soft packing.

There are many types of soft packing used in the manner shown in Fig. 24.15. The packing is composed of various types of fibers and is woven in different ways for various purposes. It is often formed into a rectangular cross section so it can be wrapped around a shaft and pushed into a packing gland as shown. As the packing nut is tightened the packing deforms and begins to press on the shaft (or sleeve). Contact or near contact with the shaft forms the seal. If the packing is overtightened the packing material will generate excessive heat from friction and burn. If it is too loose, leakage will be excessive. At the point where the packing is properly loaded, there is some small leakage which acts to lubricate between the shaft and the packing material. Although other types of sealing devices have replaced soft packing in many applications, there are still many applications (e.g., pump shafts, valve stems, and hot applications) that utilize soft packing, and there has been a continuous development of new packing materials. Soft packing for continuously rotating shafts is restricted to moderate pressures and speeds. For valve stems and other reciprocating applications, soft packing can be used at high pressure and temperature.

Figure 24.16 Lip seal.

16. Lip Seal

The lip seal (oil seal) operating on a shaft surface represents one of the most common sealing arrangements. The lip seal is made of rubber (or, much less commonly, a plastic) or similar material that can be readily deflected inward toward the shaft surface by a garter spring. The lip is very lightly loaded, and, in operation in oils with rotation, a small liquid film thickness develops between the rubber lip and the shaft. The shape of the cross section determines which way the seal will operate. As shown in Fig. 24.16 the seal will retain oil to the left. Lip seals can tolerate only moderate pressure (100000 Pa maximum). The normal failure mechanism is deterioration (stiffening) of the rubber, so lip seals have a limited speed and temperature of service. Various elastomers are best suited for the variety of applications.

The elastomeric ring as described for static seals can also be used to seal continuous or oscillating rotary motion, given low-pressure and low-speed applications. As shown in Fig. 24.17, the control of the pressure on the rubber depends on the squeeze of the rubber itself, so that compression set of the rubber will cause a loss of the seal. But, yet, if the squeeze is too high, the seal will develop too much friction heat. The use of a backup ring under high-pressure or high-gap conditions and the slipper seal to reduce friction are also shown in Fig. 24.17.

Figure 24.17 Elastomeric ring seals for rotating and reciprocating motion.
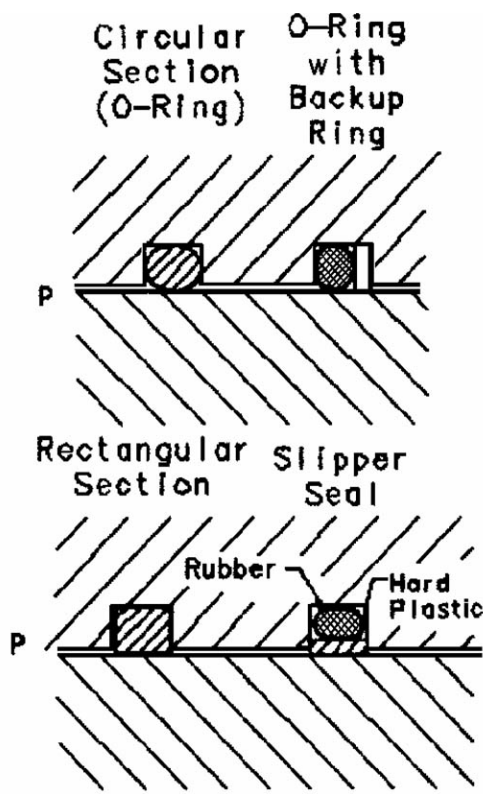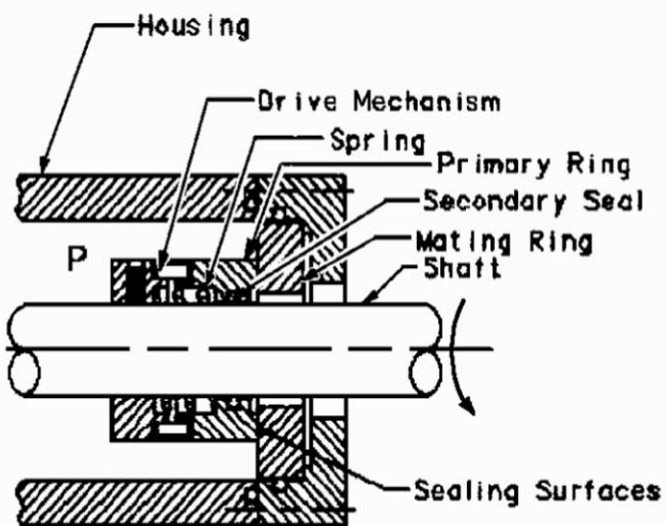
Figure 24.18 Mechanical face seal. (*Source:* Lebeck, A. O. *1991. Principles and Design of Mechanical Face Seals.* John Wiley & Sons, New York. With permission.)

Rotating Surface-Guided Seals—Annular Surface

The mechanical face seal, as shown in Fig. 24.18, has become widely used to seal rotating and oscillating shafts in pumps and equipment. The mechanical face seal consists of a self-aligning primary ring, a rigidly mounted mating ring, a secondary seal such as an O-ring or bellows that gives the primary ring freedom to self-align without permitting leakage, springs to provide loading of the seal faces, and a drive mechanism to flexibly provide the driving torque. It is common to have the pressure to be sealed on the outside, but in some cases the pressure is on the inside. The flexibly mounted primary ring may be either the rotating or the nonrotating member.

Face seal faces are initially lapped very flat (1 micrometer or better) so that when they come into contact only a very small leakage gap results. In fact, using suitable materials, such faces lap themselves into conformity so that such a seal can leak as little as a drop of liquid per hour. Face seals also can be used for sealing gas.

One may also utilize a lip seal or an elastomeric ring to seal rotationally on an annular face.

Reciprocating Fixed-Clearance Seals

The clearance or bushing seal (Fig. 24.10) and the floating-ring seal (Fig. 24.12) can also be used for reciprocating motion, such as sealing piston rods. In fact, the bushing can be made to give a near-zero clearance by deformation in such applications.

Reciprocating Surface-Guided Seals

An elastomeric ring can be used to seal the reciprocating motion of a piston, as shown in Fig. 24.19. But more commonly used for such applications are cup seals (Fig. 24.20), U-cups, V- or chevron rings, or any of a number of specialized shapes (Fig. 24.21). Various types of these seals are used to seal piston rods, hydraulic cylinders, air cylinders, pumping rods, and pistons.

Figure 24.19 Elastomeric ring seal. **Figure 24.20** Cup seal. **Figure 24.21** Elastomeric ring reciprocating seals.
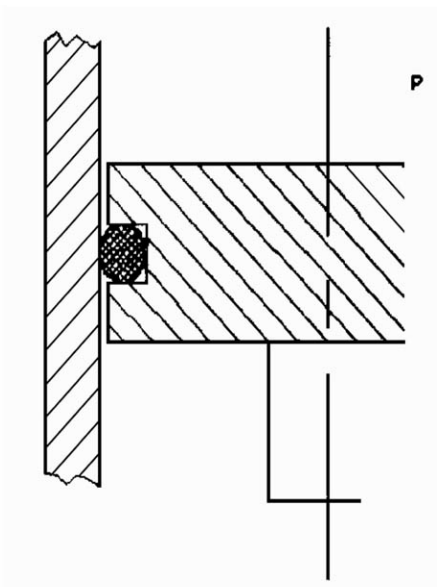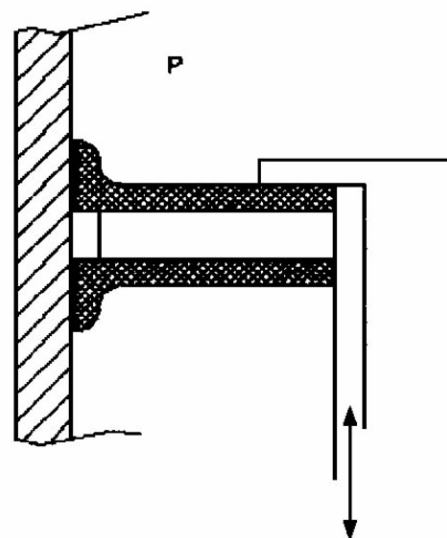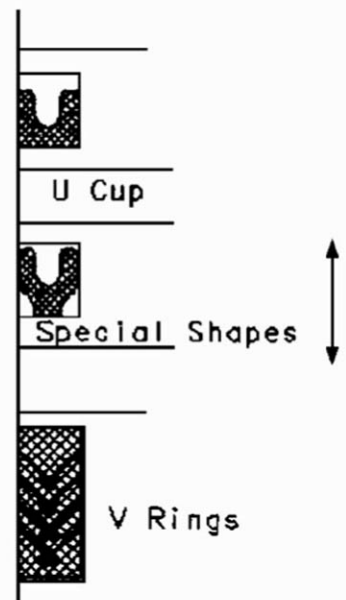
Split rings such as shown in Fig. 24.22 can be made of rigid materials. They are split for installation and so that they are loaded tightly against the wall by fluid pressure. Metal piston rings can be used in very hot environments. Plastic piston rings are suited to lower-temperature compressors.

Reciprocating Limited-Travel Seals

Most commonly used in pressure regulator and other limited-travel devices is the diaphragm shown in Fig. 24.23. Properly designed, this seal can be absolute and have significant travel. It can also allow for angular misalignment. In Fig. 24.24 is shown a metal bellows and in Fig. 24.25 is a rubber bellows. Both of these permit limited axial and angular motion. They have the advantage of being absolute seals because they do not rely on a sealing interface or suffer from wear and have no significant friction. Metal bellows may be made from edge-welded disks as shown or formed from a thin metal tube.

Figure 24.22 Split ring seal (piston ring).
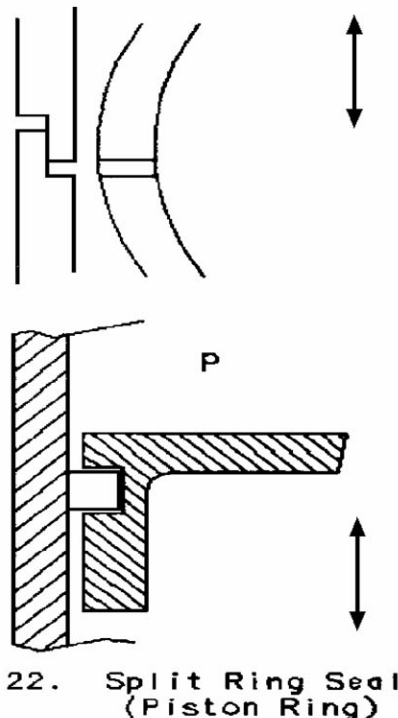
Figure 24.23 Diaphragm.
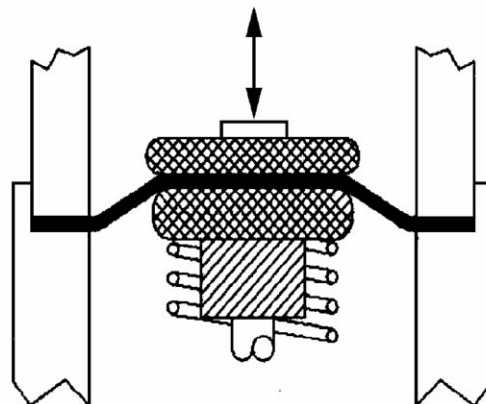
Figure 24.24 Welded metal bellows.
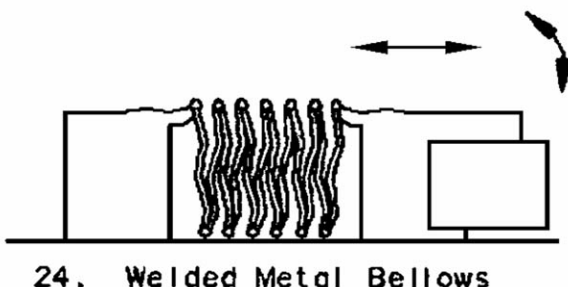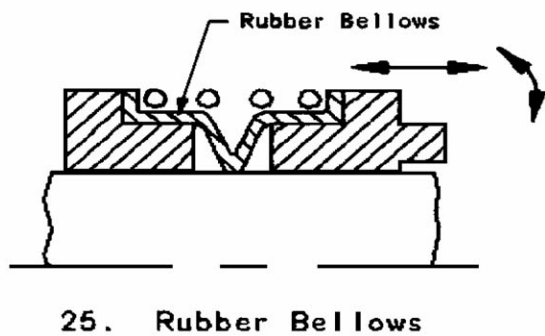
Figure 24.25 Rubber bellows.

24.4 Gasket Practice

For a gasket to seal, certain conditions must be met. There must be enough bolt or clamping force initially to seat the gasket. Then there also must be enough force to keep the gasket tightly clamped as the joint is loaded by pressure.

One may take the ASME Pressure Vessel Code [1980] formulas and simplify the gasket design procedure to illustrate the basic ideas. The clamping force, to be applied by bolts or other suitable means, must be greater than the larger of the following:

$$W_1 = \frac{\pi}{4} D^2 P + \pi 2 b D m P \qquad (24.1)$$

$$W_2 = \pi D b y \qquad (24.2)$$

where

D = effective diameter of gasket (m)

b = effective seating width of gasket (m)
$2b$ = effective width of gasket for pressure (m)
P = maximum pressure (Pa)
m = gasket factor
y = seating load (Pa)

Equation (24.1) is a statement that the clamping load must be greater than the load created by pressure plus a factor m times the same pressure applied to the area of the gasket in order to keep the gasket tight. Equation (24.2) is a statement that the initial clamping load must be greater than some load associated with a seating stress on the gasket material. To get some idea of the importance of the terms, a few m and y factors are given in Table 24.1. One should recognize that the procedure presented here is greatly simplified, and the user should consult one of the comprehensive references cited for details.
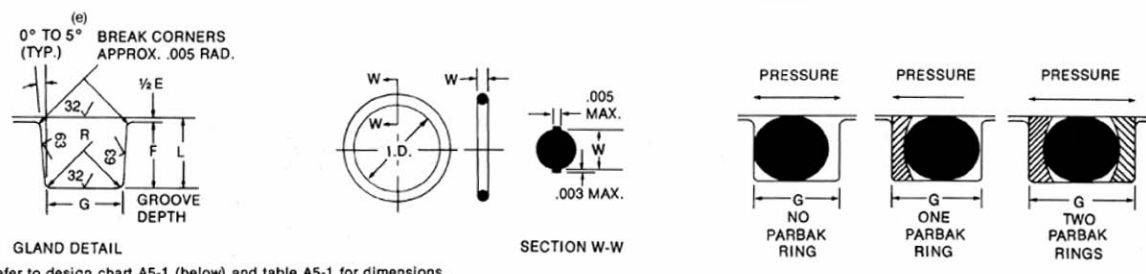
Table 24.1 Gasket Factors

Type	m	y (MPa)
Soft elastometer	0.5	0
Elastometer with fabric insertion	2.5	20
Metal jacketed and filled	3.5	55
Solid flat soft copper	4.8	90

24.5 O-Ring Practice

To seal properly, an O-ring must have the proper amount of squeeze or **preload,** have enough room to thermally expand, not have to bridge too large a gap, have a rubber hardness suitable to the job, and be made of a suitable rubber. Table 24.2 shows an abbreviated version of recommendations for static O-rings and Table 24.3 for reciprocating O-rings. In many cases one will want to span gaps larger or smaller than those recommended in the tables, so Fig. 24.26 shows permissible gap as a function of pressure and hardness based on tests.

Table 24.2 Static O-Ring Grooves—Design Chart A5-1 for Industrial O-Ring Static Seal Glands

Refer to design chart A5-1 (below) and table A5-1 for dimensions.

Table 24.2 Static O-Ring Grooves—Design Chart A5-1 for Industrial O-Ring Static Seal Glands

O-Ring Size Parker 2-	W Cross Section		L Gland Depth[1]	Squeeze[1]		E Diametral Clearance[2,3]	G Groove Width			R Groove Radius	Eccentricity Max.[4]
	Nominal	Actual		Actual	%		No Parbak Rings	One Parbak Ring	Two Parbak Rings		
004 through 050	$\frac{1}{16}$	.070 ±.003	.050 to .052	.015 to .023	22 to 32	.002 to .005	.093 to .098	.138 to .143	.205 to .210	.005 to .015	.002
102 through 178	$\frac{3}{32}$	.103 ±.003	.081 to .083	.017 to .025	17 to 24	.002 to .005	.140 to .145	.171 to .176	.238 to .243	.005 to .015	.002
201 through 284	$\frac{1}{8}$	.139 ±.004	.111 to .113	.022 to .032	16 to 23	.003 to .006	.187 to .192	.208 to .213	.275 to .280	.010 to .025	.003
309 through 395	$\frac{3}{16}$	.210 ±.005	.170 to .173	.032 to .045	15 to 21	.003 to .006	.281 to .286	.311 to .316	.410 to .415	.020 to .035	.004
425 through 475	$\frac{1}{4}$	.275 ±.006	.226 to .229	.040 to .055	15 to 20	.004 to .007	.375 to .380	.408 to .413	.538 to .543	.020 to .035	.005

[1] For ease of assembly when Parbaks are used, gland depth may be increased up to 5%.
[2] Clearance gap must be held to a minimum consis nt with design requirements for temperature range variation.
[3] Reduce maximum diametral clearance 50% when using silicone or fluorosilicone O-rings.
[4] Total indicator reading between groove and adjacent bearing surface.
(e) 0° preferred.
Source: Parker Hannifin Corporation. 1990. *Parker O-Ring Handbook.* Parker Hannifin Corporation. Cleveland, OH. With permission.

Table 24.3 Reciprocating O-Ring Grooves—Design Chart A6-5 for Industrial Reciprocating O-Ring Packing Glands

O-Ring Size Parker 2-	W Cross Section		L Gland Depth	Squeeze		E Diametral Clearance[1]	G Groove Width			R Groove Radius	Eccentricity Max.[2]
	Nominal	Actual		Actual	%		No Parbak Rings	One Parbak Ring	Two Parbak Rings		
006 through 012	$\frac{1}{16}$	.070 ±.003	.055 to .057	.010 to .018	15 to 25	.002 to .005	.093 to .098	.138 to .143	.205 to .210	.005 to .015	.002
104 through 116	$\frac{3}{32}$	.103 ±.003	.088 to .090	.010 to .018	10 to 17	.002 to .005	.140 to .145	.171 to .176	.238 to .243	.005 to .015	.002
201 through 222	$\frac{1}{8}$	.139 ±.004	.121 to .123	.012 to .022	9 to 16	.003 to .006	.187 to .192	.208 to .213	.275 to .280	.010 to .025	.003
309 through 349	$\frac{3}{16}$	.210 ±.005	.185 to .188	.017 to .030	8 to 14	.003 to .006	.281 to .286	.311 to .316	.410 to .415	.020 to .035	.004
425 through 460	$\frac{1}{4}$	.275 ±.006	.237 to .240	.029 to .044	11 to 16	.004 to .007	.375 to .380	.408 to .413	.538 to .543	.020 to .035	.005

[1] Clearance (extrusion gap) must be held to a minimum consistent with design requirements for temperature range variation.
[2] Total indicator reading between groove and adjacent bearing surface.
Source: Parker Hannifin Corporation. 1990. *Parker O-Ring Handbook.* Parker Hannifin Corporation. Cleveland, OH. With permission.

Figure 24.26 Limits for extrusion. (*Source:* Parker Hannifin Corporation. 1990. *Parker O-Ring Handbook.* Parker Hannifin Corporation. Cleveland, OH. With permission.)
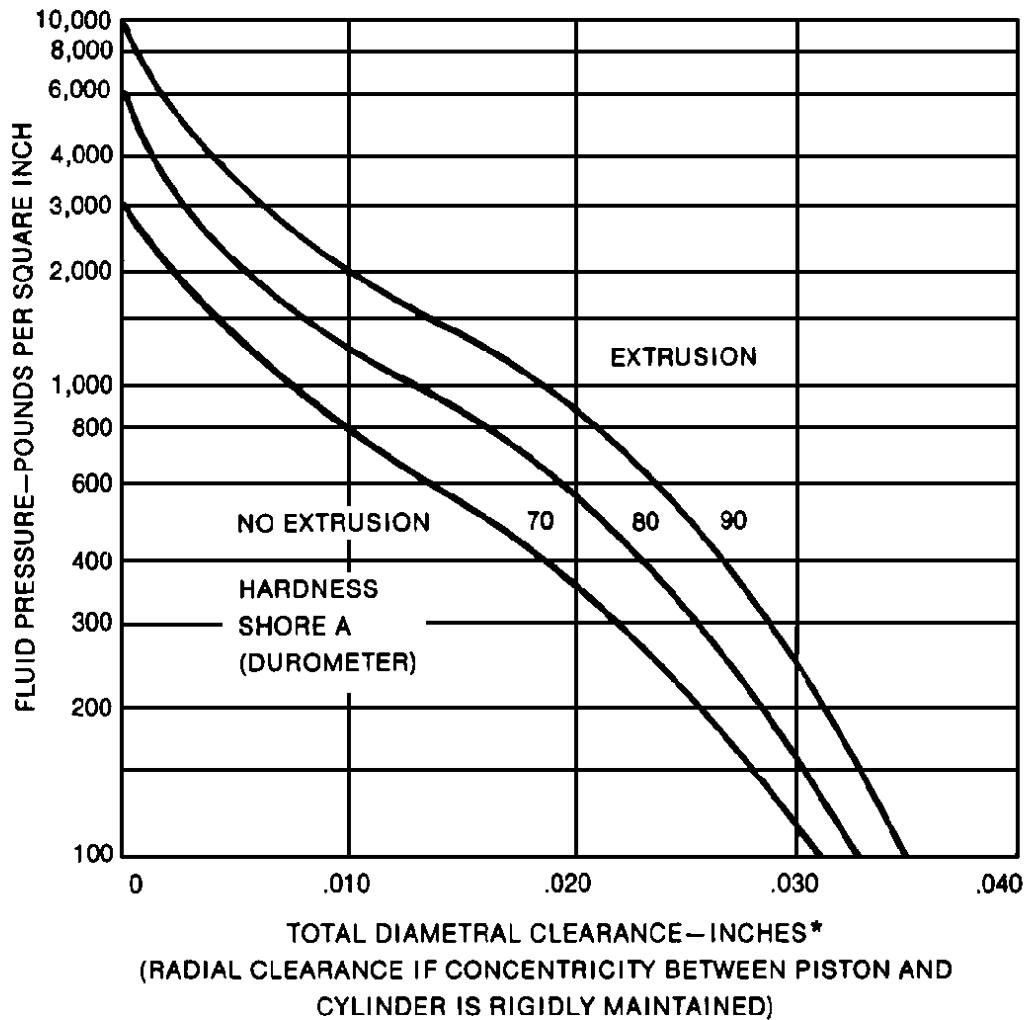
FIGURE A4-2 LIMITS FOR EXTRUSION

BASIS FOR CURVES

1. 100,000 pressure cycles at the rate of 60 per minute from zero to the indicated pressure.

2. Maximum temperature (i.e. test temperature) 160°F.

3. No back-up rings.

4. Total diametral clearance must include cylinder expansion due to pressure.

5. Apply a reasonable safety factor in practical applications to allow for excessively sharp edges and other imperfections and for higher temperatures.

Whereas nitrile rubber is most common and suitable for oils and aqueous solutions, fluorocarbon is excellent for hot oils. Many of the elastomer materials are made into O-rings and find application in certain chemical environments. Proper O-ring elastomer selection using one of the extensive recommendation tables [ASME, 1980; Lebeck, 1991] is essential for good performance.
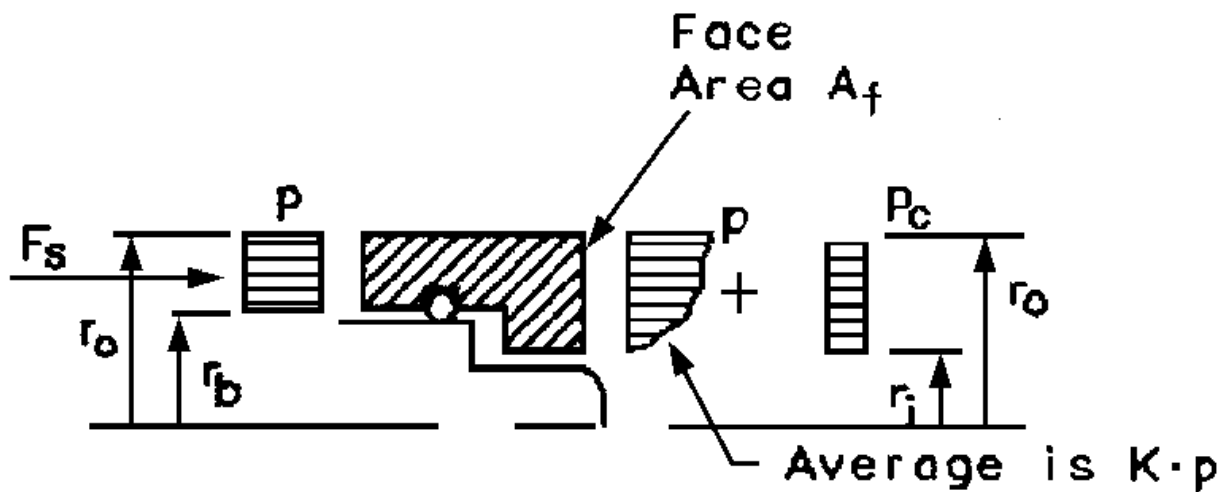
24.6 Mechanical Face Seal Practice

Figure 24.27 shows how, in general, the area on which the pressure is acting to load the primary ring may be smaller (or larger) than the area of the face. Thus, the balance ratio for a mechanical seal is defined as

$$B = \frac{r_o^2 - r_b^2}{r_o^2 - r_i^2} \qquad (24.3)$$

where balance ratios less than 1.0 are considered to be "balanced" seals where in fact the face load pressure is made less than the sealed pressure. If balance ratio is greater than 1.0, the seal is "unbalanced."

Figure 24.27 Mechanical seal elementary theory.

27. Mechanical Seal Elementary Theory

Balance radius (r_b) of a seal is used by seal designers to change balance ratio and thus to change the load on the seal face. With reference to Fig. 24.27, and noting that the face area is

$$A_f = \pi(r_o^2 - r_i^2) \qquad (24.4)$$

the average **contact pressure** (load pressure not supported by fluid pressure) on the face is given by

$$p_c = (B - K)p + \frac{F_s}{A_f} \qquad (24.5)$$

where the K factor represents the average value of the distribution of the fluid pressure across the face. For well-worn seals in liquid, $K = 1/2$ and, for a compressible fluid, K approaches $2/3$.

The sliding speed of the seal is based on the average face radius, or

$$V = \frac{r_o + r_i}{2}\omega \qquad (24.6)$$

The severity of service for the seal is taken as the pressure times the sliding speed, or

$$(PV)_{\text{total}} = pV \qquad (24.7)$$

The severity of operating conditions for the seal materials is the contact pressure times the sliding speed, or

$$(PV)_{\text{net}} = p_c V \qquad (24.8)$$

The maximum allowable net PV is materials- and environment-dependent. For liquids the limiting values of Table 24.4 are generally used.

Table 24.4 Limiting Values for Liquids

Materials	$(PV)_{\text{net}}$ (psi·ft/min)	$(PV)_{\text{net}}$ (Pa·m/s) · 10^6
Carbon graphite/alumina	100 000	$3.5 \cdot 10^6$
Carbon graphite/tungsten carbide	500 000	$17.5 \cdot 10^6$
Carbon graphite/silicon carbide	> 500 000	$> 17.5 \cdot 10^6$

Friction or seal power can be estimated from

$$P = p_c A_f f_c V \qquad (24.9)$$

where P is the power and f_c is the friction coefficient, with values ranging from 0.07 for carbon graphite on silicon carbide to 0.1 for carbon graphite on tungsten carbide.

Defining Terms

Annulus: The radial face of a rectangular cross-section ring.

Contact pressure: At a seal interface a part of the force needed for equilibrium is supplied by fluid pressure and a part by contact pressure.

Elastomer(ic): A material having the property of recovery of shape after deformation; rubberlike materials.

Ferrofluid: A liquid containing a suspension of magnetic particles.

Preload: The clamping load before pressure is applied.

Sealing clearance: The effective gap between two surfaces.

Self-energized: The preload is supplied by the elastic behavior of the material itself.

References

American Society of Mechanical Engineers. 1980. *Code for Pressure Vessels,* Section VIII, Div 1. ASME, New York.

Lebeck, A. O. 1991. *Principles and Design of Mechanical Face Seals.* John Wiley & Sons, New York.

Parker Hannifin Corporation. 1990. *Parker O-Ring Handbook.* Parker Hannifin Corporation. Cleveland, OH.

Further Information

Brink, R. V., Czernik, D. E., and Horve, L. A. 1993. *Handbook of Fluid Sealing.* McGraw-Hill, New York.

Buchter, H. H. 1979. *Industrial Sealing Technology.* John Wiley & Sons, New York.

Kaydon Ring & Seals, Inc. 1987. *Engineer's Handbook—Piston Rings, Seal Rings, Mechanical Shaft Seals.* Kaydon Rings & Seals, Inc. Baltimore, MD.

Warring, R. H. 1981. *Seals and Sealing Handbook.* Gulf, Houston, TX.